Doctoral Thesis

Development of Cancer Therapeutics and Diagnostics

Targeting Telomere and Telomerase

March, 2014

Faculty of Frontiers of Innovative Research

in Science and Technology (FIRST),

Konan University Graduate School

Hidenobu Yaku

Contents

1. Abstract

Telomeres at ends of eukaryotic chromosomes contain accessory proteins and telomeric DNA, which is composed of tandem repeats of a G-rich motif (5'-TTAGGG-3' in humans) with 3' overhang termed G-tail. In normal somatic cells, telomeric DNA shortens with every cell division due to an end replication problem. The shortening of telomeric DNA finally leads to apoptosis. In contrast, in most of tumor cells (85-90%), highly-activated telomerase maintains the length of telomeric DNA, which is a critical biological event for carcinogenesis. The specificity and universality of the telomerase activity for tumor cells implies two important suggestions: (i) inhibition of the telomerase activity should allow an anticancer therapy with few side-effects and (ii) detection of the telomerase activity should allow a precise cancer diagnosis. Thus, the author attempted to achieve two purposes: (i) elucidation of rules to design anticancer drugs with efficient telomerase inhibitory effect, and (ii) development of an assay for telomerase activity without false results.

1.1. Elucidation of Rules to Design Anticancer Drugs with Efficient Telomerase Inhibitory Effect (Main Papers 1 and 2)

Since it was found that G-quadruplex structure formed by telomeric DNA inhibits telomerase activity, many G-quadruplex-ligands have been screened or developed toward development of anticancer drugs. Most of them contain a large π planar core with peripheral cationic groups in order to bind to G-quadruplex *via* π-π stacking and electrostatic attractive interactions. However, cationic G-quadruplex-ligands did not often show the desired anticancer effects in cellular assays despite of their highly efficient telomerase inhibition *in vitro*. This divergence is at least partly due to differences between chemical conditions *in vitro* and *in vivo*. Based on previous studies on the conventional G-quadruplex-ligands, it was expected that excess double-stranded DNA (dsDNA) found in genome DNA and molecular crowding (MC) in cell nuclei may reduce their capacities to bind to G-quadruplex and to inhibit telomerase activity. Therefore, in order to acquire a strategy to design G-quadruplex-ligands that exert the desired functions even in cell nuclei, the author systematically examined various cationic and anionic G-quadruplex-ligands under cell nuclei-mimicking conditions, in which excess dsDNA and MC cosolutes exist.

The capacities of an anionic copper phthalocyanine with four sodium salt forms of sulfo groups, copper (II) phthalocyanine 3,4',4'',4'''-tetrasulfonic acid, tetrasodium salt (Cu-APC), to bind to a human telomeric oligo G-quadruplex and to inhibit telomerase

activity were investigated. Based on visible absorbance titration experiments, Cu-APC bound to the G-quadruplex with a K_d value of 42 μM in the presence of 100 mM KCl at 25°C, and little or no absorbance change was observed for single-stranded DNA (ssDNA) or dsDNA. These results indicate that Cu-APC can bind to the G-quadruplex with high selectivity over ssDNA and dsDNA. Notably, the K_d value of Cu-APC for the G-quadruplex in the presence of excess decoy dsDNA, λ DNA, was almost the same as that in the absence of λ DNA. This high selectivity is attributed to that an electrostatic repulsion between anionic groups of Cu-APC and phosphate groups of dsDNA prevents Cu-APC from binding to dsDNA, although interaction between Cu-APC and the G-quadruplex is kept *via* π-π stacking interaction. Results obtained with a modified telomeric repeat amplification protocol (TRAP) assay were in accordance with results from the binding studies; Cu-APC inhibited telomerase activity with an IC50 value of 1.2 μM in both the absence and presence of λ DNA. In addition, the telomerase inhibitory effect of metal-free and nickel anionic phthalocyanines was not significantly affected by λ DNA. These results indicate that the coordination metal has very little effect on anionic phthalocyanine-mediated telomerase inhibition. In contrast, 5,10,15,20-tetra(N-methyl-4-pyridyl)porphyrin (TMPyP4), which is a cationic porphyrin, bound to not only the G-quadruplexdid but also ssDNA and dsDNA. In accordance with these results, TMPyP4 lost its telomerase inhibitory effect in the presence of λ DNA, although it inhibited telomerase activity in the absence of λ DNA. The loss of the telomerase inhibitory effect of TMPyP4 should be due to non-specific binding between cationic groups of TMPyP4 and phosphate groups of λ DNA. Based on these findings, it is possible to conclude that, even in the presence of excess genomic dsDNA in cell nuclei, anionic phthalocyanines could efficiently inhibit telomerase activity.

Next, the telomeric G-quadruplex-binding and telomerase-inhibiting capacities of two cationic (TMPyP4 and N,N'-bis[2-(1-piperidino)ethyl]-3,4,9,10-perylenetetracarboxylic diimide (PIPER)) and two anionic (Cu-APC and Fe(III)-protoporphyrin IX (Hemin)) G-quadruplex-ligands were examined under MC conditions. Osmotic experiments showed that binding of the anionic ligands, which bind to G-quadruplex DNA *via* π-π stacking interactions, caused some water molecules to be released from the G-quadruplex/ligand complex; in contrast, a substantial number of water molecules were taken up upon electrostatic binding of the cationic ligands to G-quadruplex DNA. These behaviors of water molecules maintained and reduced the binding affinities of the anionic and the cationic ligands, respectively, under MC conditions. Consequently, the anionic ligands (Cu-APC and Hemin) robustly inhibited telomerase activity even with

MC; in contrast, the inhibition of telomerase caused by cationic TMPyP4 was drastically reduced by MC. These results indicate that the binding of G-quadruplex-ligands to G-quadruplex *via* non-electrostatic interactions is preferable for telomerase inhibition under physiological conditions. Collating all these results, it is reasonable to support that anionic ligands such as Cu-APC are promising anticancer drug candidates that efficiently inhibit telomerase activity even in cell nuclei.

1.2. Development of an Assay for Telomerase Activity without False Negative Results (Main Paper 3)

TRAP assay, which is a most widely-used telomerase assay, can detect telomerase activity with high sensitivity, because it amplifies telomerase reaction products by polymerase chain reaction (PCR). However, this assay is susceptible to PCR inhibitors in clinical samples, which include bile acid, bilirubin, heparin, and hemoglobin. Since such reaction inhibition by these inhibitors causes false negative results, TRAP assay should not be appropriate for clinical applications. Thus, the author developed a telomerase assay without false negative results, which is based on asymmetric PCR (A-PCR) on magnetic beads (MBs) and subsequent application of cycling probe technology (CPT). In this assay, the telomerase reaction products are immobilized on MBs, which are then washed to remove PCR inhibitors in clinical samples. The guanine-rich sequences (5’-(TTAGGG)*n*-3’) of the telomerase reaction products on MBs are then preferentially amplified by A-PCR, and the amplified products are subsequently detected *via* CPT. In CPT, a probe RNA with a fluorophore at the 5’ end and a quencher at the 3’ end is hydrolyzed by RNase H in the presence of the target DNA. The catalyst-mediated cleavage of the probe RNA enhances fluorescence from the 5’ end of the probe. Furthermore, the reactions including hybridization and hydrolysis of the probe RNA occur repetitively, which leads to fluorescence signal amplification. The assay successfully enabled detection of HeLa cells selectively over normal human dermal fibroblast (NHDF) cells. Importantly, this selectivity produced identical results with regard to detection of HeLa cells in the absence and presence of excess NHDF cells; therefore, this assay can be used for practical clinical applications. The lower limit of detection for HeLa cells was 50 cells, which is lower than that achieved with conventional TRAP assays. The present assay also eliminated false negative results caused by PCR inhibitors such as bile salt, heparin, and hemoglobin. Furthermore, it was shown that this assay is appropriate for screening among G-quadruplex-ligands to find those that inhibit telomerase activity. Therefore, the present assay should make a contribution to not only cancer diagnosis but also

development of new anticancer drugs.

1.3. Short Summary

Telomerase has not been detected in various normal somatic cells except proliferating progenitor cells and stimulated lymphocytes despite of the high activity in almost of all cancer types including cancer stem or stem-like cells. Thus, telomerase is promising as a target for anticancer therapy and cancer diagnosis. Through this thesis, it was elucidated that anionic functional groups of G-quadruplex-ligands contribute to G-quadruplex-binding and telomerase-inhibiting capacity of the ligands under abundant dsDNA condition and MC conditions. These results imply that anionic G-quadruplex-ligands can be promising candidates of anticancer drugs. Also, the present telomerase assay utilizing A-PCR on MBs and CPT technology was developed. This assay allowed high-sensitive detection of cancer cells without false negative results caused by PCR inhibitors. Consequently, the findings in this thesis should make a contribution to anticancer therapy without side-effects and accurate cancer diagnosis targeting telomerase.

2. Introduction

Cancer threatens human health *via* uncontrolled cell proliferation, invasion, and metastasis. Cancer has the highest risk for death among diseases and the number of deaths from cancer reached more than 20,000 a day in the world according to World Health Statistics by World Health Organization (WHO) (Fig. 2-1). For reduction of the death number from cancer, fairly extensive studies have been done. Especially, in 1980's molecular biological studies on many cancer-related genes such as oncogens and tumor suppressor genes made a huge contribution to elucidation of a carcinogenesis mechanism. Oncogenes, which are related to signal transduction promoting cell growth, are categorized into viral oncogenes and cellular oncogenes. Expression of cellular oncogenes is adequately controlled under normal conditions. However, point mutation, translocation, and amplification of those genes abnormally activate or amplify the expressed proteins, leading to carcinogenesis. Viral oncogenes are also host cell-derived genes that contain mutations or abnormally activated by viral promoters. In contrast to oncogenes, tumor suppressor genes usually play a role in inhibition of carcinogenesis by involving inhibition of cell divisions, and induction of DNA repair and apoptosis. Thus, mutations that reduce functions and expression levels of tumor suppressor genes induce carsinogenesis. It has been thought that at least several mutations of cancer-related genes are required for human cancer iniciation. For example, mutations of BRCA1 and BRCA2 genes, which are tumor suppressor genes, increase an incidence of breast cancer to 85%. Thus, an affordable technology for accurate detection of such mutations should be greatly-helpful to expect the incidence. The author succeeded in an electrochemical genotyping of mutations by developping a novel allele-spcific primer extenstion technology, and an electrochemical detection technology for pyrophosphate,

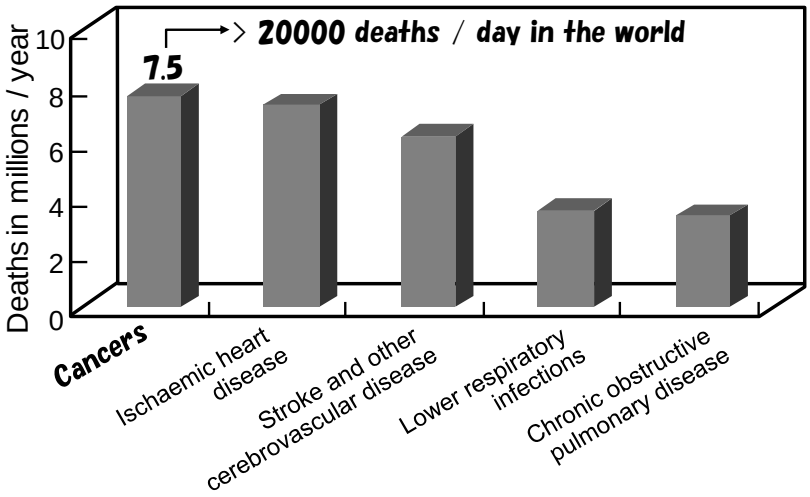

Fig. 2-1. The worldwide top 5 causes of death (2008) from WHO report.

which is produced during a primer extension reaction (Fig. 2-2A) [1]. Furthermore, a μ-total analysis sytem (μ-TAS) chip utilizing these technologies allowed accurate genotyping in one hour from several μL of blood (Fig. 2-2B) [2, 3]. In the future, this device should contribute to low-cost and accurate diagnosis of the cancer incidence.

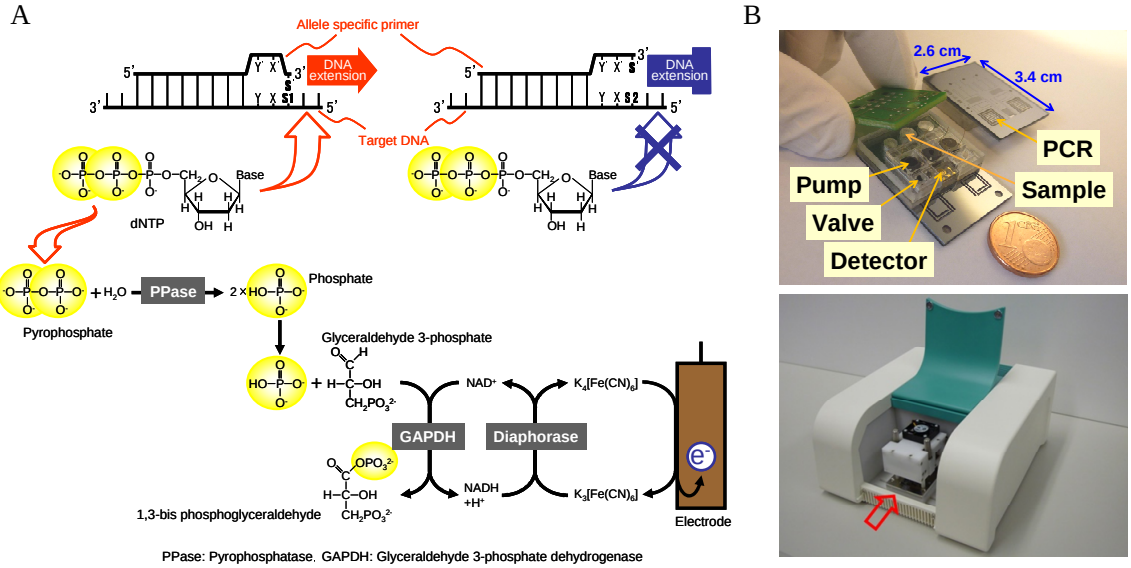

Fig. 2-2. (A) Electrochemical genotyping principle, and (B) electrochemical genotyping chip and reader (http://panasonic.co.jp/corp/news/official.data/data.dir/2013/02/jn130214-1/jn130214-1.html)

2.1. Structure and Function of Telomeric DNA

There can be no doubt about that oncogenes and tumor suppressor genes are important triggers for carcinogenesis. However, the mutations of these genes are not sufficient factors for carcinogenesis. Immortal cell growth is an essential event for carcinogenesis, and is regurally controlled by telomeres at ends of chromosme and telomerase catalyzing a telomeric DNA extension. In this section, the structural and functional features of telomeres will be explained.

Telomeres at ends of eukaryotic chromosomes contain telomeric DNA with tandem repeats of a G-rich motif (Fig. 2-3) [4-7]. The sequence of the G-rich motif and the number of repeats varies among species, from a fixed 4.5 repeats of 5'-TTTTGGGG-3' in the ciliate *Oxytricha nova* to ~350-500 bp in *Saccharomyces cerevisiae*, and variable numbers of 5'-TTAGGG-3' repeats encompassing 10-15 kb in humans and 20-50 kb in certain mouse and rat species (Table 2-1) [5-7]. Telomeric DNA further has a structural

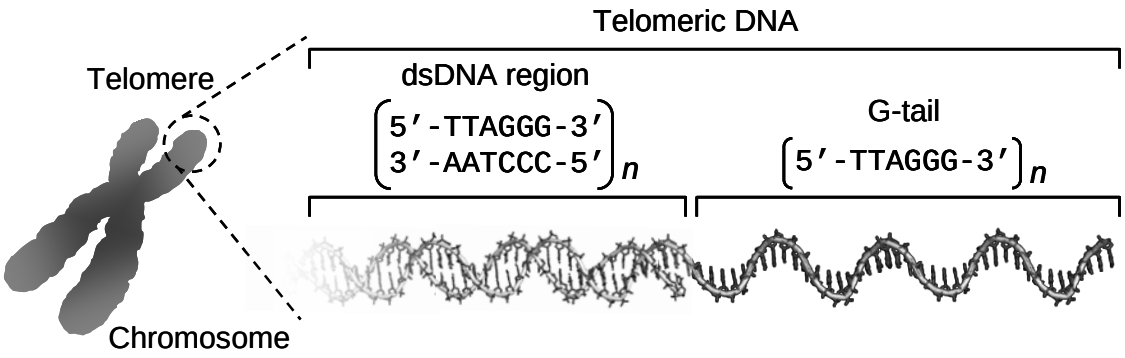

Fig. 2-3. Human telomeric DNA.

Table 2-1. Telomeric G-rich sequences.

Sequences (5'→3')	Species
TTGGGG	*Tetrahymena thermophila*
TTAGGG	*Human*
TTTAGGG	*Arabidopsis thaliana*
TTTTGGGG	*Oxytricha nova*
TTTTGGGG	*Stylonychia lemnae*

feature of the 3'-ends with a single-stranded G-rich overhang called G-tail (Fig. 2-3) [6-12]. In humans, the length of the G-tail, 5'-TTAGGG-3', is 150-250 bases. Intrinsically, a linear DNA is recognized as a damaged DNA and the ends are rapidly joined *via* catalysis of various nucleases and DNA ligases. However, chromosomal DNA is protected from illicit DNA end-joining events [6, 7, 13, 14], because at least six telomeric proteins including telomeric repeat-binding factor 1 (TRF1), TRF2, repressor and activator protein 1 (RAP1), TRF1-interacting nuclear protein 2 (TIN2), protection of telomeres 1 (POT1) and TPP1, bind to telomeric DNA to form a capped complex known as shelterin (Fig. 2-4) [6, 7]. TRF1 and TRF2 directly bind to telomeric dsDNA *via* forming each homodimer [6, 7]. On the other hand, POT1 directly binds to G-tail.

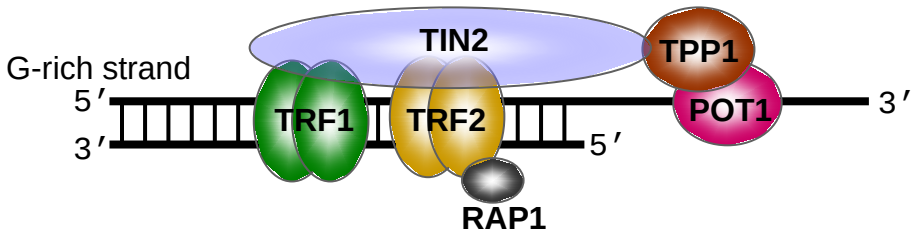

Fig. 2-4. Shelterin composed of telomeric DNA and accessory proteins.

TIN2 forms a bridge between TRF1, TRF2, and TPP1, and TPP1 forms another bridge between TIN2 and POT1 [6, 7]. RAP1 homologue in humans associates with telomeric DNA *via* its interaction with TRF2 [6, 7].

Telomeric DNA can form an alternative structure termed Telomere loop (T-loop) (Fig. 2-5) [15]. T-loop is a lariat-like configuration, in which the G-tail invades the dsDNA region to form D-loop. Since T-loop is not thermodynamically favorable, the telomeric accessory proteins should be implicated in the formation. This structure may be also another option to protect chromosomal DNA.

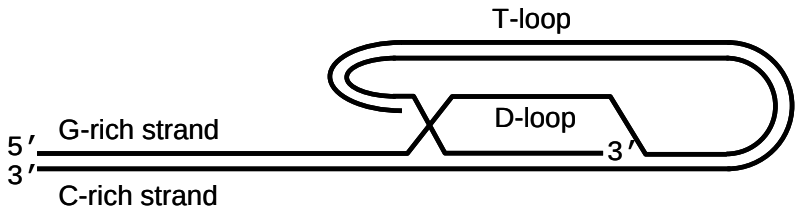

Fig. 2-5. Structure of T-loop.

Telomeric DNA is responsible for not only the protection of chromosomal ends but also a control of cell life time. During S-phase of the cell cycle, chromosomal DNA is replicated from RNA primers by DNA polymerase, and then RNA primers are removed by exonuclease (Fig. 2-6A). Thus, daughter strands are shorter than parent strands. This end replication problem causes lost of 50-100 bp of telomeric DNA with every cell division in normal somatic cells. The shortening of telomeric DNA finally leads to inefficiency of the protection of chromosome ends by telomeric DNA (Fig. 2-6B) [16]. Furthermore, this deprotection results in end-to-end fusions of chromosomal DNA, which causes apoptosis [16]. A series of these biological events serves as a huge barrier to carcinogenesis. Even though oncogenic mutations occur, carcinogenesis

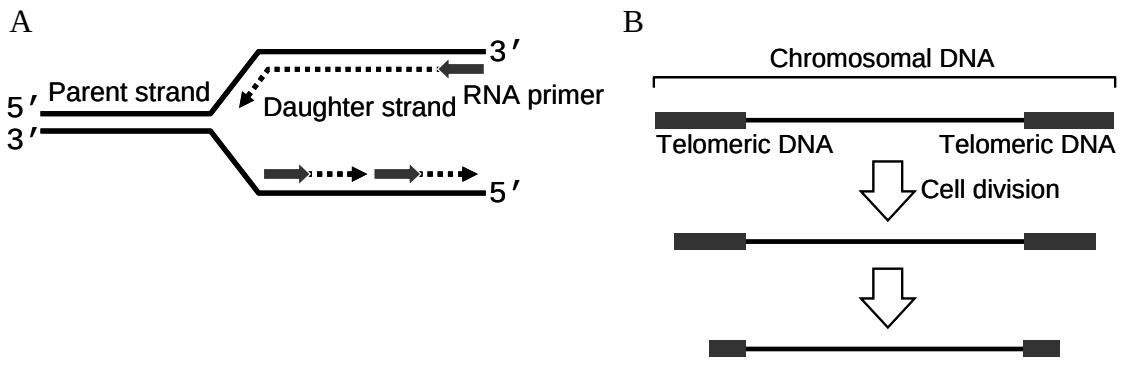

Fig. 2-6. (A) End replication problem and (B) loss of telomeric DNA with every cell division.

should be prevented as long as telomeric DNA shortens in a normal way.

2.2. Structure and Function of Telomerase

Not only tumor cells but also germ cells and stem cells can proliferate indefinitely [17, 18]. These immortalized cells solve the end replication problem by telomeric DNA extension using telomerase (Fig. 2-7A) [19-22]. Telomerase has a complex structure composed of many subunits, but not all of them are well-understood. Previous studies showed that two subunits, which are found in a central part of a human telomerase holoenzyme, have critical functions in telomeric DNA extension [23-26]. One of the subunits is telomerase reverse transcriptase (abbre*via*ted to TERT, or hTERT in humans), which can synthesize DNA using RNA template (Fig. 2-7A) [23, 24]. Another subunit is a telomerase RNA component (abbre*via*ted to TR, or hTR in humans) including a template sequence for telomeric DNA extension (Fig. 2-7A) [25, 26]. TR is involved at multiple stages of telomerase biogenesis and function. For example, TR provides a template boundary element that limits the extent of reverse transcription. In humans, 11 nucleotides of hTR, 5'-CUAACCCUAAC-3', hybridize with G-tail and serve as the template for the extension reaction from the hybridized G-tail (Fig. 2-7A). As a result,

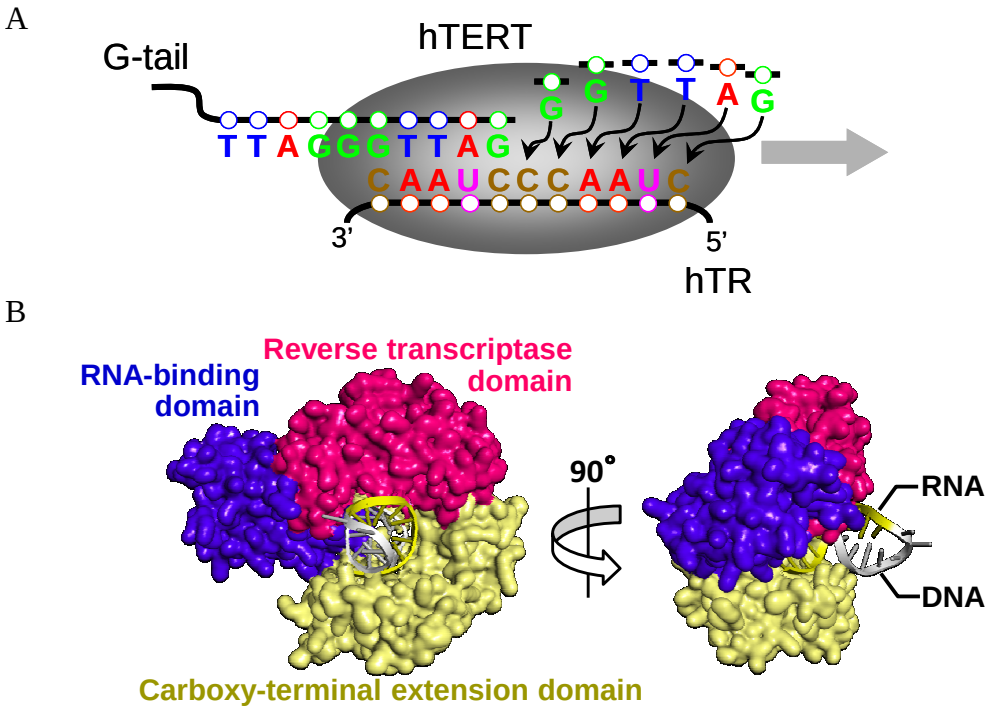

Fig. 2-7. (A) Telomeric DNA extension by telomerase and (B) crystal structural analysis of TERT of *Tribolium castaneum* with RNA-DNA hairpin of putative hTR (Yellow) and telomeric DNA (Gray) (PDB ID: 3KYL) [28].

new six nucleotides, 5'-GGTTAG-3', are added at the 3'-end of telomeric DNA (Fig. 2-7A). Crystal structural studies on *Tribolium castaneum* TERT and *Tetrahymena* telomerase holoenzyme in 2008, 2010, and 2013, respectively, strongly supported these reaction mechanisms including hybridization and addition of the six nucleotides [27, 28, 29]. These studies demonstrated that TERT consists of three highly conserved domains, organized into a ring-like structure, and the structure has an interior cavity, which is large enough for RNA/DNA duplex to dock in (Fig. 2-7B) [27, 28, 29].

Importantly, in 85-90 % of human tumor cells, telomerase is highly activated [22]. Antisense RNA can inhibit the telomerase activation in tumor cells [30]. For example, antisence RNA of hTR competitively prevented human telomerase from binding to telomeric DNA by binding to hTR [30]. This competitive prevention caused reduction in telomerase activity, and then tumor cells stopped proliferation in 23 to 26 days. A dominant-negative mutant of hTERT also inhibited proliferation of tumor cells [30]. These results indicate that constituous telomerase activation is essential for carcinogenesis as well as activation and inactivation of oncogenes and tumor supressor genes, respectively. More importantly, most of normal cells excepting germ cells, stem cells, and activated lymphocytes show little or no telomerase activity [17, 18, 31]. The specificity and universality of the telomerase activity for cancer cells implies two important suggestions: (i) inhibition of the telomerase activity should allow an anticancer therapy without any side effects, and (ii) detection of the telomerase activity should allow a precise cancer diagnosis.

2.3. Telomerase Inhibition by G-Quadruplex

In association with the demonstration of telomeric DNA extension by telomerase, a significant finding was reported that telomeric DNA can form a non-canonical DNA structure termed G-quadruplex (Fig. 2-8A) [32, 33]. G-quadruplex is a four-stranded DNA structure with stacked guanine tetrads, G-quartets, which are held together *via* eight Hoogsteen hydrogen bonds (Fig. 2-8A). The existence and possible structure of G-quartets was proposed about 50 years ago [34]. Since then, G-quadruplexes formed by various G-rich sequences have been reported [32, 33, 35-45]. Structural studies of G-quadruplexes have demonstrated that the G-rich sequences can form highly polymorphic G-quadruplexes, and the variation in these structures depends on the sequences and the experimental conditions (e.g., coexisting metal ion, metal ion concentration, and degree of molecular crowding) (Fig. 2-9) [46-66]. Among these polymorphic G-quadruplexes, G-quadruplexes formed by human telomeric DNA, in particular, have been investigated extensively, because G-quadruplex DNA inhibits

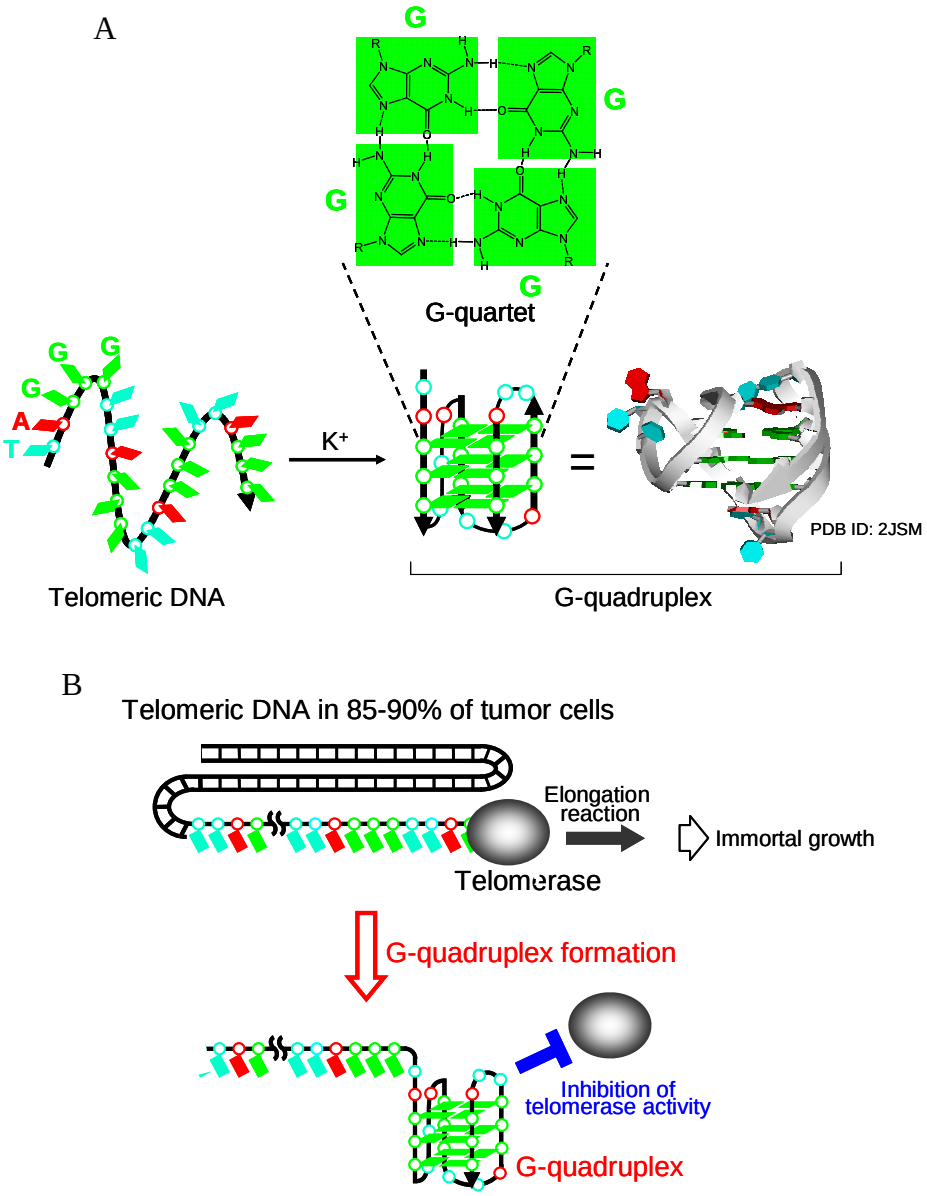

Fig. 2-8. (A) G-quadruplex formation by human telomeric DNA and (B) telomerase inhibition by G-quadruplex in tumor cells.

telomerase activity by preventing telomerase from binding to telomeric DNA (Fig. 2-8B) [67]. This finding indicates that G-quadruplex-ligands that inhibit telomerase activity *via* induction or stabilization of G-quadruplex are promising candidates of anticancer drugs without side effects. Thus, development of G-quadruplex-ligands has become an area of great interest. Moreover, recent bioinformatic studies showed that about 370,000 putative G-quadruplex-forming sequences exist throughout the human genome [68, 69]. Many of the putative G-quadruplex-forming sequences are enriched in promoter regions of oncogenes, including *c-MYC*, *c-kit*, *HRAS*, and *KRAS* [53,

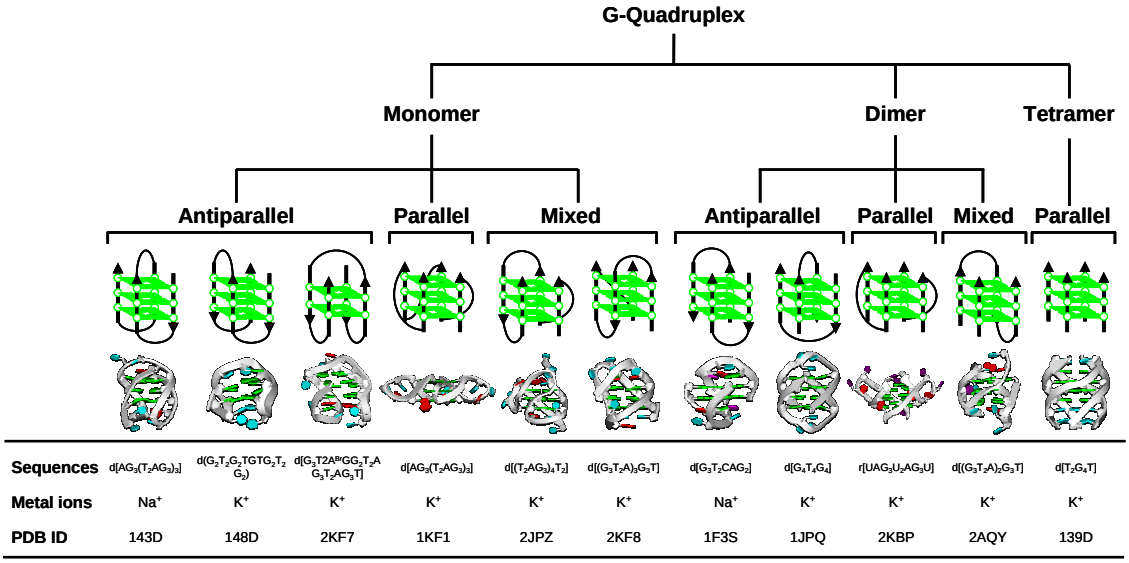

Fig. 2-9. G-quadruplex polymorphism depending on sequences and metal ions.

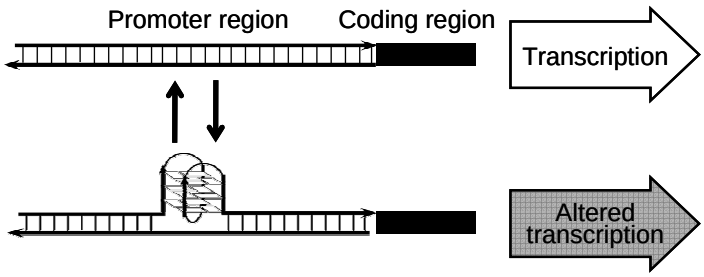

Fig. 2-10. Transcriptional regulation by G-quadruplex.

70-88]. These bioinformatic studies strongly indicate that G-quadruplexes can influence carcinogenesis by modulating transcription of oncogenes (Fig. 2-10). Importantly, some G-quadruplex-ligands regulate the expression of these oncogenes by binding to G-quadruplexes in the promoter regions [70-76, 78, 80, 82, 86, 88]. Thus, ligands that recognize and bind to G-quadruplexes in telomeric DNA and/or promoter regions of oncogenes are promising anticancer drugs.

2.4. G-Quadruplex-Ligand as Anticancer Drug

Many G-quadruplex-ligands developed to date contain a π-planar structure, of which size is similar to that of G-quartet, because the plane aromatic surface is essential for making strong π-π stacking interactions with G-quartet (Fig. 2-11) [89-91]. Most of

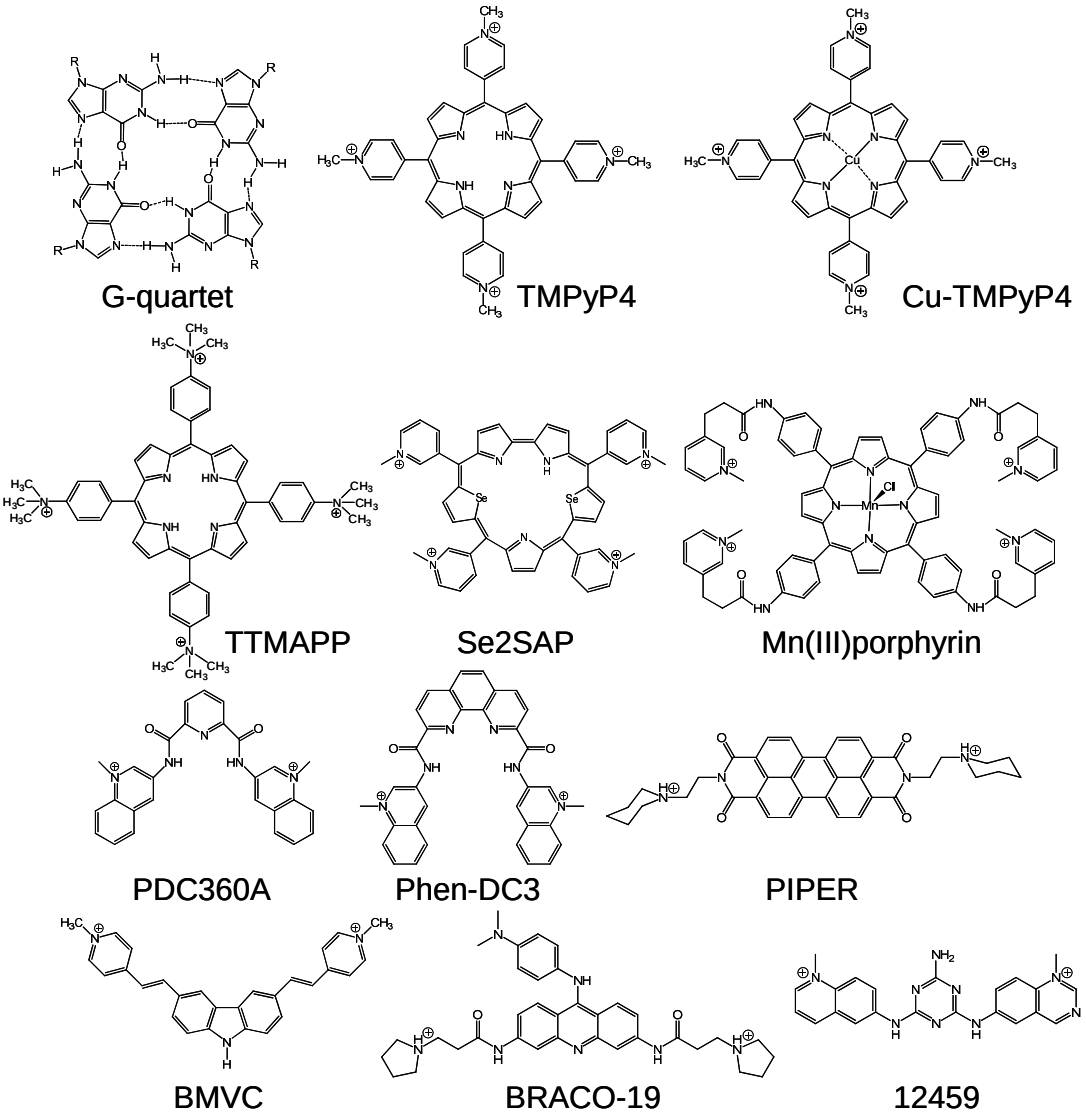

Fig. 2-11. Chemical structures of G-quartet and cationic G-quadruplex-ligands.

them further contain cationic functional groups in order to form electrostatic attractive interactions with G-quadruplex (Fig. 2-11) [89-91]. One of the most extensively studied G-quadruplex-ligands is 5,10,15,20-tetra(N-methyl-4-pyridyl)porphyrin, TMPyP4 (Fig. 2-11) [89-97]. This cationic porphyrin derivative is composed of four modified pyrrol units and four cationic functional groups. Based on results from UV titration experiment, NMR, and photocleavage assay, Hurley's group reported for the first time that TMPyP4 bound to a human telomeric oligo G-quadruplex [92]. Other groups also showed that TMPyP4 bound to the G-quadruplex with multiple binding modes (Fig. 2-12A) [80, 98]. It was further demonstrated that TMPyP4 inhibited telomerase activity in a cell-free system [92]. TMPyP4 inhibits proliferation of various tumor cells including human pancreatic, breast, and prostate carcinomas. Furthermore, TMPyP4 can

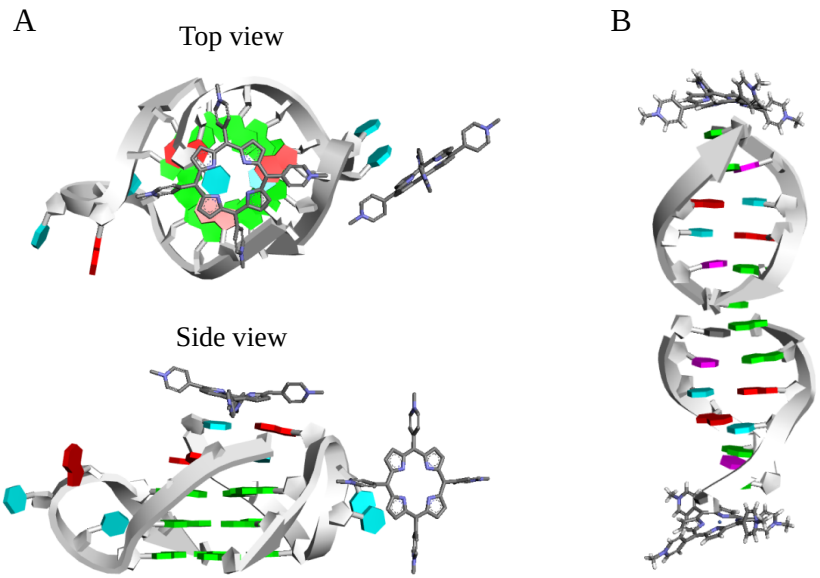

Fig. 2-12. Structural analysis of binding TMPyP4 with parallel G-quadruplex formed by human telomeric DNA (A) and dsDNA (B).

downregulate the expression of oncogenes like *C-MYC*, *VEGF*, and *K-RAS* [74-76, 78, 80, 82, 89, 99, 100]. Similarly, it has been shown that other cationic G-quadruplex-ligands such as BRACO-19 [101], 12459 [102], and PIPER [103] also inhibit the telomerase activity by binding the telomeric G-quadruplex. However, TMPyP4 inhibits growth of not only cancer cells but also normal cells [104]. This non-specific antiproliferative capacity of TMPyP4 is attributable to non-specific binding of TMPyP4 with dsDNA (Fig. 2-12B) [105-108]. TMPyP4 can bind to dsDNA non-specifically because the cationic functional groups interact with anionic phosphate groups of dsDNA electrostatically. Thus, many cationic ligands including TMPyP4 should bind to dsDNA region of chromosomal DNA even in normal cells, which may lead to antiproliferative effect on normal cells. In addition, most of cationic G-quadruplex-ligands with highly efficient telomerase inhibition *in vitro* showed low anticancer effects in cellular assays [18-20]. This reduced effect may be because living cells contain various macromolecules, of which concentrations reach 400 g/L [109-111], although diluted solutions are usually used for test tube experiments. Such high-concentrated biomolecules in cells, which is known as molecular crowding (MC) [109-111], have an impact on various reactions involving biomolecules by affecting several aspects to a solution in cells, such as a decrease in dielectric constant [110] and water activity [59, 64, 112, 113], and an increase in viscosity [114] and excluded

Table. 2-2. The number of water molecules (Δn_w) released upon the binding of ligand to dsDNA

DNA sequence	DNA structure	Ligand	Cosolute	Δn_w	Reference
Calf thymus DNA	dsDNA	Ethidium	Sucrose (Triethylene glycol, Betaine)	-0.25	116, 117
		Propidium	Sucrose (Triethylene glycol, Betaine)	-6.4	
		Proflavine	Sucrose (Triethylene glycol, Betaine)	-30	
		Daunomycin	Sucrose (Triethylene glycol, Betaine)	-18	
		7-aminoactionomycin D	Sucrose (Triethylene glycol, Betaine)	-32	
d(CGCGCAATTGCGCG)$_2$	dsDNA	Hoechst 33258	Triethylene glycol	-78	118
			Acetamide	-51	
			Betaine	-51	
			Tetraethylene glycol	-67	
d(CGCGCAATTGCGCG)$_2$	dsDNA	DAPI	Triethylene glycol (Actamide, Betaine, Trimethylamine N-oxide)	-35	119
		Netropsin	Triethylene glycol (Actamide, Betaine, Trimethylamine N-oxide)	-26	
		Pentamidine	Triethylene glycol (Actamide, Betaine, Trimethylamine N-oxide)	-34	
Calf thymus DNA	dsDNA	Daumocycin	Sucrose (Triethylene glycol, Betaine)	-17.8	120
		Adriamycin	Sucrose (Triethylene glycol, Betaine)	-35.8	
Calf thymus DNA	dsDNA	Hoechst 33258	Triethylene glycol	-74	121
			Sucrose	-30	
d(GGGTTA)$_3$GGG	G-quadruplex	TMPyP4	Glycerol	-30	122

volume [115]. Previous studies on interaction between dsDNA and its cationic ligands showed that almost all of the ligands acquire a significant number of water molecules upon binding to dsDNA (Table 2-2) [116-121]. Under a condition of decreased water activity caused by MC, uptake of water molecules is unfavorable and thus the affinity of the ligands with dsDNA are drastically reduced. More importantly, it was recently reported that cationic G-quadruplex-ligands including TMPyP4, BMVC, and Hoechst 33258 reduced their binding affinity to the telomeric G-quadruplex and the subsequent telomerase inhibitory effect under MC conditions due to uptake of water molecules upon binding to the G-quadruplex [122].

2.5. Telomeric Repeat Amplification Protcol (TRAP) Assay

In most human tumor cells, telomerase is highly-activated and plays a key role of the immortal cell proliferation, although the activity has not been detected in various

normal somatic cells [22, 31]. Thus, telomerase has been suggested as a promising marker for cancer diagnosis. Several studies showed the association between telomerase activity and a number of prognostic and clinopathological features in colorectal cancer [123-129]. For the diagnosis with the telomerase activity as a marker, the assay for the telomerase activity, which is precise and sensitive, is required.

A conventional procedure for telomerase activity assay is TRAP assay (Fig. 2-13) [22]. In the assay, a telomerase reaction is carried out using biological samples such as

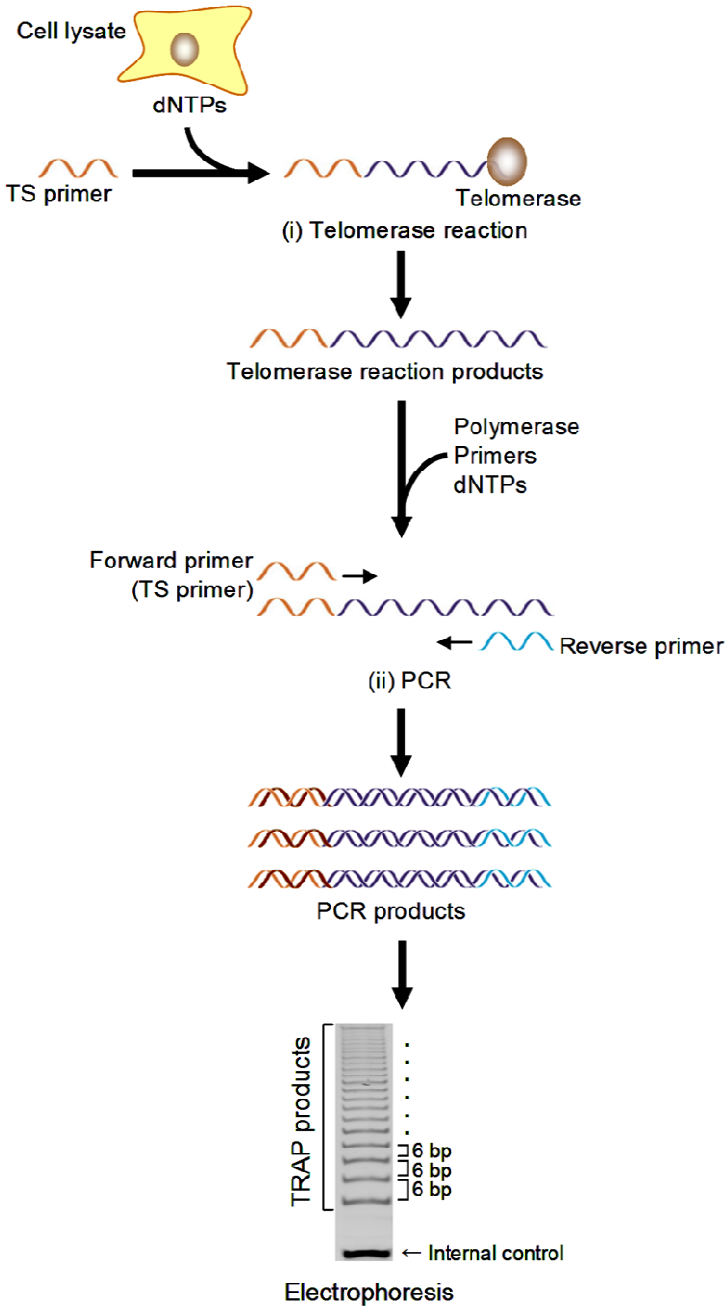

Fig. 2-13. TRAP assay.

cell lysate including telomerase, and a telomerase substrate primer. Following the telomerase reaction, the reaction products are amplified by PCR using the telomerase substrate primer as a forward primer. Finally, the amplification products are analyzed electrophoretically. Because telomerase adds six nucleotides with every extension reaction, a ladder of PCR products with six base pair (bp) increments is observed. Given simply a principle of TRAP assay, the telomerase substrate primer and a reverse primer in PCR should be a telomeric repetitive oligonucleotide and its complementary oligonucleotide, respectively. However, such primers generate primer dimers with different length because of their repetitive complementary sequences (Fig. 2-14). The primer dimers further bind to the primers, leading to longer primer artifacts with six bp increments. To avoid the false positive result, TS (telomerase substrate) primer, which is a non-telomeric oligonucleotide, is used as the telomerase substrate primer (Table 2-3) [22]. In addition, several reverse primers, which have uncomplementary sequences with the telomeric sequence, have been designed (Table 2-3) [22, 130-132]. These improvements drastically reduce the false positive result. However, TRAP assay still has a severe problem that some polymerase inhibitors in clinical samples inhibit PCR, which leads to the false negative results [131]. Thus, a novel telomerase assay that can avoid the false negative results has been required for practical cancer diagnostics.

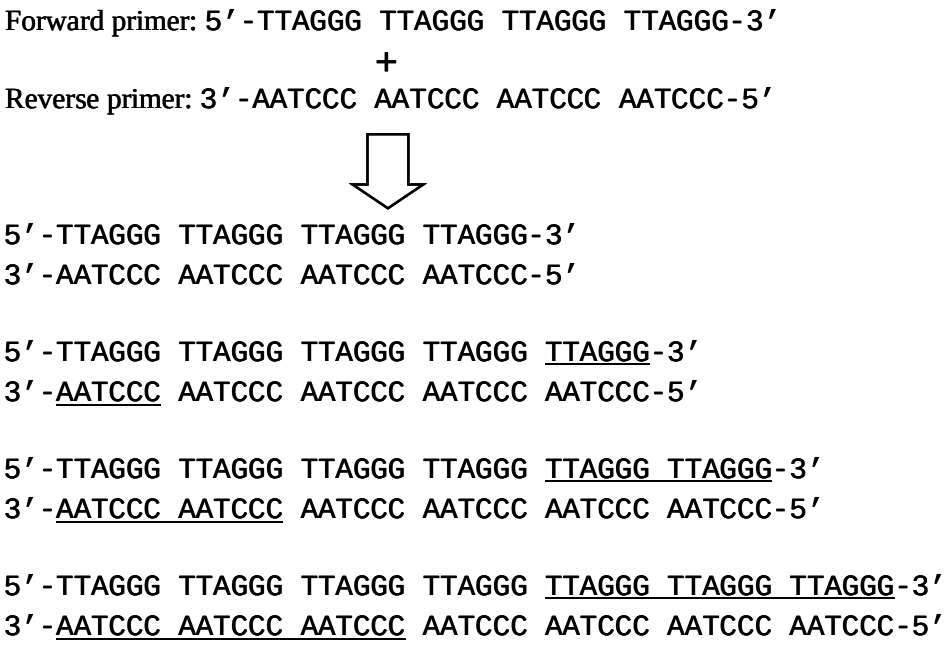

Fig. 2-14. Example of primer dimmers with different length caused by the telomeric repetitive forward primer and its complementary reverse primer. Underlined sequences are elongated products *via* PCR.

Table 2-3. Primers used in TRAP assay.

Name	Function	Sequence [a]	Ref.
TS	Telomerase substrate primer and forward primer	5'-AATCCGTCGAGCAGAGTT-3'	[22]
CX	Reverse primer	5'-CCCTTACCCTTACCCTTACCCTAA-3'	[22]
CX-ext	Reverse primer	5'-GTGCCCTTACCCTTACCCTTACCCTAA-3'	[130]
ACX	Reverse primer	5'-GCGCGGCTTACCCTTACCCTTACCCTAACC-3'	[131]
ACT	Reverse primer	5'-GCGCGGCTAACCCTAACCCTAACC-3'	[131]
Cxa	Reverse primer	5'-GTGTAACCCTAACCCTAACCC-3'	[132]

[a] Underlined sequences of reverse primers are uncomplimentary with telomeric repetitive sequences.

2.6. Purposes in This Study

2.6.1. Elucidation of Rules to Design Anticancer Drugs with Efficient Telomerase Inhibitory Effect (Main Papers 1 and 2)

G-quadruplex-ligands should be promising as the anticancer drug candidate without side effects. However, most of cationic G-quadruplex-ligands did not show the desired anticancer effects in cellular assays despite of their highly efficient telomerase inhibition *in vitro*. Importantly, previous studies on the conventional G-quadruplex-ligands imply that cationic functional groups may prevent G-qaudruplex ligands from binding to the human telomeric G-quadruplex in cell nuclei because of non-specific interaction with dsDNA and uptake of water molecules upon binding, which is unfavorable under the condition of decreased water activity. Therefore, an alternative strategy to improve the binding efficiency to the G-quadruplex in cell nuclei is required. A possible solution is to make the ligand non-ionic or anionic. In fact, a non-ionic ligand, telomestatin [104], can bind to the G-quadruplex with remarkable selectivity, whereas non-ionic ligands have problems such as low water solubility and difficulty of chemical synthesis. On the other hand, few anionic molecules have been investigated for the binding abilities to the G-quadruplex and the telomerase inhibitory effects. Thus, in this thesis, in order to acquire the strategy to design G-quadruplex-ligands that exert the desired effect even in cell nuclei, various cationic and anionic G-quadruplex-ligands were systematically examined under cell nuclei-mimicking conditions, in which excess dsDNA and MC cosolutes exist.

2.6.2. Development of an Assay for Telomerase Activity without False Negative Results (Main Paper 3)

Telomerase activity is an ideal target for cancer diagnosis, because it is specifically

activated in tumor cells. Thus, TRAP assay can be a critical technique for accurate cancer diagnosis. However, TRAP assay is not used for practical cancer diagnostics, because it should cause the false negative results. Thus, some research groups have developed other telomerase assays based on various sensors or methodologies, such as optical fiber [133], magnetic resonance reader [134], magneto-mechanical detector [135], ISFET (ion-sensitive field-effect transmitter) [136], electrochemical method [137], photonic microring device [138], and surface plasmon resonance method [136, 139] , but in general such assays do not utilize any signal amplification processes like PCR and were therefore less sensitive than TRAP assays. Other groups proposed telomerase assays with novel signal amplification processes involving enzymes [140-143], DNAzymes [144-146], and nanoparticles [147-150] instead of PCR. Although some of these assays with novel amplification reactions detected telomerase activity with high sensitivity [140, 143], the enzymes used for catalysis-based amplification may also be inhibited by components in clinical samples. Then, in this thesis, a novel telomerase assay that can absolutely avoid the false negative results was attempted to be developed toward cancer diagnosis without wrong diagnosis.

2.7. References

1. Yaku, H.; Yukimasa, T.; Nakano, S. I.; Sugimoto, N.; Oka, H., Design of Allele-Specific Primers and Detection of the Human ABO Genotyping to Avoid the Pseudopositive Problem. *Electrophoresis* **2008**, 29, 4130-4140.
2. Majeed, B.; Jones, B.; Tezcan, D. S.; Tutunjyan, N.; Haspeslagh, L.; Peeters, S.; Fiorini, P.; Op de Beeck, M.; Van Hoof, C.; Hiraoka, M.; Tanaka, H.; Yamashita, I., Silicon Based System for Single-Nucleotide-Polymorphism Detection: Chip Fabrication and Thermal Characterization of Polymerase Chain Reaction Microchamber. *Jpn. J. Appl. Phys.* **2012**, 51, 04DL01-04DL01-9.
3. Tanaka, H.; Fiorini, P.; Peeters, S.; Majeed, B.; Sterken, T.; Op de Beeck, M.; Hayashi, M.; Yaku, H.; Yamashita, I., Sub-Micro-Liter Electrochemical Single-Nucleotide-Polymorphism Detector for Lab-on-a-Chip System. *Jpn. J. Appl. Phys.* **2012**, 51, 04DL02-1-04DL02-6.
4. Szostak, J. W.; Blackburn, E. H., Cloning Yeast Telomeres on Linear Plasmid Vectors. *Cell* **1982**, 29, 245-255.
5. Moyzis, R. K.; Buckingham, J. M.; Cram, L. S.; Dani, M.; Deaven, L. L.; Jones, M. D.; Meyne, J.; Ratliff, R. L.; Wu, J. R., A Highly Conserved Repetitive DNA-Sequence, (TTAGGG)n, Present at the Telomeres of Human-Chromosomes. *Proc. Natl. Acad. Sci. USA* **1988**, 85, 6622-6626.

6. Palm, W.; de Lange, T., How Shelterin Protects Mammalian Telomeres. *Annu. Rev. Genet.* **2008**, 42, 301-334.
7. Nandakurnar, J.; Cech, T. R., Finding the End: Recruitment of Telomerase to Telomeres. *Nat. Rev. Mol. Cell. Bio.* **2013**, 14, 69-82.
8. Wellinger, R. J.; Wolf, A. J.; Zakian, V. A., Saccharomyces Telomeres Acquire Single-strand TG(1-3) Tails Late in S-Phase. *Cell* **1993**, 72, 51-60.
9. Makarov, V. L.; Hirose, Y.; Langmore, J. P., Long G Tails at Both Ends of Human Chromosomes Suggest a C Strand Degradation Mechanism for Telomere Shortening. *Cell* **1997**, 88, 657-666.
10. McElligott, R.; Wellinger, R. J., The Terminal DNA Structure of Mammalian Chromosomes. *EMBO J.* **1997**, 16, 3705-3714.
11. Wright, W. E.; Tesmer, V. M.; Huffman, K. E.; Levene, S. D.; Shay, J. W., Normal Human Chromosomes Have Long G-Rich Telomeric Overhangs at One End. *Gene. Dev.* **1997**, 11, 2801-2809.
12. Henderson, E. R.; Blackburn, E. H., An Overhanging 3' Terminus is a Conserved Feature of Telomeres. *Mol. Cell. Biol.* **1989**, 9, 345-348.
13. de Lange, T., T-Loops and the Origin of Telomeres. *Nat. Rev. Mol. Cell Bio.* **2004**, 5, 323-329.
14. de Lange, T., Shelterin: the Protein Complex that Shapes and Safeguards Human Telomeres. *Gene. Dev.* **2005**, 19, 2100-2110.
15. Griffith, J. D.; Comeau, L.; Rosenfield, S.; Stansel, R. M.; Bianchi, A.; Moss, H.; de Lange, T., Mammalian Telomeres End in a Large Duplex Loop. *Cell* **1999**, 97, 503-514.
16. Verdun, R. E.; Karlseder, J., Replication and Protection of Telomeres. *Nature* **2007**, 447, 924-931.
17. Harley, C. B.; Futcher, A. B.; Greider, C. W., Telomeres Shorten During Ageing of Human Fibroblasts. *Nature* **1990**, 345, 458-60.
18. Wright, W. E.; Piatyszek, M. A.; Rainey, W. E.; Byrd, W.; Shay, J. W., Telomerase Activity in Human Germline and Embryonic Tissues and Cells. *Dev. Genet.* **1996**, 18, 173-179.
19. Greider, C. W.; Blackburn, E. H., Identification of a Specific Telomere Terminal Transferase-Activity in Tetrahymena Extracts. *Cell* **1985**, 43, 405-413.
20. Greider, C. W.; Blackburn, E. H., A Telomeric Sequence in the RNA of Tetrahymena Telomerase Required for Telomere Repeat Synthesis. *Nature* **1989**, 337, 331-337.
21. Morin, G. B., The Human Telomere Terminal Transferase Enzyme Is a

Ribonucleoprotein That Synthesizes TTAGGG Repeats. *Cell* **1989**, 59, 521-529.

22. Kim, N. W.; Piatyszek, M. A.; Prowse, K. R.; Harley, C. B.; West, M. D.; Ho, P. L. C.; Coviello, G. M.; Wright, W. E.; Weinrich, S. L.; Shay, J. W., Specific Association of Human Telomerase Activity with Immortal Cells and Cancer TTAGGG Repeats. *Science* **1994**, 266, 2011-2015.
23. Counter, C. M.; Meyerson, M.; Eaton, E. N.; Weinberg, R. A., The Catalytic Subunit of Yeast Telomerase. *Proc. Natl. Acad. Sci. USA***1997**, 94, 9202-9207.
24. Lingner, J.; Hughes, T. R.; Shevchenko, A.; Mann, M.; Lundblad, V.; Cech, T. R., Reverse Transcriptase Motifs in the Catalytic Subunit of Telomerase. *Science* **1997**, 276, 561-567.
25. Chen, J. L.; Greider, C. W., An Emerging Consensus for Telomerase RNA Structure. *Proc. Natl. Acad. Sci. USA***2004**, 101, 14683-14684.
26. Ly, H.; Blackburn, E. H.; Parslow, T. G., Comprehensive Structure-Function Analysis of the Core Domain of Human Telomerase RNA. *Mol. Cell. Biol.* **2003**, 23, 6849-6856.
27. Gillis, A. J.; Schuller, A. P.; Skordalakes, E., Structure of the *Tribolium castaneum* Telomerase Catalytic Subunit TERT. *Nature* **2008**, 455, 633-637.
28. Mitchell, M.; Gillis, A.; Futahashi, M.; Fujisawa, H.; Skordalakes, E., Structural Basis for Telomerase Catalytic Subunit TERT Binding to RNA Template and Telomeric DNA. *Nat. Struct. Mol. Biol.* **2010**, 17, 513-518.
29. Jiang, J. S.; Miracco, E. J.; Hong, K.; Eckert, B.; Chan, H.; Cash, D. D.; Min, B. S.; Zhou, Z. H.; Collins, K.; Feigon, J., The Architecture of *Tetrahymena* Telomerase Holoenzyme. *Nature* **2013**, 496, 187-192.
30. White, L. K.; Wright, W. E.; Shay, J. W., Telomerase Inhibitors. *Trends Biotechnol.* **2001**, 19, 114-120.
31. Masutomi, K.; Yu, E. Y.; Khurts, S.; Ben-Porath, I.; Currier, J. L.; Metz, G. B.; Brooks, M. W.; Kaneko, S.; Murakami, S.; DeCaprio, J. A.; Weinberg, R. A.; Stewart, S. A.; Hahn, W. C., Telomerase Maintains Telomere Structure in Normal Human Cells. *Cell* **2003**, 114, 241-253.
32. Sundquist, W. I.; Klug, A., Telomeric DNA Dimerizes by Formation of Guanine Tetrads between Hairpin Loops. *Nature* **1989**, 342, 825-829.
33. Williamson, J. R.; Raghuraman, M. K.; Cech, T. R., Mono-Valent Cation Induced Structure of Telomeric DNA - the G-quartet Model. *Cell* **1989**, 59, 871-880.
34. Gellert, M.; Lipsett, M. N.; Davies, D. R., Helix Formation by Guanylic Acid. *Proc. Natl. Acad. Sci. USA* **1962**, 48, 2013-2018.

35. Henderson, E.; Hardin, C. C.; Walk, S. K.; Tinoco, I.; Blackburn, E. H., Telomeric DNA Oligonucleotides Form Novel Intramolecular Structures Containing Guanine Guanine Base-Pairs. *Cell* **1987**, 51, 899-908.
36. Williamson, J. R., Guanine Quartets. *Curr. Opin. Struc. Biol.* **1993**, 3, 357-362.
37. Williamson, J. R., G-Quartet Structures in Telomeric DNA. *Annu. Rev. Bioph. Biom.***1994**, 23, 703-730.
38. Gilbert, D. E.; Feigon, J., Multistranded DNA Structures. *Curr. Opin. Struc. Biol.* **1999**, 9, 305-314.
39. Simonsson, T., G-Quadruplex DNA Structures - Variations on a Theme. *Biol. Chem.* **2001**, 382, 621-628.
40. Arthanari, H.; Bolton, P. H., Functional and Dysfunctional Roles of Quadruplex DNA in Cells. *Chem. Biol.* **2001**, 8, 221-230.
41. Davis, J. T., G-Quartets 40 Years Later: from 5 ‘-GMP to Molecular Biology and Supramolecular Chemistry. *Angew. Chem., Int. Ed.* **2004**, 43, 668-698.
42. Burge, S.; Parkinson, G. N.; Hazel, P.; Todd, A. K.; Neidle, S., Quadruplex DNA: Sequence, Topology and Structure. *Nucleic Acids Res.* **2006**, 34, 5402-5415.
43. Patel, D. J.; Phan, A. T.; Kuryavyi, V., Human Telomere, Oncogenic Promoter and 5’-UTR G-quadruplexes: Diverse Higher Order DNA and RNA Targets for Cancer Therapeutics. *Nucleic Acids Res.* **2007**, 35, 7429-7455.
44. Lipps, H. J.; Rhodes, D., G-Quadruplex Structures: *in Vivo* Evidence and Function. *Trends Cell Biol.* **2009**, 19, 414-422.
45. Wu, Y. L.; Brosh, R. M., G-Quadruplex Nucleic Acids and Human Disease. *FEBS J.* **2010**, 277, 3470-3488.
46. Wang, Y.; Patel, D. J., Solution Structure of the Human Telomeric Repeat d[$AG_3(T_2AG_3)_3$] G-Tetraplex. *Structure* **1993**, 1, 263-282.
47. Wang, Y.; Patel, D. J., Solution Structure of a Parallel-Stranded G-Quadruplex DNA. *J. Mol. Biol.* **1993**, 234, 1171-1183.
48. Schultze, P.; Macaya, R. F.; Feigon, J., 3-dimensional Solution Structure of the Thrombin-Binding DNA Aptamer d(GGTTGGTGTGGTTGG). *J. Mol. Biol.* **1994**, 235, 1532-1547.
49. Kettani, A.; Basu, G.; Gorin, A.; Majumdar, A.; Skripkin, E.; Patel, D. J., A Two-Stranded Template-Based Approach to G·(C-A) Triad Formation: Designing Novel Structural Elements into an Existing DNA Framework. *J. Mol. Biol.* **2000**, 301, 129-146.
50. Parkinson, G. N.; Lee, M. P. H.; Neidle, S., Crystal Structure of Parallel

Quadruplexes from Human Telomeric DNA. *Nature* **2002**, 417, 876-880.

51. Miyoshi, D.; Nakao, A.; Sugimoto, N., Molecular Crowding Regulates the Structural Switch of the DNA G-Quadruplex. *Biochemistry* **2002**, 41, 15017-15024.
52. Miyoshi, D.; Nakao, A.; Sugimoto, N., Structural Transition from Antiparallel to Parallel G-Quadruplex of d($G_4T_4G_4$) Induced by Ca^{2+}. *Nucleic Acids Res.* **2003**, 31, 1156-1163.
53. Phan, A. T.; Modi, Y. S.; Patel, D. J., Propeller-Type Parallel-Stranded G-Quadruplexes in the Human *c-myc* Promoter. *J. Am. Chem. Soc.* **2004**, 126, 8710-8716.
54. Zhang, N.; Phan, A. T.; Patel, D. J., (3+1) Assembly of Three Human Telomeric Repeats into an Asymmetric Dimeric G-Quadruplex. *J. Am. Chem. Soc.* **2005**, 127, 17277-17285.
55. Miyoshi, D.; Karimata, H.; Sugimoto, N., Drastic Effect of a Single Base Difference between Human and *Tetrahymena* Telomere Sequences on Their Structures under Molecular Crowding Conditions. *Angew. Chem., Int. Ed.* **2005**, 44, 3740-3744.
56. Luu, K. N.; Phan, A. T.; Kuryavyi, V.; Lacroix, L.; Patel, D. J., Structure of the Human Telomere in K^+ Solution: an Intramolecular (3+1) G-Quadruplex Scaffold. *J. Am. Chem. Soc.* **2006**, 128, 9963-9970.
57. Xu, Y.; Noguchi, Y.; Sugiyama, H., The New Models of the Human Telomere d[AGGG($TTAGGG)_3$] in K^+ Solution. *Bioorgan. Med. Chem.* **2006**, 14, 5584-5591.
58. Ambrus, A.; Chen, D.; Dai, J. X.; Bialis, T.; Jones, R. A.; Yang, D. Z., Human Telomeric Sequence Forms a Hybrid-Type Intramolecular G-Quadruplex Structure with Mixed Parallel/Antiparallel Strands in Potassium Solution. *Nucleic Acids Res.* **2006**, 34, 2723-2735.
59. Miyoshi, D.; Karimata, H.; Sugimoto, N., Hydration Regulates Thermodynamics of G-Quadruplex Formation under Molecular Crowding Conditions. *J. Am. Chem. Soc.* **2006**, 128, 7957-7963.
60. Dai, J. X.; Carver, M.; Punchihewa, C.; Jones, R. A.; Yang, D. Z., Structure of the Hybrid-2 Type Intramolecular Human Telomeric G-Quadruplex in K^+ Solution: Insights into Structure Polymorphism of the Human Telomeric Sequence. *Nucleic Acids Res.* **2007**, 35, 4927-4940.
61. Miyoshi, D.; Sugimoto, N., Molecular Crowding Effects on Structure and Stability of DNA. *Biochimie* **2008**, 90, 1040-1051.

62. Lim, K. W.; Amrane, S.; Bouaziz, S.; Xu, W. X.; Mu, Y. G.; Patel, D. J.; Luu, K. N.; Phan, A. T., Structure of the Human Telomere in K^+ Solution: a Stable Basket-Type G-Quadruplex with Only Two G-Tetrad Layers. *J. Am. Chem. Soc.* **2009**, 131, 4301-4309.
63. Martadinata, H.; Phan, A. T., Structure of Propeller-Type Parallel-Stranded RNA G-Quadruplexes, Formed by Human Telomeric RNA Sequences in K^+ Solution. *J. Am. Chem. Soc.* **2009**, 131, 2570-2578.
64. Miyoshi, D.; Nakamura, K.; Tateishi-Karimata, H.; Ohmichi, T.; Sugimoto, N., Hydration of Watson-Crick Base Pairs and Dehydration of Hoogsteen Base Pairs Inducing Structural Polymorphism under Molecular Crowding Conditions. *J. Am. Chem. Soc.* **2009**, 131, 3522-3531.
65. Zhang, D. H.; Fujimoto, T.; Saxena, S.; Yu, H. Q.; Miyoshi, D.; Sugimoto, N., Monomorphic RNA G-Quadruplex and Polymorphic DNA G-Quadruplex Structures Responding to Cellular Environmental Factors. *Biochemistry* **2010**, 49, 4554-4563.
66. Pramanik, S.; Nakamura, K.; Usui, K.; Nakano, S.; Saxena, S.; Matsui, J.; Miyoshi, D.; Sugimoto, N., Thermodynamic Stability of Hoogsteen and Watson-Crick Base Pairs in the Presence of Histone H3-Mimicking Peptide. *Chem. Commun.* **2011**, 47, 2790-2792.
67. Zahler, A. M.; Williamson, J. R.; Cech, T. R.; Prescott, D. M., Inhibition of Telomerase by G-Quartet DNA Structures. *Nature* **1991**, 350, 718-720.
68. Huppert, J. L.; Balasubramanian, S., Prevalence of Quadruplexes in the Human Genome. *Nucleic Acids Res.* **2005**, 33, 2908-2916.
69. Todd, A. K.; Johnston, M.; Neidle, S., Highly Prevalent Putative Quadruplex Sequence Motifs in Human DNA. *Nucleic Acids Res.* **2005**, 33, 2901-2907.
70. Grand, C. L.; Han, H. Y.; Munoz, R. M.; Weitman, S.; Von Hoff, D. D.; Hurley, L. H.; Bearss, D. J., The Cationic Porphyrin TMPyP4 Down-Regulates c-*MYC* and Human Telomerase Reverse Transcriptase Expression and Inhibits Tumor Growth *in Vivo*. *Mol. Cancer Ther.* **2002**, 1, 565-573.
71. Seenisamy, J.; Bashyam, S.; Gokhale, V.; Vankayalapati, H.; Sun, D.; Siddiqui-Jain, A.; Streiner, N.; Shin-ya, K.; White, E.; Wilson, W. D.; Hurley, L. H., Design and Synthesis of an Expanded Porphyrin That Has Selectivity for the c-*MYC* G-Quadruplex Structure. *J. Am. Chem. Soc.* **2005**, 127, 2944-2959.
72. Alzeer, J.; Vummidi, B. R.; Roth, P. J. C.; Luedtke, N. W., Guanidinium-Modified Phthalocyanines as High-Affinity G-Quadruplex Fluorescent Probes and Transcriptional Regulators. *Angew. Chem., Int. Ed.* **2009**,

48, 9362-9365.

73. Alzeer, J.; Luedtke, N. W., pH-Mediated Fluorescence and G-quadruplex Binding of Amido Phthalocyanines. *Biochemistry* **2010**, 49, 4339-4348.
74. Siddiqui-Jain, A.; Grand, C. L.; Bearss, D. J.; Hurley, L. H., Direct Evidence for a G-Quadruplex in a Promoter Region and Its Targeting with a Small Molecule to Repress c-*MYC* Transcription. *Proc. Natl. Acad. Sci. USA* **2002**, 99, 11593-11598.
75. Seenisamy, J.; Rezler, E. M.; Powell, T. J.; Tye, D.; Gokhale, V.; Joshi, C. S.; Siddiqui-Jain, A.; Hurley, L. H., The Dynamic Character of the G-Quadruplex Element in the c-*MYC* Promoter and Modification by TMPyP4. *J. Am. Chem. Soc.* **2004**, 126, 8702-8709.
76. Lemarteleur, T.; Gomez, D.; Paterski, R.; Mandine, E.; Mailliet, P.; Riou, J. F., Stabilization of the c-*Myc* Gene Promoter Quadruplex by Specific Ligands' Inhibitors of Telomerase. *Biochem. Biophys. Res. Commun.* **2004**, 323, 802-808.
77. De Armond, R.; Wood, S.; Sun, D. Y.; Hurley, L. H.; Ebbinghaus, S. W., Evidence for the Presence of a Guanine Quadruplex Forming Region within a Polypurine Tract of the Hypoxia Inducible Factor 1 Alpha Promoter. *Biochemistry* **2005**, 44, 16341-16350.
78. Sun, D. Y.; Guo, K. X.; Rusche, J. J.; Hurley, L. H., Facilitation of a Structural Transition in the Polypurine/Polypyrimidine Tract within the Proximal Promoter Region of the Human *VEGF* Gene by the Presence of Potassium and G-Quadruplex-Interactive Agents. *Nucleic Acids Res.* **2005**, 33, 6070-6080.
79. Rankin, S.; Reszka, A. P.; Huppert, J.; Zloh, M.; Parkinson, G. N.; Todd, A. K.; Ladame, S.; Balasubramanian, S.; Neidle, S., Putative DNA Quadruplex Formation within the Human *c-kit* Oncogene. *J. Am. Chem. Soc.* **2005**, 127, 10584-10589.
80. Phan, A. T.; Kuryavyi, V.; Gaw, H. Y.; Patel, D. J., Small-Molecule Interaction with a Five-Guanine-Tract G-Quadruplex Structure from the Human *MYC* Promoter. *Nat. Chem. Biol.* **2005**, 1, 167-173.
81. Ambrus, A.; Chen, D.; Dai, J. X.; Jones, R. A.; Yang, D. Z., Solution Structure of the Biologically Relevant G-Quadruplex Element in the Human c-*MYC* Promoter. Implications for G-Quadruplex Stabilization. *Biochemistry* **2005**, 44, 2048-2058.
82. Cogoi, S.; Xodo, L. E., G-Quadruplex Formation within the Promoter of the *KRAS* Proto-Oncogene and Its Effect on Transcription. *Nucleic Acids Res.* **2006**, 34, 2536-2549.

83. Dai, J. X.; Dexheimer, T. S.; Chen, D.; Carver, M.; Ambrus, A.; Jones, R. A.; Yang, D. Z., An Intramolecular G-Quadruplex Structure with Mixed Parallel/Antiparallel G-Strands Formed in the Human BCL-2 Promoter Region in Solution. *J. Am. Chem. Soc.* **2006**, 128, 1096-1098.
84. Huppert, J. L.; Balasubramanian, S., G-Quadruplexes in Promoters throughout the Human Genome. *Nucleic Acids Res.* **2007**, 35, 406-413.
85. Phan, A. T.; Kuryavyi, V.; Burge, S.; Neidle, S.; Patel, D. J., Structure of an Unprecedented G-Quadruplex Scaffold in the Human *c-kit* Promoter. *J. Am. Chem. Soc.* **2007**, 129, 4386-4392.
86. Bejugam, M.; Sewitz, S.; Shirude, P. S.; Rodriguez, R.; Shahid, R.; Balasubramanian, S., Trisubstituted Isoalloxazines as a New Class of G-Quadruplex Binding Ligands: Small Molecule Regulation of *c-kit* Oncogene Expression. *J. Am. Chem. Soc.* **2007**, 129, 12926-12927.
87. Palumbo, S. L.; Memmott, R. M.; Uribe, D. J.; Krotova-Khan, Y.; Hurley, L. H.; Ebbinghaus, S. W., A Novel G-Quadruplex-Forming GGA Repeat Region in the *c-myb* Promoter is a Critical Regulator of Promoter Activity. *Nucleic Acids Res.* **2008**, 36, 1755-1769.
88. Membrino, A.; Paramasivam, M.; Cogoi, S.; Alzeer, J.; Luedtke, N. W.; Xodo, L. E., Cellular Uptake and Binding of Guanidine-Modified Phthalocyanines to *KRAS*/*HRAS* G-Quadruplexes. *Chem. Commun.* **2010**, 46, 625-627.
89. Monchaud, D.; Teulade-Fichou, M. P., A Hitchhiker's Guide to G-Quadruplex Ligands. *Org. Biomol. Chem.* **2008**, 6, 627-636.
90. Ou, T. M.; Lu, Y. J.; Tan, J. H.; Huang, Z. S.; Wong, K. Y.; Gu, L. Q., G-Quadruplexes: Targets in Anticancer Drug Design. *ChemMedChem* **2008**, 3, 690-713.
91. Georgiades, S. N.; Abd Karim, N. H.; Suntharalingam, K.; Vilar, R., Interaction of Metal Complexes with G-Quadruplex DNA. *Angew. Chem., Int. Ed.* **2010**, 49, 4020-4034.
92. Wheelhouse, R. T.; Sun, D. K.; Han, H. Y.; Han, F. X. G.; Hurley, L. H., Cationic Porphyrins as Telomerase Inhibitors: the Interaction of Tetra-(N-methyl-4-pyridyl)porphine with Quadruplex DNA. *J. Am. Chem. Soc.* **1998**, 120, 3261-3262.
93. Mergny, J. L.; Helene, C., G-Quadruplex DNA: a Target for Drug Design. *Nat. Med.* **1998**, 4, 1366-1367.
94. Han, H. Y.; Hurley, L. H., G-Quadruplex DNA: a Potential Target for Anti-Cancer Drug Design. *Trends Pharmacol. Sci.* **2000**, 21, 136-142.

95. Neidle, S.; Parkinson, G., Telomere Maintenance as a Target for Anticancer Drug Discovery. *Nat. Rev. Drug Discov.* **2002**, 1, 383-393.
96. De Cian, A.; Lacroix, L.; Douarre, C.; Temime-Smaali, N.; Trentesaux, C.; Riou, J. F.; Mergny, J. L., Targeting Telomeres and Telomerase. *Biochimie* **2008**, 90, 131-155.
97. Neidle, S., Human Telomeric G-Quadruplex: the Current Status of Telomeric G-Quadruplexes as Therapeutic Targets in Human Cancer. *FEBS J.* **2010**, 277, 1118-1125.
98. Parkinson, G. N.; Ghosh, R.; Neidle, S., Structural Basis for Binding of Porphyrin to Human Telomeres. *Biochemistry* **2007**, 46, 2390-2397.
99. Tan, J. H.; Gu, L. Q.; Wu, J. Y., Design of Selective G-Quadruplex Ligands as Potential Anticancer Agents. *Mini-Rev. Med. Chem.* **2008**, 8, 1163-1178.
100. Neidle, S., The Structures of Quadruplex Nucleic Acids and Their Drug Complexes. *Curr. Opin. Struc. Biol.* **2009**, 19, 239-250.
101. Harrison, R. J.; Reszka, A. P.; Haider, S. M.; Romagnoli, B.; Morrell, J.; Read, M. A.; Gowan, S. M.; Incles, C. M.; Kelland, L. R.; Neidle, S., Evaluation of by Disubstituted Acridone Derivatives as Telomerase Inhibitors: the Importance of G-Quadruplex Binding. *Bioorg. Med. Chem. Lett.* **2004**, 14, 5845-5849.
102. Riou, J. F.; Guittat, L.; Mailliet, P.; Laoui, A.; Renou, E.; Petitgenet, O.; Megnin-Chanet, F.; Helene, C.; Mergny, J. L., Cell Senescence and Telomere Shortening Induced by a New Series of Specific G-Quadruplex DNA Ligands. *Proc. Natl. Acad. Sci. USA* **2002**, 99, 2672-2677.
103. Sissi, C.; Lucatello, L.; Krapcho, A. P.; Maloney, D. J.; Boxer, M. B.; Camarasa, M. V.; Pezzoni, G.; Menta, E.; Palumbo, M., Tri-, Tetra- and Heptacyclic Perylene Analogues as New Potential Antineoplastic Agents Based on DNA Telomerase Inhibition. *Bioorgan. Med. Chem.* **2007**, 15, 555-562.
104. Kim, M. Y.; Gleason-Guzman, M.; Izbicka, E.; Nishioka, D.; Hurley, L. H., The Different Biological Effects of Telomestatin and TMPyP4 Can Be Attributed to Their Selectivity for Interaction with Intramolecular or Intermolecular G-Quadruplex Structures. *Cancer Res.* **2003**, 63, 3247-3256.
105. Lipscomb, L. A.; Zhou, F. X.; Presnell, S. R.; Woo, R. J.; Peek, M. E.; Plaskon, R. R.; Williams, L. D., Structure of a DNA-Porphyrin Complex. *Biochemistry* **1996**, 35, 2818-2823.
106. Arthanari, H.; Basu, S.; Kawano, T. L.; Bolton, P. H., Fluorescent Dyes Specific for Quadruplex DNA. *Nucleic Acids Res.* **1998**, 26, 3724-3728.
107. Ren, J. S.; Chaires, J. B., Sequence and Structural Selectivity of Nucleic Acid

Binding Ligands. *Biochemistry* **1999**, 38, 16067-16075.

108. Bennett, M.; Krah, A.; Wien, F.; Garman, E.; McKenna, R.; Sanderson, M.; Neidle, S., A DNA-Porphyrin Minor-Groove Complex at Atomic Resolution: the Structural Consequences of Porphyrin Ruffling. *Proc. Natl. Acad. Sci. USA* **2000**, 97, 9476-9481.
109. Zimmerman, S. B.; Minton, A. P., Macromolecular Crowding - Biochemical, Biophysical, and Physiological Consequences. *Annu. Rev. Bioph. Biom.* **1993**, 22, 27-65.
110. Minton, A. P., The Influence of Macromolecular Crowding and Macromolecular Confinement on Biochemical Reactions in Physiological Media. *J. Biol. Chem.* **2001**, 276, 10577-10580.
111. Ellis, R. J.; Minton, A. P., Cell Biology - Join the Crowd. *Nature* **2003**, 425, 27-28.
112. Nakano, S.; Karimata, H.; Ohmichi, T.; Kawakami, J.; Sugimoto, N., The Effect of Molecular Crowding with Nucleotide Length and Cosolute Structure on DNA Duplex Stability. *J. Am. Chem. Soc.* **2004**, 126, 14330-14331.
113. Ninni, L.; Camargo, M. S.; Meirelles, A. J. A., Water Activity in Poly(ethylene glycol) Aqueous Solutions. *Thermochim. Acta* **1999**, 328, 169-176.
114. Kozer, N.; Kuttner, Y. Y.; Haran, G.; Schreiber, G., Protein-Protein Association in Polymer Solutions: from Dilute to Semidilute to Concentrated. *Biophys. J.* **2007**, 92, 2139-2149.
115. Minton, A. P. Molecular Crowding: Analysis of Effects of High Concentrations of Inert Cosolutes on Biochemical Equilibria and Rates in Terms of Volume Exclusion. *Method Enzymol.* **1998**, *295*, 127-149.
116. Qu, X. G.; Chaires, J. B., Contrasting Hydration Changes for Ethidium and Daunomycin Binding to DNA. *J. Am. Chem. Soc.* **1999**, 121, 2649-2650.
117. Qu, X. G.; Chaires, J. B., Hydration Changes for DNA Intercalation Reactions. *J. Am. Chem. Soc.* **2001**, 123, 1-7.
118. Kiser, J. R.; Monk, R. W.; Smalls, R. L.; Petty, J. T., Hydration Changes in the Association of Hoechst 33258 with DNA. *Biochemistry* **2005**, 44, 16988-16997.
119. Degtyareva, N. N.; Wallace, B. D.; Bryant, A. R.; Loo, K. M.; Petty, J. T., Hydration Changes Accompanying the Binding of Minor Groove Ligands with DNA. *Biophys. J.* **2007**, 92, 959-965.
120. Yu, H. J.; Ren, J. S.; Chaires, J. B.; Qu, X. G., Hydration of Drug-DNA Complexes: Greater Water Uptake for Adriamycin Compared to Daunomycin. *J. Med. Chem.* **2008**, 51, 5909-5911.

121. Anuradha; Alam, M. S.; Chaudhury, N. K., Osmolyte Changes the Binding Affinity and Mode of Interaction of Minor Groove Binder Hoechst 33258 with Calf Thymus DNA. *Chem. Pharm. Bull.* **2010**, 58, 1447-1454.
122. Chen, Z.; Zheng, K. W.; Hao, Y. H.; Tan, Z., Reduced or Diminished Stabilization of the Telomere G-Quadruplex and Inhibition of Telomerase by Small Chemical Ligands under Molecular Crowding Condition. *J. Am. Chem. Soc.* **2009**, 131, 10430-10438.
123. Vidaurreta, M.; Maestro, M.; Rafael, S.; Veganzones, S.; Sanz-Casla, M.; Cerdan, J.; Arroyo, M., Telomerase Activity in Colorectal Cancer, Prognostic Factor and Implications in the Microsatellite Instability Pathway. *World J. Gastroentero.* **2007**, 13, 3868-3872.
124. Uen, Y. H.; Lin, S. R.; Wu, D. C.; Su, Y. C.; Wu, J. Y.; Cheng, T. L.; Chi, C. W.; Wang, J. Y., Prognostic Significance of Multiple Molecular Markers for Patients with Stage II Colorectal Cancer Undergoing Curative Resection. *Ann. Surg.* **2007**, 246, 1040-1046.
125. Saleh, S.; Lam, A. K. Y.; Ho, Y. H., Real-Time PCR Quantification of Human Telomerase Reverse Transcriptase (hTERT) in Colorectal Cancer. *Pathology* **2008**, 40, 25-30.
126. Lam, A. K. Y.; Ong, K.; Ho, Y. H., Aurora Kinase Expression in Colorectal Adenocarcinoma: Correlations with Clinicopathological Features, p16 Expression, and Telomerase Activity. *Hum. Pathol.* **2008**, 39, 599-604.
127. Lam, A. K. Y.; Saleh, S.; Smith, R. A.; Ho, Y. H., Quantitative Analysis of Survivin in Colorectal Adenocarcinoma: Increased Expression and Correlation with Telomerase Activity. *Hum. Pathol.* **2008**, 39, 1229-1233.
128. Soreide, K.; Gudlaugsson, E.; Skaland, I.; Janssen, E. A. M.; Van Diermen, B.; Korner, H.; Baak, J. P. A., Metachronous Cancer Development in Patients with Sporadic Colorectal Adenomas - Multivariate Risk Model with Independent and Combined Value of hTERT and Survivin. *Int. J. Colorectal Dis.* **2008**, 23, 389-400.
129. Lam, A. K. Y.; Ong, K.; Ho, Y. H., hTERT Expression in Colorectal Adenocarcinoma: Correlations with p21, p53 Expressions and Clinicopathological Features. *Int. J. Colorectal Dis.* **2008**, 23, 587-594.
130. Krupp, G.; Kuhne, K.; Tamm, S.; Klapper, W.; Heidorn, K.; Rott, A.; Parwaresch, R., Molecular Basis of Artifacts in the Detection of Telomerase Activity and a Modified Primer for a More Robust 'TRAP' Assay. *Nucleic Acids Res.* **1997**, 25, 919-921.

131. Kim, N. W.; Wu, F., Advances in Quantification and Characterization of Telomerase Activity by the Telomeric Repeat Amplification Protocol (TRAP). *Nucleic Acids Res.* **1997**, 25, 2595-2597.
132. Falchetti, M. L.; Levi, A.; Molinari, P.; Verna, R.; D'Ambrosio, E., Increased Sensitivity and Reproducibility of TRAP Assay by Avoiding Direct Primers Interaction. *Nucleic Acids Res.* **1998**, 26, 862-863.
133. Schmidt, P. M.; Lehmann, C.; Matthes, E.; Bier, F. F., Detection of Activity of Telomerase in Tumor Cells Using Fiber Optical Biosensors. *Biosens. Bioelectron.* **2002**, 17, 1081-1087.
134. Grimm, J.; Perez, J. M.; Josephson, L.; Weissleder, R., Novel Nanosensors for Rapid Analysis of Telomerase Activity. *Cancer Res.* **2004**, 64, 639-643.
135. Weizmann, Y.; Patolsky, F.; Lioubashevski, O.; Willner, I., Magneto-Mechanical Detection of Nucleic Acids and Telomerase Activity in Cancer Cells. *J. Am. Chem. Soc.* **2004**, 126, 1073-1080.
136. Sharon, E.; Freeman, R.; Riskin, M.; Gil, N.; Tzfati, Y.; Willner, I., Optical, Electrical and Surface Plasmon Resonance Methods for Detecting Telomerase Activity. *Anal. Chem.* **2010**, 82, 8390-8397.
137. Sato, S.; Kondo, H.; Nojima, T.; Takenaka, S., Electrochemical Telomerase Assay with Ferrocenyl Naphthalene Diimide as a Tetraplex DNA-Specific Binder. *Anal. Chem.* **2005**, 77, 7304-7309.
138. Kim, K. W.; Shin, Y.; Perera, A. P.; Liu, Q.; Kee, J. S.; Han, K.; Yoon, Y.-J.; Park, M. K., Label-Free, PCR-Free Chip-Based Detection of Telomerase Activity in Bladder Cancer Cells. *Biosens. Bioelectron.* **2013**, 45, 152-157.
139. Maesawa, C.; Inaba, T.; Sato, H.; Iijima, S.; Ishida, K.; Terashima, M.; Sato, R.; Suzuki, M.; Yashima, A.; Ogasawara, S.; Oikawa, H.; Sato, N.; Saito, K.; Masuda, T., A Rapid Biosensor Chip Assay for Measuring of Telomerase Activity Using Surface Plasmon Resonance. *Nucleic Acids Res.* **2003**, 31, e4.
140. Xu, S. Q.; He, M.; Yu, H. P.; Wang, X. Y.; Tan, X. L.; Lu, B.; Sun, X.; Zhou, Y. K.; Yao, Q. F.; Xu, Y. J.; Zhang, Z. R., Bioluminescent Method for Detecting Telomerase Activity. *Clin. Chem.* **2002**, 48, 1016-1020.
141. Kha, H.; Zhou, W.; Chen, K.; Karan-Tamir, B.; Miguel, T. S.; Zeni, L.; Kearns, K.; Mladenovic, A.; Rasnow, B.; Robinson, M.; Wahl, R. C., A Telomerase Enzymatic Assay That Does Not Use Polymerase Chain Reaction, Radioactivity, or Electrophoresis. *Anal. Biochem.* **2004**, 331, 230-234.
142. Pavlov, V.; Willner, I.; Dishon, A.; Kotler, M., Amplified Detection of Telomerase Activity Using Electrochemical and Quartz Crystal Microbalance

Measurements. *Biosens. Bioelectron.* **2004**, 20, 1011-1021.

143. Ding, C. F.; Li, X. L.; Ge, Y.; Zhang, S. S., Fluorescence Detection of Telomerase Activity in Cancer Cells Based on Isothermal Circular Strand-Displacement Polymerization Reaction. *Anal. Chem.* **2010**, 82, 2850-2855.
144. Pavlov, V.; Xiao, Y.; Gill, R.; Dishon, A.; Kotler, M.; Willner, I., Amplified Chemiluminescence Surface Detection of DNA and Telomerase Activity Using Catalytic Nucleic Acid Labels. *Anal. Chem.* **2004**, 76, 2152-2156.
145. Yi, X.; Pavlov, V.; Gill, R.; Bourenko, T.; Willner, I., Lighting up Biochemiluminescence by the Surface Self-Assembly of DNA-Hemin Complexes. *Chembiochem* **2004**, 5, 374-379.
146. Xiao, Y.; Pavlov, V.; Niazov, T.; Dishon, A.; Kotler, M.; Willner, I., Catalytic Beacons for the Detection of DNA and Telomerase Activity. *J. Am. Chem. Soc.* **2004**, 126, 7430-7431.
147. Patolsky, F.; Gill, R.; Weizmann, Y.; Mokari, T.; Banin, U.; Willner, I., Lighting-up the Dynamics of Telomerization and DNA Replication by CdSe-ZnS Quantum Dots. *J. Am. Chem. Soc.* **2003**, 125, 13918-13919.
148. Zheng, G. F.; Daniel, W. L.; Mirkin, C. A., A New Approach to Amplified Telomerase Detection with Polyvalent Oligonucleotide Nanoparticle Conjugates. *J. Am. Chem. Soc.* **2008**, 130, 9644-9645.
149. Zhou, X. M.; Xing, D.; Zhu, D. B.; Jia, L., Magnetic Bead and Nanoparticle Based Electrochemiluminescence Amplification Assay for Direct and Sensitive Measuring of Telomerase Activity. *Anal. Chem.* **2009**, 81, 255-261.
150. Li, Y.; Liu, B. W.; Li, X.; Wei, Q. L., Highly Sensitive Electrochemical Detection of Human Telomerase Activity Based on Bio-Barcode Method. *Biosens. Bioelectron.* **2010**, 25, 2543-2547.

3. Elucidation of Rules to Design Anticancer Drugs with Efficient Telomerase Inhibitory Effect

3.1. Introduction

Since G-quadruplex DNA inhibits telomerase activity by preventing telomerase binding to telomeric DNA [1], development of G-quadruplex-ligands has become an area of great interest [2-16]. Many G-quadruplex-ligands developed to date contain a π-planar structure, of which size is similar to that of G-quartet, and cationic functional groups in order to bind to G-quadruplex *via* π-π stacking interaction and electrostatic attractive interaction, respectively [11-13]. However, most of cationic G-quadruplex-ligands with highly efficient telomerase inhibition *in vitro* showed lower anticancer effects in cellular assays [17-19]. This divergence is at least partly due to differences between chemical conditions *in vitro* and *in vivo*. Living cells contain various macromolecules, of which concentrations reach 400 g/L [20-22], despite a diluted solution under test tube conditions. Existence of the excess macromolecules often leads to unexpected interactions between the drug and the off-target molecules and have an impact on several aspects to a solution in cells including a decrease in dielectric constant [21] and water activity [23-26], and an increase in viscosity [27] and excluded volume [28]. Thus, for the rational design of drugs including G-quadruplex-ligands, one should consider how intracellular factors influence their functions.

At least two intracellular environmental factors should inhibit the properties of cationic G-quadruplex-ligands. First, abundant dsDNA found in genome DNA should prevent cationic G-quadruplex-ligands from binding to the human telomeric G-quadruplex, because positive charges of the cationic ligands also mediate high-affinity and non-specific interactions with the dsDNA [29-32]. The diminished affinity to the telomeric G-quadruplex should lead to low efficiency for telomerase inhibition in cell nuclei. In addition, non-specific interactions of cationic G-quadruplex-ligands to the dsDNA in genome DNA probably cause severe toxicity to normal cells. Second, high-concentrated biomolecules in cells, which is known as MC [20-22], also affect the binding property of cationic G-quadruplex-ligands [33]. It was reported that MC reduced the binding affinity of cationic G-quadruplex-ligands including TMPyP4 and their telomerase inhibition [33]. This reduction is attributed to that water molecules are acquired upon cationic ligands binding to the G-quadruplex and the hydration reaction is unfavorable under a decreased water activity condition by MC [33]. Therefore, an alternative strategy to improve the telomerase inhibitory effect of G-quadruplex-ligands in cell nuclei is required. A possible solution is to make the

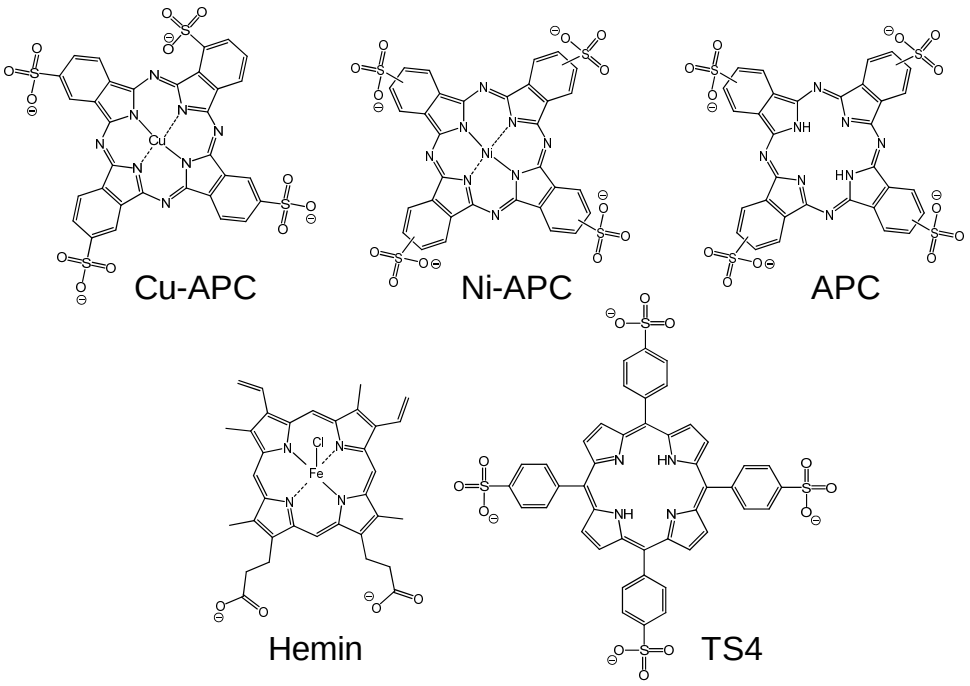

Fig. 3-1. Anionic G-quadruplex-ligand candidates used in this study.

ligand non-ionic or anionic. In fact, a non-ionic ligand, telomestatin, can bind the telomeric G-quadruplex with remarkable selectivity over dsDNA and inhibit proliferation of cancer cells efficiently but not normal cells [34]. However, telomestatin have less water solubility due to its non-ionic property. In addition, telomestatin is a natural compound and difficult to synthesize chemically. On the other hand, few anionic molecules have been investigated for the binding abilities to the G-quadruplex and the telomerase inhibitory effects.

Herein, in order to develop G-quadruplex-ligands that exert desired functions in cell nuclei, G-quadruplex-binding and telomerase-inhibiting capacity of eight G-quadruplex-ligands was systematically examined: three cationic, TMPyP4 (Fig. 2-11) [3-5, 10-14, 35], copper-coordinating TMPyP4 (Cu-TMPyP4; Fig. 2-11), and PIPER (Fig. 2-11) [36]; and five anionic, Cu-APC (Fig. 3-1), nickel(II) phthalocyanine tetrasulfonic acid, tetrasodium salt (Ni-APC; Fig. 3-1), phthalocyanine tetrasulfonate hydrate (APC; Fig. 3-1), Hemin (Fig. 3-1) [37], and 5,10,15,20-tetraphenyl-21*H*,23*H*-porphine-*p*,*p*′,*p*″,*p*‴-tetrasulfonic acid, tetrasodium hydrate (TS4; Fig. 3-1) [30]. Experimental conditions included excess decoy dsDNA or molecular crowding cosolutes.

3.2. Materials and Methods

3.2.1. Materials

High-performance liquid chromatography (HPLC) purification grade DNA oligonucleotides were purchased from Tsukuba Oligo Service Co., Ltd. (Ibaraki, Japan). Cu-APC, Ni-APC, APC, and TS4 were purchased from Sigma-Aldrich (St. Louis, MO, USA) and were used without further purification. TMPyP4, PIPER, and Hemin were purchased from Dojindo Laboratories (Kumamoto, Japan), Merck KGaA (Darmstadt, Germany), and Tokyo Chemical Industry Co., Ltd. (Tokyo, Japan), respectively, and were used without further purification. Cu-TMPyP4, a Cu^{2+} derivative of TMPyP4, was synthesized as follows. A 101.7 mg (0.15 mmol) sample of TMPyP4 was dissolved in 40 mL of freshly distilled water, and the solution was heated to reflux. 6.65 g (50 mmol) of $CuCl_2$ was added to the resulting solution, and the mixture was allowed to continue refluxing for 2 h with vigorously stirring. The reaction mixture was cooled below 4 °C, then the excess amount of sodium perchlorate was added to precipitate the Cu-TMPyP4. The resulting mixture was allowed to stand overnight below 0 °C. The precipitate was filtered and washed several times with dilute perchloric acid. Ethylene glycol (EG), poly ethylene glycol with an average molecular weight of 200 (PEG 200), and poly ethylene glycol with an average molecular weight of 8000 (PEG 8000) were purchased from Wako Pure Chemical Industries Ltd. (Osaka, Japan), and were used without further purification. To generate stock solutions for each ligand, Cu-APC, Ni-APC, APC, TTMAPP, TS4, TMPyP4, and Cu-TMPyP4 were dissolved in distilled water, and PIPER and Hemin were dissolved in 3% CH_3COOH and 10 mM NaOH, respectively.

3.2.2. Circular Dichroism (CD) Spectroscopy

CD experiment for 20 μM human telomeric oligo DNA, 5'-$(GGGTTA)_3GGG$-3' (Htelo-DNA) in a buffer containing 50 mM MES-LiOH (pH 7.0) and 100 mM KCl was carried out using a J-820 spectropolarimeter (JASCO Co., Ltd., Hachioji, Japan) with a 0.1-cm path-length quartz cell at 25°C. The CD spectrum was obtained by taking the average of three scans made at 0.5-nm intervals from 200 to 350 nm. Before measurement, the DNA sample was heated at 80°C for 2 min, gently cooled at 2°C min^{-1}.

3.2.3. Binding Assay

Absorbance for ligands including TMPyP4 (1.0 μM), Cu-APC (2.5 μM), Ni-APC (2.5 μM), APC (2.5 μM), Cu-TMPyP4 (1.0 μM), PIPER (10 μM), Hemin (12.5 μM) or TTMAPP (1.0μM) with various concentrations of Htelo-DNA was recorded at 20°C or 25°C; a UV-1700 spectrophotometer (Shimadzu) connected to a Shimadzu TMSPC-8 thermoprogrammer (Shimadzu) was used with a 1.0-cm path-length quartz cell. The

measurements for these ligands were carried out in a buffer containing 50 mM MES-LiOH (pH 7.0) and 100 mM KCl in the absence or presence of 128 μg/ml λ DNA or cosolute (0–40 wt% EG, 0–40 wt% PEG 200 or 0–20 wt% PEG 8000). Exceptionally, the buffer further comprised CH_3COOH (0.25% or 1.5%) or NaOH (2 mM) for the measurements for PIPER or Hemin, respectively. Before measurement, each sample was heated to 80°C for 2 min and gently cooled to 25°C at 2°C min^{-1}.

3.2.4. Stoichiometric Titration Assay

Absorbance at 690 nm for Cu-APC (100 μM) with 0-500 μM Htelo-DNA was recorded at 25°C; a UV-1700 spectrophotometer (Shimadzu) connected to a Shimadzu TMSPC-8 thermoprogrammer (Shimadzu) was used with a 0.1-cm path-length quartz cell. The measurement was carried out in a buffer containing 50 mM MES-LiOH (pH 7.0), 100 mM KCl, and 10 mM $MgCl_2$. Before measurement, each sample was heated to 80°C for 2 min and gently cooled to 25°C at 2°C min^{-1}.

3.2.5. Evaluation of the Association Constant

The fractional degree (v) of saturation of each ligand-binding site to DNA can be expressed by the following equation based on the model that is based on the assumption of one binding site to estimate the equilibrium parameters [38]:

$$v = \left\{K_d + [\text{ligand}] + [\text{DNA}] - \sqrt{(K_d + [\text{ligand}] + [\text{DNA}])^2 - 4[\text{ligand}][\text{DNA}]}\right\} / 2[\text{ligand}] \quad (1)$$

where K_d is the dissociation constant, [DNA] is the concentration of DNA, and [ligand] is the concentration of the ligand. Equation (1) can be transformed into equation (2). The association constant (K_a) for each DNA for each ligand was determined with equation (2):

$$\theta = a\left\{K_a[\text{ligand}] + K_a[\text{DNA}] + 1 - \sqrt{(K_a[\text{ligand}] + K_a[\text{DNA}] + 1)^2 - 4K_a{}^2[\text{ligand}][\text{DNA}]}\right\} / 2K_a[\text{ligand}] + b \quad (2)$$

where θ is the absorbance value, K_a is the apparent association constant of DNA binding, a is a scale factor, and b is the initial θ value.

3.2.6. Determination of the Number of Water Molecules Released upon G-Quadruplex/Ligand Complex Formation

3.2.6.1. Theoretical Equation

Formation of a G-quadruplex/ligand complex in a solution containing a cosolute (e.g., PEG 200) and a cation (e.g., K^+) can be represented as follows:

$$\mathrm{G-quadruplex + Ligand} \rightleftarrows \mathrm{G-quadruplex/ligand} + \Delta n_{\mathrm{w}}\mathrm{H_2O} + \Delta n_{\mathrm{CS}}\mathrm{CS} + \Delta n_{\mathrm{M^+}}\mathrm{M^+} \quad (4)$$

where CS and M^+ represent a cosolute and cation, respectively. Δn_{w}, Δn_{cs}, and $\Delta n_{\mathrm{M+}}$ represent the numbers of water molecules, cosolute molecules, and cations, respectively, that are released upon the complex formation. The observed equilibrium constant (K_{a}) for the complex formation is:

$$K_0 = K_{\mathrm{a}} a_{\mathrm{w}}^{\ \Delta n_{\mathrm{w}}} a_{\mathrm{CS}}^{\ \Delta n_{\mathrm{CS}}} a_{\mathrm{M^+}}^{\ \Delta n_{\mathrm{M^+}}} \quad (5)$$

where K_0 is the true thermodynamic equilibrium constant, and a_{w}, a_{cs}, and $a_{\mathrm{M+}}$ are the activities of water, the cosolute, and the cation, respectively. At a constant temperature and pressure, the first derivatives of ln K_{a} by ln a_{w} are represented by the following equation [23-25].

$$\frac{\mathrm{d}\ln K_{\mathrm{a}}}{\mathrm{d}\ln a_{\mathrm{w}}} = -\left[\Delta n_{\mathrm{w}} + \Delta n_{\mathrm{cs}}\left(\frac{\mathrm{d}\ln a_{\mathrm{cs}}}{\mathrm{d}\ln a_{\mathrm{w}}}\right) + \Delta n_{\mathrm{M^+}}\left(\frac{\mathrm{d}\ln a_{\mathrm{M^+}}}{\mathrm{d}\ln a_{\mathrm{w}}}\right)\right] \quad (6)$$

3.2.6.2. Experimental Procedure

(i) The observed equilibrium constants for the formation of the G-quadruplex/ligand complexes were measured in the absence and presence of various amounts (10, 20, 30, and 40 wt%) of cosolute (e.g., PEG 200) at a constant cation concentration.

(ii) The water activity was determined using a vapor phase osmometer or a freezing point depression osmometer at room temperature under the assumption that cosolutes do not directly interact with DNA. Although the osmotic pressure values for most cosolutes can be measured using a vapor phase osmometer, the osmotic pressure of cosolutes (cosolvents) with boiling points less than 100°C should be obtained using a freezing point depression osmometer. In contrast, the freezing point depression osmometer is unsuitable for osmotic pressure measurements of high molecular weight cosolutes because solutions containing high molecular weight cosolutes sometimes do not freeze uniformly.

A model 5520XR pressure osmometer (Wescor Inc., Logan, UT, USA) and the osmotic stressing method were used to measure *via* the vapor phase the osmotic

pressure for EG, PEG 200, and PEG 8000.

(iii) In calculating the water activity from the osmotic pressure, it was assumed that the temperature dependence of the water activity was small between 25 and 80°C; this assumption has been confirmed experimentally. The logarithm of water activities (a_w) was calculated from the measured osmolality (mmol kg^{-1}) with the following equation:

$$\psi = (RT / M_w) \ln a_w \quad (7)$$

where Ψ is the water potential, M_w is the molecular weight of water (0.018 kg/mol), R is the gas constant (8.314 J mol^{-1} K^{-1}), and T is the temperature in Kelvin. The relationship between water potential (MPa) and osmolality (mmol kg^{-1}), in the cases where the water potential is independent of temperature, was calculated using the following equation:

$$\psi = \text{osmolality} / -400 \quad (8)$$

(iv) The values of ln K_a at 25°C at different cosolute concentrations were plotted on the y-axis and the values of ln a_w for each solution were plotted on the x-axis.

For example, the stability (ln K_a) of G-quadruplex/TMPyP4 complex decreased linearly with the decrease in ln a_w. Although the slope of the plot included two variable terms responsible for the cosolute and cation bindings, the linear plot (described by eq. 6) indicated that these variable terms were insignificant, and the slope approximately equaled the constant term $-\Delta n_w$. If the slope of the linear plot was positive, water molecules were taken up upon formation of the G-quadruplex/ligand complex; if the slope was negative, water molecules were released during complex formation.

3.2.7. Two-Step TRAP Assay

The two-step telomere repeat amplification protocol (tsTRAP) assay was improved on the basis of the manufacturer's protocol for the TRAPEZE telomerase detection kit manufactured by Millipore Corporation (Billerica, MA, USA) [39, 40]. In the tsTRAP assay, the telomerase reaction mixture containing G-quadruplex-ligand was first diluted and then used as a template for the PCR step described below. Thus, diluted G-quadruplex-ligand did not affect PCR efficiency. Each 10-μL telomerase reaction mixture contained telomerase, 1× TRAP reaction buffer, 1× dNTP mix, and 0.2 μL TS primer, and either lacked G-quadruplex-ligand or contained 2 μL of a defined

concentration of G-quadruplex-ligand. In the first step, each reaction was incubated at 30°C for 60 min; each mixture was then heated at 90°C for 10 min. In the second step, telomerase reaction products were amplified in a 10-μL PCR reaction mixture containing 50-fold diluted telomerase mixture, 0.2 μL TS primer, 0.2 μL TRAP primer mix, 1× dNTP mix, 1× LA Taq polymerase buffer, and LA Taq polymerase manufactured by Takara Bio Inc. (Shiga, Japan); the PCR was carried out over 30 cycles each comprising denaturation at 94°C for 30 s, annealing at 59°C for 30 s, and extension at 72°C for 30 s. The TRAP assay products were resolved by non-denaturing electrophoresis at 400 V through a 10% nondenaturing polyacrylamide gel in Tris-borate-EDTA buffer (pH 8.5). The gels were stained with GelStar nucleic acid gel stain manufactured by Cambrex Corporation (East Rutherford, NJ, USA), and imaged using FLS-5100 film manufactured by Fujifilm Corporation (Tokyo, Japan). Telomerase activity was measured according to the protocol provided with the TRAPEZE telomerase detection kit. For the negative control reactions, lysis buffer was added in the place of telomerase. For the positive control reactions, telomerase extract was added to a reaction solution that lacked any G-quadruplex-ligand. Relative activity (A) was calculated *via* the following equation:

$$A = \{(X - X_0)/C\}/\{(X_p - X_0)/C_p\} \quad (3)$$

where X is the signal intensity of the region of the gel lane corresponding to the TRAP product ladder bands and C is the signal intensity of the region of the gel lane corresponding to the internal control product. Subscripts "*p*" and "*0*" indicate the positive and negative controls, respectively.

3.3. Results

3.3.1. Excess dsDNA Effects on Functional Capacities of G-Quadruplex-Ligands

3.3.1.1. Effects of Excess dsDNA on Binding Capacities

Selectivity to G-quadruplex over dsDNA is essential for G-quadruplex-ligands, because a non-specific binding of G-quadruplex-ligands to a part of genomic DNA that forms dsDNA not only reduces their binding efficiency to G-quadruplex but also causes side effects. To study the selectivity of Cu-APC (Fig. 3-1), the binding affinity of Cu-APC was evaluated by UV-Vis titration with an annealed human telomeric oligo DNA, 5'-GGG(TTAGGG)$_3$-3' (Htelo-DNA); dsDNA, 5'-AGAAGAGAAAGA-3'/5'-TCTTTCTCTTCT-3' (DS-DNA); and ssDNA, 5'-T$_{21}$-3'

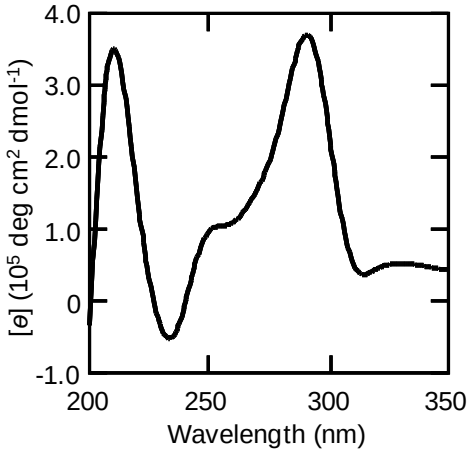

Fig. 3-2. CD spectrum of 20 μM Htelo-DNA in a buffer containing 50 mM MES-LiOH (pH 7.0) and 100 mM KCl at 25°C.

(SS-DNA) in a buffer containing 50 mM MES-LiOH (pH 7.0) and 100 mM KCl at 25°C. Under this condition, Htelo-DNA showed a CD spectrum with a positive peak and a negative peak at 295 nm and 240 nm, respectively. This result indicates that Htelo-DNA formed a (3+1) G-quadruplex (Fig. 3-2) [41-43]. A new peak around 690 nm in the Q band increased as a function of Htelo-DNA concentration (Fig. 3-3A), which indicates that Cu-APC bound to the G-quadruplex formed by Htelo-DNA. Furthermore, the stoichiometry was studied with higher concentrations of Cu-APC and Htelo-DNA (100 μM Cu-APC and 0-500 μM Htelo-DNA) in a buffer containing 50 mM MES-LiOH (pH 7.0), 100 mM KCl, and 10 mM $MgCl_2$. $MgCl_2$ was added into the buffer because Mg^{2+} reduces the electrostatic repulsion between Cu-APC and DNA, resulting in a higher affinity of Cu-APC with Htelo-DNA. A stoichiometric point around 100 μM Htelo-DNA was observed (Fig. 3-4), suggesting a 1:1 binding of Cu-APC and Htelo-DNA. Based on the assumption that the 1:1 binding stoichiometry does not depend on the experimental conditions, the absorbance at 690 nm was plotted against the concentration of Htelo-DNA (Fig. 3-3B) and the K_a value for Htelo-DNA was determined to be $(2.4 \pm 0.2) \times 10^4$ M^{-1} at 25°C (see 3.2.5. Evaluation of the association constant). Notably, in contrast to Htelo-DNA, the K_a values for DS-DNA and SS-DNA could not be determined because of the small change in the peak at 690 nm with addition of DS-DNA or SS-DNA (Fig. 3-3B). These results demonstrate the significantly high selectivity of Cu-APC to the G-quadruplex.

To obtain further insight into the selectivity of Cu-APC to the G-quadruplex, UV-Vis titrations in the presence of λ DNA, which is a double-stranded DNA isolated from bacteriophage λ and 48502 base pairs in length, corresponding to 400 μM in base

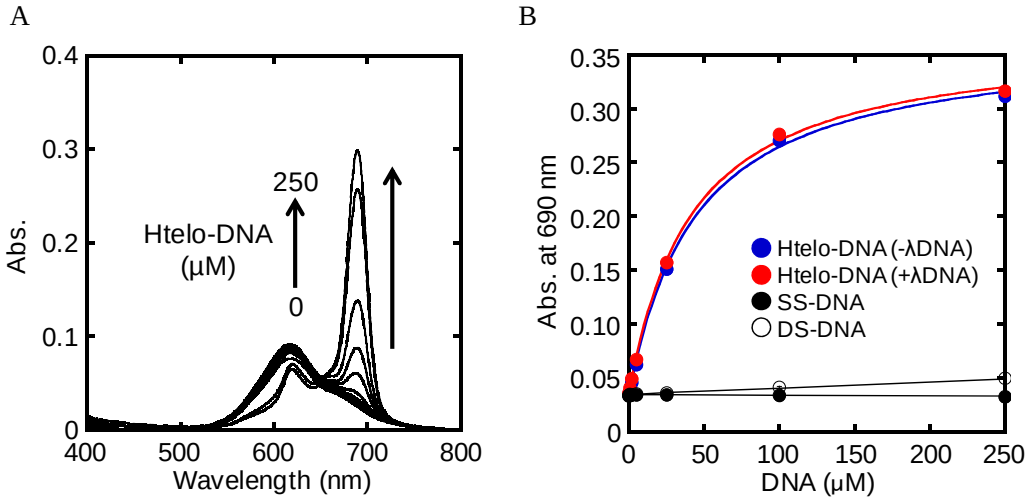

Fig. 3-3. Cu-APC binding to G-quadruplex with high selectivity. (A) UV-Vis spectra of Cu-APC with Htelo-DNA (0, 0.1, 0.2, 0.5, 1, 2, 5, 10, 25, 100 or 250 μM) in a buffer containing 50 mM MES-LiOH (pH 7.0) and 100 mM KCl at 25°C. (B) Plots of absorbance at 690 nm of Cu-APC as a function of Htelo-DNA, SS-DNA and DS-DNA in the absence of λ DNA, and Htelo-DNA in the presence of λ DNA.

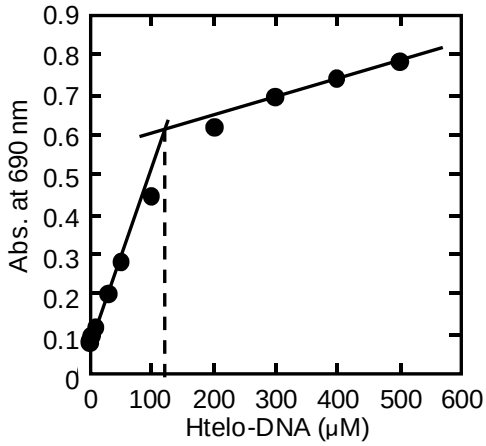

Fig. 3-4. Change in absorbance at 690 nm of 100 μM Cu-APC with 0-500 μM Htelo-DNA in a buffer containing 50 mM MES-LiOH (pH 7.0), 100 mM KCl, and 10 mM $MgCl_2$ at 25°C.

units were conducted. Increase in the same peak at 690 nm in the presence of λ DNA demonstrated that Cu-APC bound to the G-quadruplex with the K_a value of $(2.5 \pm 0.2) \times 10^4$ M^{-1} at 25°C (Fig. 3-3B), which is almost the same as that in the absence of λ DNA. These results suggest that excess dsDNA has no effect on the binding properties of Cu-APC to the G-quadruplex. Furthermore, the K_a values of Ni-APC (Fig. 3-1), a nickel-coordinating anionic phthalosyanine, for Htelo-DNA in the absence and the

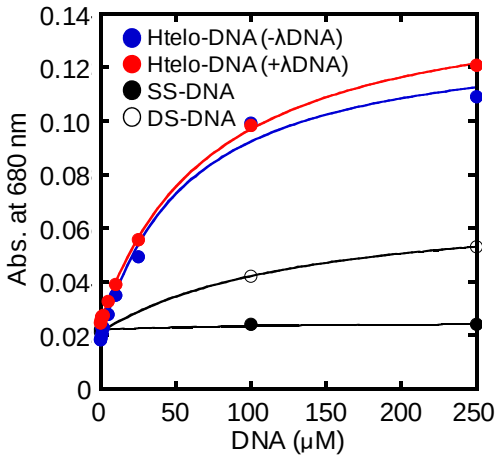

Fig. 3-5. Ni-APC binding to G-quadruplex with high selectivity. Plots of absorbance at 680 nm of Ni-APC as a function of Htelo-DNA, SS-DNA and DS-DNA in the absence of λ DNA, and Htelo-DNA in the presence of λ DNA at 20°C.

presence of λ DNA were (1.8 ± 0.3) × 10^4 M^{-1} and (1.4 ± 0.1) × 10^4 M^{-1} at 20°C, respectively (Fig. 3-5). These results were similar to those with Cu-APC, suggesting that the binding properties of anionic phthalocyanines to the G-quadruplex are independent of the coordinating metal.

Next, the binding affinity of a cationic porphyrin, TMPyP4 (Fig. 3-1), was investigated by UV-Vis titration as control experiments. A significant increase and decrease of absorbance at 440 nm and 424 nm, respectively, was observed with the annealed Htelo-DNA (Fig. 3-6A), indicating that TMPyP4 bound to the G-quadruplex formed by Htelo-DNA. The binding stoichiometry of TMPyP4 with the telomeric G-quadruplex remains to be elucidated. Previous studies using UV-Vis and ITC showed stoichiometries of 1:1 (G-quadruplex:TMPyP4) and 1:2 for the strong and weak binding modes, respectively [44]. Thus, based on the assumption that the dominant stoichiometry is 1:1, the K_a value was estimated to be (3.6 ± 1.8) × 10^6 M^{-1} at 25°C according to the plot of absorbance of TMPyP4 at 424 nm vs. Htelo-DNA concentration (Fig. 3-6B). More importantly, DS-DNA and SS-DNA also decreased the peak at 424 nm (Fig. 3-6B). These results indicate that, in contrast to anionic phthalocyanines, the selectivity of TMPyP4 to the G-quadruplex was extremely low as reported previously because of its cationic groups [29-32]. In addition, UV-Vis spectra of an anionic porphyrin, TS4 (Fig. 3-1), showed no change with the addition of Htelo-DNA, indicating that TS4 did not bind to the G-quadruplex [30]. These results support that a combination of large π-planar surface and peripheral anionic groups allows the anionic phthalocyanines to specifically bind to the G-quadruplex *via* stacking interaction.

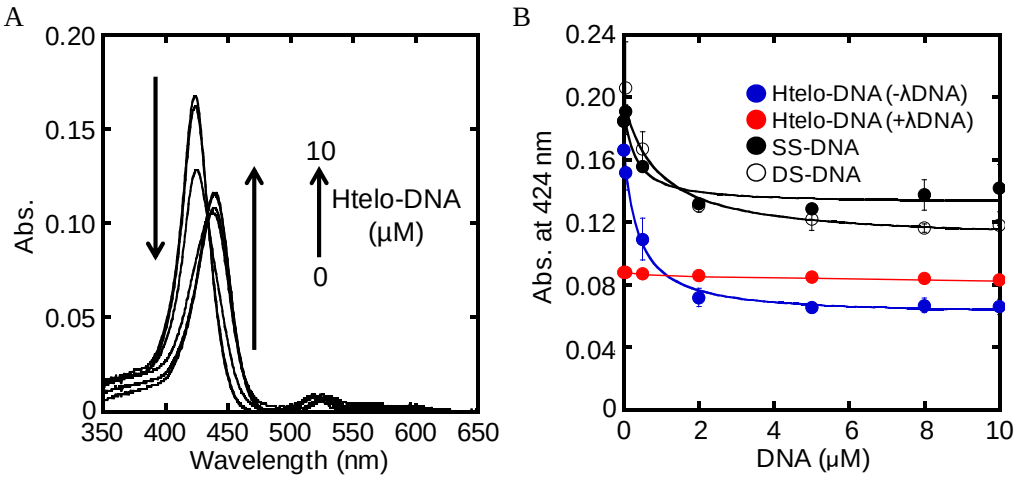

Fig. 3-6. TMPyP4 binding to G-quadruplex, dsDNA, and ssDNA, non-specifically. (A) UV-Vis spectra of TMPyP4 with Htelo-DNA (0, 0.05, 0.5, 2, 5, 8, or 10 μM) in a buffer containing 50 mM MES-LiOH (pH 7.0) and 100 mM KCl at 25°C. (B) Plots of absorbance at 440 nm of TMPyP4 as a function of Htelo-DNA, SS-DNA, and DS-DNA.

3.3.1.2. Effects of Excess dsDNA on Telomerase Inhibition Capacities

The high selectivity of anionic phthalocyanines to the telomeric G-quadruplex should

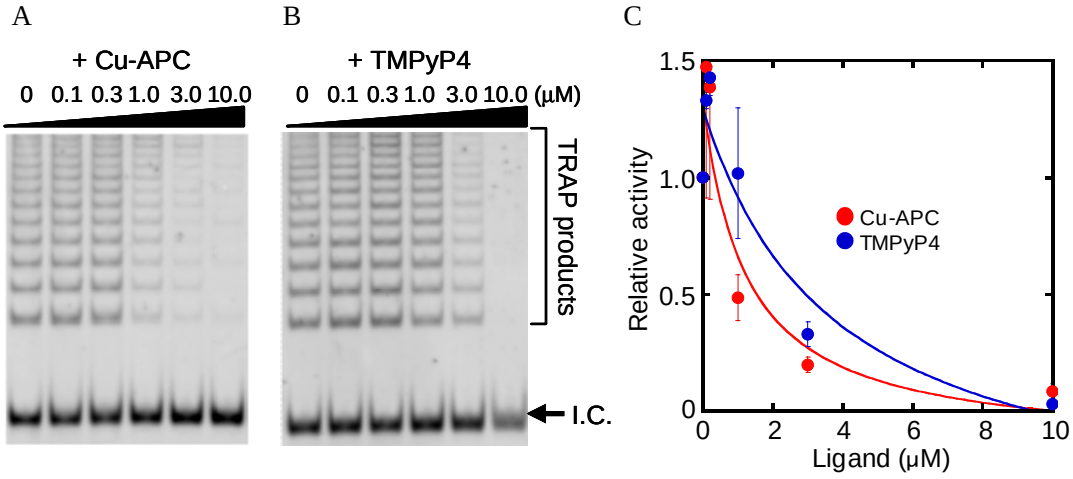

Fig. 3-7. Results of the tsTRAP assay with various concentrations of Cu-APC (A) and TMPyP4 (B). I.C. stands for the internal control. (C) The relative activity of telomerase with various concentrations (0, 0.1, 0.3, 1.0, 3.0 or 10 μM) of Cu-APC (red) and TMPyP4 (blue) in the absence of λ DNA. The relative activity value of 1 corresponds to the positive control, namely without Cu-APC or TMPyP4 (For details of the calculation of the relative activity, see the experimental section).

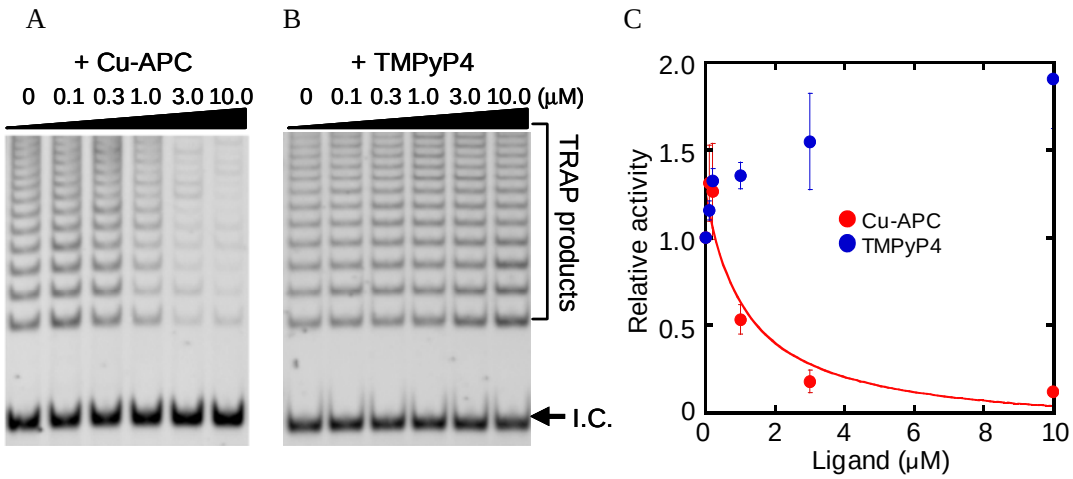

Fig. 3-8. Results of the tsTRAP assay with various concentrations of Cu-APC (A) and TMPyP4 (B) in the presence of λ DNA. I.C. stands for the internal control. (C) The relative activity of telomerase with various concentrations (0, 0.1, 0.3, 1.0, 3.0 or 10 μM) of Cu-APC (red) and TMPyP4 (blue) in the presence of λ DNA. The relative activity value of 1 corresponds to the positive control, namely without Cu-APC or TMPyP4.

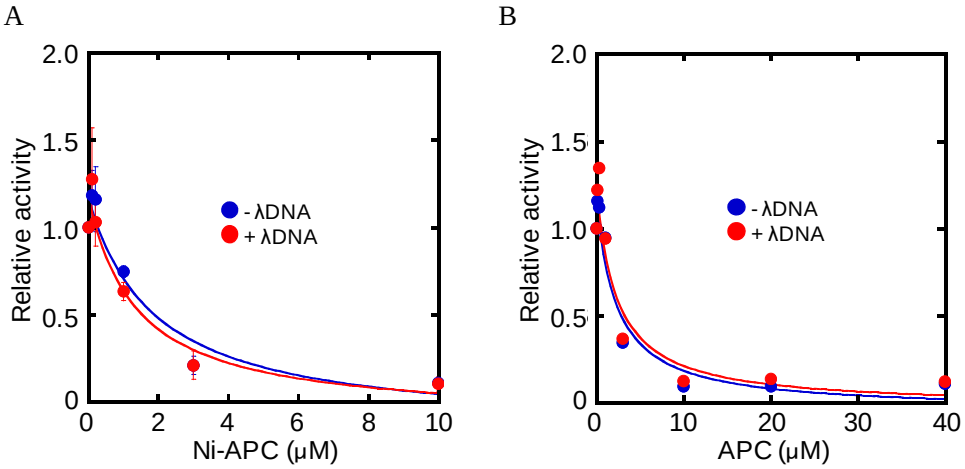

Fig. 3-9. The relative activity of telomerase with various concentrations of Ni-APC (A) and APC (B) in the absence or presence of λ DNA. The relative activity value of 1 corresponds to the positive control, namely without Ni-APC or APC.

inhibit telomerase activity even in the presence of excess dsDNA as found in cell nuclei. The inhibitory effects were studied in the absence or presence of λ DNA, mimicking genomic DNA, by a tsTRAP assay. In this improved TRAP assay, PCR was carried out with 50-fold diluted products of the telomerase reaction in order to inhibit ligands from interfering with PCR [39, 40]. In the absence of λ DNA, higher concentrations of

Cu-APC reduced the tsTRAP products (Figs. 3-7A and 3-7C), and the IC 50 value (the concentration of ligand at 50% relative activity, see Materials and Methods) was estimated to be 1.2 μM. More importantly, Cu-APC inhibited telomerase activity even in the presence of λ DNA with the IC 50 value of 1.2 μM (Figs. 3-8A and 3-8C), which is identical to that in the absence of λ DNA. These results are in agreement with the spectroscopic studies and demonstrate that selective binding to the telomeric G-quadruplex enables Cu-APC to inhibit telomerase activity specifically even in the presence of excess dsDNA. Furthermore, Ni-APC and APC (Fig. 3-1) also inhibited telomerase reaction activity both in the absence and presence of λ DNA (Figs. 3-9A and 3-9B). These results indicate that coordinating metal has little impact on telomerase inhibition by anionic phthalocyanines. In contrast to anionic phthalocyanines, both cationic porphyrins, TMPyP4 and Cu-TMPyP4, drastically lost their telomerase inhibition effects in the presence of λ DNA, while they reduced tsTRAP products in the absence of λ DNA (Figs. 3-7B, 3-7C, 3-8B and 3-8C). These results indicate that the non-specific binding of the cationic groups to λ DNA prevented these porphyrins from inhibiting telomerase activity.

3.3.2. MC Effects on Functional Capacities of G-Quadruplex-Ligands

3.3.2.1. MC Effects on Binding Capacities

In order to study the effects of MC on the binding affinity between TMPyP4 and the

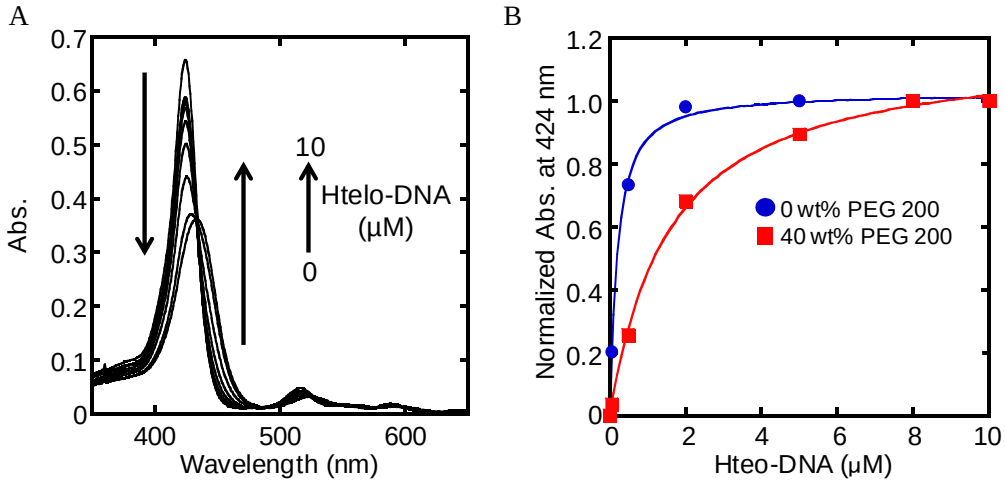

Fig. 3-10. (A) UV-Vis spectra of 1 μM TMPyP4 with 0-10 μM Htelo-DNA in a buffer containing 50 mM MES-LiOH (pH 7.0), 100 mM KCl, and 40 wt% PEG 200 at 25°C. (B) Plots of normalized absorbance at 424 nm of 1 μM TMPyP4 as a function of Htelo-DNA at 0 (blue) and 40 (red) wt% PEG 200 at 25°C.

G-quadruplex formed by Htelo-DNA, UV-Vis absorbance spectra of TMPyP4 with the annealed Htelo-DNA were measured in a buffer containing 100 mM KCl and 50 mM MES-LiOH (pH7.0) at 25°C; PEG 200 content was 0 or 40 wt% in each sample. The addition of Htelo-DNA decreased the absorbance of TMPyP4 at 424 nm both at 0 wt% and 40 wt% PEG 200 (Fig. 3-10A), indicating that TMPyP4 bound to the Htelo-DNA G-quadruplex under both conditions. According to the plot of the absorbance at 424 nm versus Htelo-DNA concentration (Fig. 3-10B), the K_a value at 40 wt% PEG 200 was calculated to be $(4.3 \pm 3.3) \times 10^5$ M^{-1}, which was less by one order of magnitude than that at 0 wt% of PEG 200, $(3.6 \pm 1.8) \times 10^6$ M^{-1}, at 25°C. These results show that MC reduced the binding affinity of TMPyP4 for the G-quadruplex, which is consistent with Tan's report that the elevation of the stability of the G-quadruplex, 5'-$(GGGTTA)_3GGG$-3', by TMPyP4 was decreased under MC conditions compared to the diluted condition [33].

It is known that TMPyP4 binds to G-quadruplexes *via* two kinds of binding modes, π-π stacking and electrostatic interactions. In order to determine which binding mode was inhibited by MC, PIPER (Fig. 2-11), another cationic G-quadruplex-ligand, which also binds to the G-quadruplex *via* π-π stacking and electrostatic interactions was further studied [36]. Unlike TMPyP4, the affinity of PIPER for the G-quadruplex decreased as pH increased from 6.0 to 8.0; this decrease in affinity was attributed to the

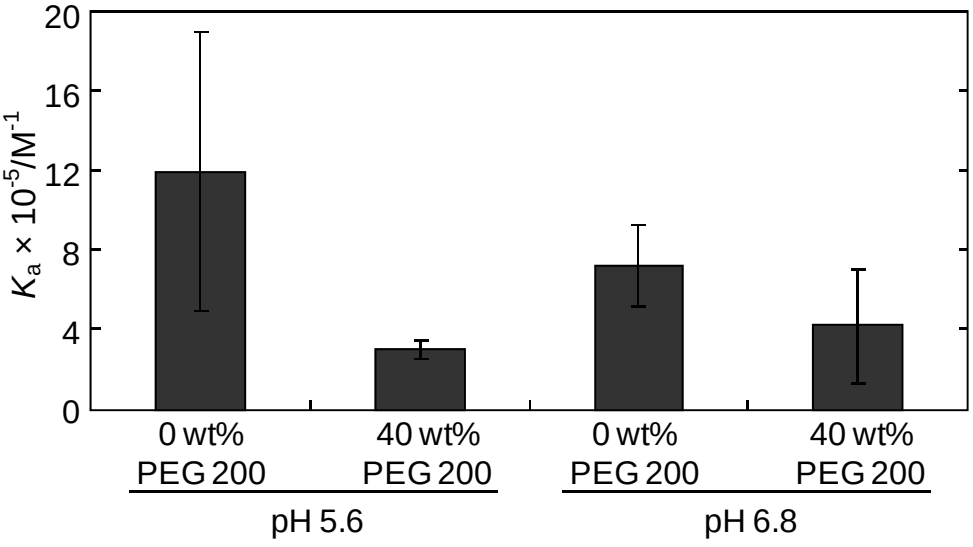

Fig. 3-11. Comparison of K_a values of PIPER for the Htelo-DNA G-quadruplex in the absence and presence of PEG 200 at pH 5.6 and 6.8 at 25°C. Each value is the average of three repeated measurements.

decrease in net positive charges on PIPER [36]. Thus, the electrostatic interaction between PIPER and the G-quadruplex could be controlled *via* the pH of the solution. UV-Vis titration of PIPER with Htelo-DNA showed that, at 25°C, the K_a values for 0 or 40 wt% PEG 200 at pH 5.6 were $(1.2 \pm 0.7) \times 10^6$ M^{-1} or $(3.0 \pm 0.5) \times 10^5$ M^{-1}, respectively, and the K_a values for 0 or 40 wt% PEG 200 at pH6.8 were $(7.2 \pm 2.0) \times 10^5$ M^{-1} or $(4.2 \pm 2.9) \times 10^5$ M^{-1}, respectively (Fig. 3-11). As was the case for TMPyP4, the K_a values of PIPER for Htelo-DNA decreased with MC at both pHs. Notably, the K_a values for 40 wt% PEG 200 were 4.0 times (pH 5.6) and 1.7 times (pH 6.8) smaller than those for 0 wt% PEG 200. MC caused a larger decrease in the binding affinity between PIPER and Htelo-DNA at pH 5.6 more than it did at pH 6.8. The electrostatic attraction between PIPER and the G-quadruplex should have been enhanced at pH 5.6 relative to that at pH 6.8 due to the increase in net positive charges [36]. Therefore, these results further support the hypothesis that MC with PEG 200 inhibited the electrostatic attraction between cationic ligands and the G-quadruplex.

Since it is conceivable that MC can inhibit electrostatic interactions between ligands and the G-quadruplex, it was attempted to further assess whether π-π stacking interactions can maintain their binding energy under MC conditions. Cu-APC should not engage in electrostatic interactions with G-quadruplexes because of their negative charges; however, it should engage in π-π stacking interactions with G-quadruplexes. Thus, in order to examine MC effects on π-π stacking interaction, the binding affinity between Cu-APC and the G-quadruplex formed by Htelo-DNA was investigated under MC conditions. UV-Vis spectra of Cu-APC were measured with the annealed Htelo-DNA at 0 wt% and at 40 wt% PEG 200 (Figs. 3-12A and 3-12B). Based on the plots of the absorbance at 690 nm versus Htelo-DNA concentration, the K_a values at 25°C were determined to be $(2.8 \pm 1.2) \times 10^4$ M^{-1} and $(3.4 \pm 1.5) \times 10^4$ M^{-1} at 0 wt% and 40 wt% PEG 200, respectively (Fig. 3-12B). These results demonstrated that the binding affinity of Cu-APC for the G-quadruplex was not influenced by MC. In addition, the binding between Hemin (Fig. 3-1), another anionic ligand, and Htelo-DNA was also examined (Fig. 3-13). At 25°C, the K_a values at 0 wt% PEG 200 were almost the same as those at 40 wt% PEG 200 ($(2.7 \pm 1.1) \times 10^5$ M^{-1} and $(3.2 \pm 1.2) \times 10^5$ M^{-1} at 0 and 40 wt% PEG 200, respectively). These results for Cu-APC and Hemin support the notion that anionic G-quadruplex-ligands can maintain their binding affinity for the G-quadruplex even under conditions of MC. Thus, it is possible to conclude that π-π stacking interactions are able to maintain binding between anionic ligands and the G-quadruplex under conditions of MC. The mechanism of the maintenance was further explored as described in 3.3.3.

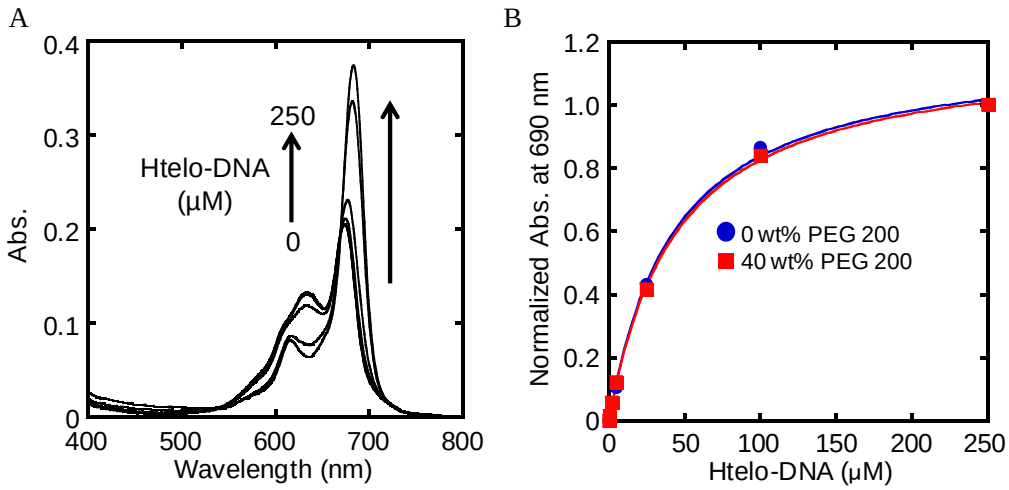

Fig. 3-12. (A) UV-Vis spectra of 2.5 μM Cu-APC with 0-250 μM Htelo-DNA in a buffer containing 50 mM MES-LiOH (pH 7.0), 100 mM KCl, 40 wt% PEG 200 at 25°C. (B) Plots of normalized absorbance at 690 nm of 2.5 μM Cu-APC as a function of Htelo-DNA at 0 (blue) and 40 (red) wt% PEG 200.

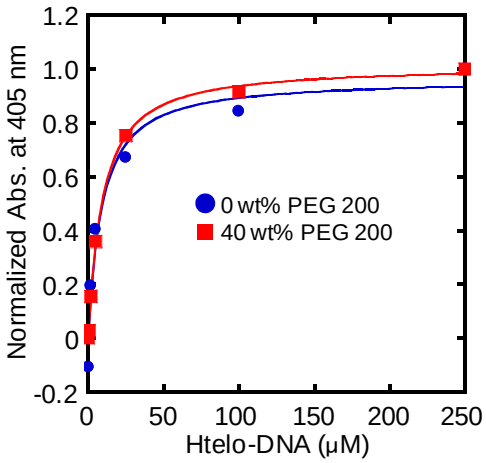

Fig. 3-13. Plots of normalized absorbance at 405 nm of 12.5 μM Hemin as a function of Htelo-DNA concentration in a buffer containing 50 mM MES-LiOH (pH 7.0) and 100 mM KCl at 0 (blue) and 40 (red) wt% PEG 200.

3.3.2.2. MC Effects on Telomerase Inhibition Capacities

Decrease in the binding affinity of TMPyP4 with the G-quadruplex should prevent TMPyP4 from inhibiting telomerase activity under MC conditions. To investigate this hypothesis, the tsTRAP assay with TMPyP4 was carried out under MC condition [39, 40]. As expected, the IC50 value at 20 wt% PEG 200 was 14 ± 1.0 μM, which was obviously larger than that at 0 wt% PEG 200, 2.3 ± 1.1 μM (Figs. 3-14A and 3-14B).

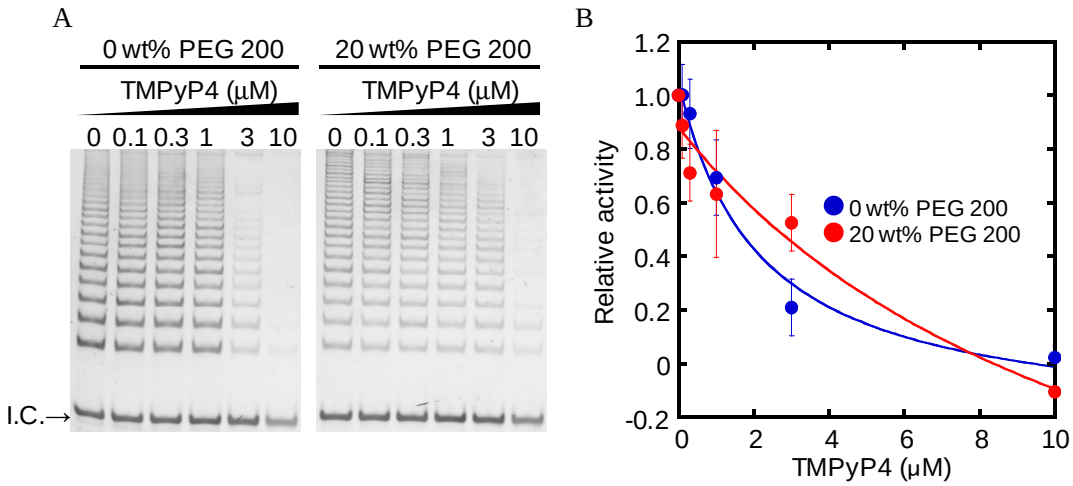

Fig. 3-14. (A) Results of the tsTRAP assay with various concentrations of TMPyP4 at 0 (left) and 20 (right) wt% PEG 200. I.C. stands for the internal control. (B) The relative activity of telomerase as a function of TMPyP4 at 0 (blue) and 20 (red) wt% PEG 200.

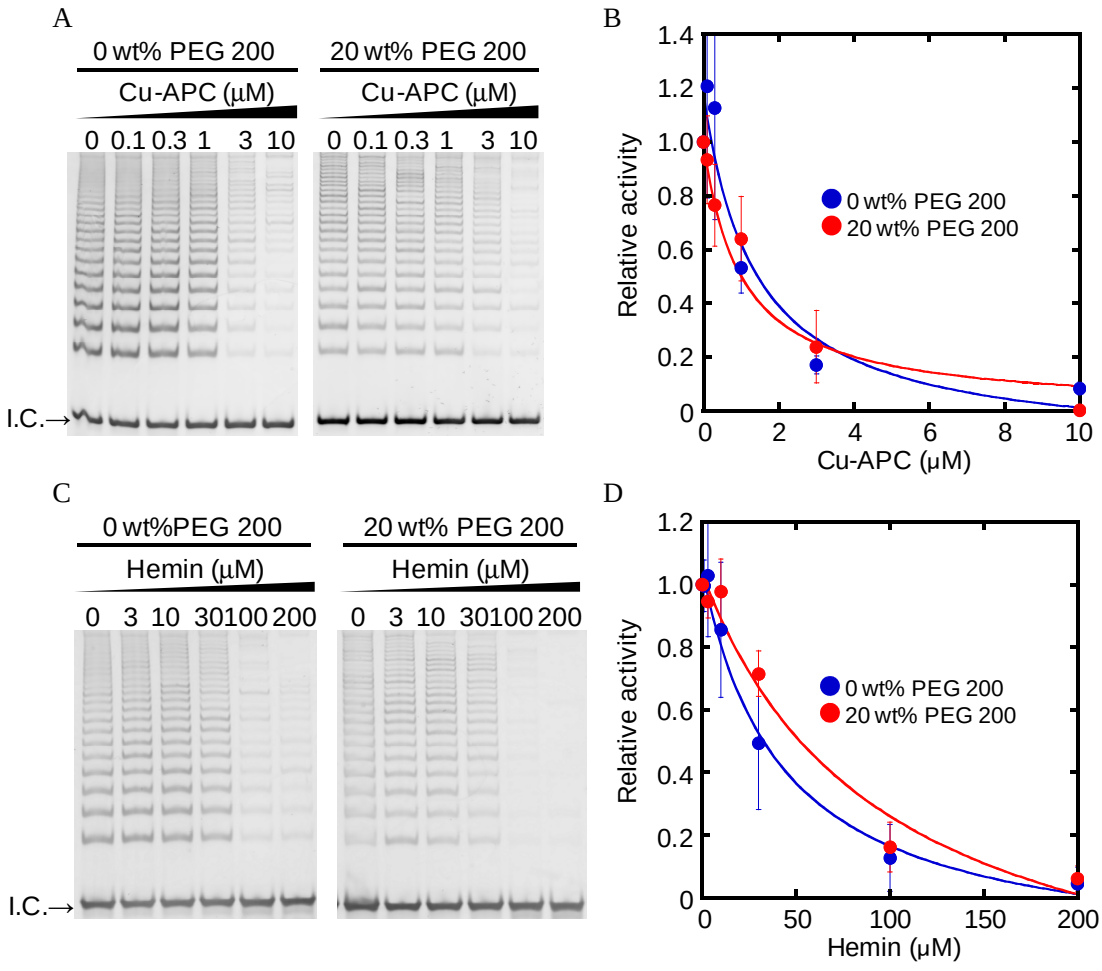

Fig. 3-15. (A) Results of the tsTRAP assay with various concentrations of Cu-APC at 0 (left) and 20 (right) wt% PEG 200. I.C. stands for the internal control. (B) The relative activity of telomerase as a function of Cu-APC at 0 (blue) and 20 (red) wt% PEG 200. (C) Results of the tsTRAP assay with various concentrations of Hemin at 0 (left) and 20 (right) wt% PEG 200. I.C. stands for the internal control. (D) The relative activity of telomerase as a function of Hemin at 0 (blue) and 20 (red) wt% PEG 200.

These MC effects were consistent with reduced telomerase inhibitory effect of TMPyP4 in the presence of PEG 200 in Tan's report [33]. Taken together, the results of the binding and tsTRAP assays indicated that MC reduced TMPyP4-mediated telomerase inhibition by decreasing the binding affinity between TMPyP4 and the G-quadruplex. On the other hand, the lack of MC effects on the binding of Cu-APC or Hemin to the G-quadruplex indicates that inhibitory effects that these ligand have on telomerase can be maintained even under MC condition. The tsTRAP assays with Cu-APC at 0 or 20 wt% PEG 200 revealed that the IC50 values at 0 and 20 wt% PEG 200 were 1.0 ± 0.2 μM and 1.8 ± 0.8 μM (Figs. 3-15A and 3-15B). Similar to Cu-APC, the IC50 values of Hemin were also almost independent of PEG 200 concentration (38 ± 24 μM and 99 ± 24 μM at 0 and 20 wt% PEG 200, respectively) (Figs. 3-15C and 3-15D). These results demonstrated for the first time that anionic G-quadruplex-ligands can inhibit telomerase activity under conditions of MC as efficiently as in the absence of MC.

3.3.3. Behavior of Water Molecules upon Binding of G-Quadruplex-Ligands

The UV-Vis titration assays showed that MC prevented cationic G-quadruplex-ligands, but not anionic G-quadruplex-ligands, from binding to the G-quadruplex. To date, the effects of osmotic pressure as it relates to the activity of water molecules altered by MC have been investigated mainly on various dsDNA-ligands including intercalators and groove binders [45-50]. MC reduced the affinities of the most ligands for dsDNA by decreasing water activity. Moreover, 0.25 to 78 water molecules are taken up upon the binding of ligands to dsDNA (Table 3-1) [45-50]. Because a hydration reaction is unfavorable under conditions where the concentration and activity of water molecules is decreased, the reduction of ligand affinity should be attributed to the water molecules taken up upon binding. Therefore, the binding affinities of TMPyP4 or Cu-APC to the G-quadruplex at PEG 200 concentrations between 0 and 40 wt% was further studied in order to examine how the activity of water molecules affected G-quadruplex-ligand binding (Figs. 3-16A and

Table 3-1. The number of water molecules (Δn_w) released upon the binding of ligand to DNA

DNA sequence	DNA structure	Ligand	Cosolute	Δn_w	Reference
Calf thymus DNA	dsDNA	Ethidium	Sucrose (Triethylene glycol, Betaine)	-0.25	45,46
		Propidium	Sucrose (Triethylene glycol, Betaine)	-6.4	
		Proflavine	Sucrose (Triethylene glycol, Betaine)	-30	
		Daunomycin	Sucrose (Triethylene glycol, Betaine)	-18	
		7-aminoactionomycin D	Sucrose (Triethylene glycol, Betaine)	-32	
$d(CGCGCAATTGCGCG)_2$	dsDNA	Hoechst 33258	Triethylene glycol	-78	47
			Acetamide	-51	
			Betaine	-51	
			Tetraethylene glycol	-67	
$d(CGCGCAATTGCGCG)_2$	dsDNA	DAPI	Triethylene glycol (Actamide, Betaine,	-35	48
		Netropsin	Triethylene glycol (Actamide, Betaine,	-26	
		Pentamidine	Triethylene glycol (Actamide, Betaine,	-34	
Calf thymus DNA	dsDNA	Daumocycin	Sucrose (Triethylene glycol, Betaine)	-17.8	49
		Adriamycin	Sucrose (Triethylene glycol, Betaine)	-35.8	
Calf thymus DNA	dsDNA	Hoechst 33258	Triethylene glycol	-74	50
			Sucrose	-30	
$d(GGGTTA)_3GGG$	G-quadruplex	TMPyP4	Glycerol	-30	33
$dA(GGGTTA)_3GGG$	G-quadruplex	Berberine	Low molecular weight cosolute	-13	51
$d(GGGTTA)_3GGG$	G-quadruplex	TMPyP4	EG	-16	This thesis
			PEG 200	-32	
			PEG 8000	-40	
		PIPER	PEG 200 (pH 5.6)	-30	
			PEG 200 (pH 6.8)	-13	
		Cu-APC	EG	-5.5	
			PEG 200	7.0	
			PEG 8000	5.3	
		Hemin	PEG 200	8.4	

3-16B). It was found that the relationships between ln K_a (the observed equilibrium constant) for binding of TMPyP4 to the G-quadruplex and ln a_w (the water activity) were linear and that they depended upon the concentration of PEG 200 (Fig. 3-17A), although MC induced a conformational change of the Htelo-DNA G-quadruplex. Based on the plots of ln K_a versus ln a_w (Fig. 3-17A), approximately 32 ±1.7 water molecules were taken up upon binding of TMPyP4 to G-quadruplex. The numbers of Δn_w

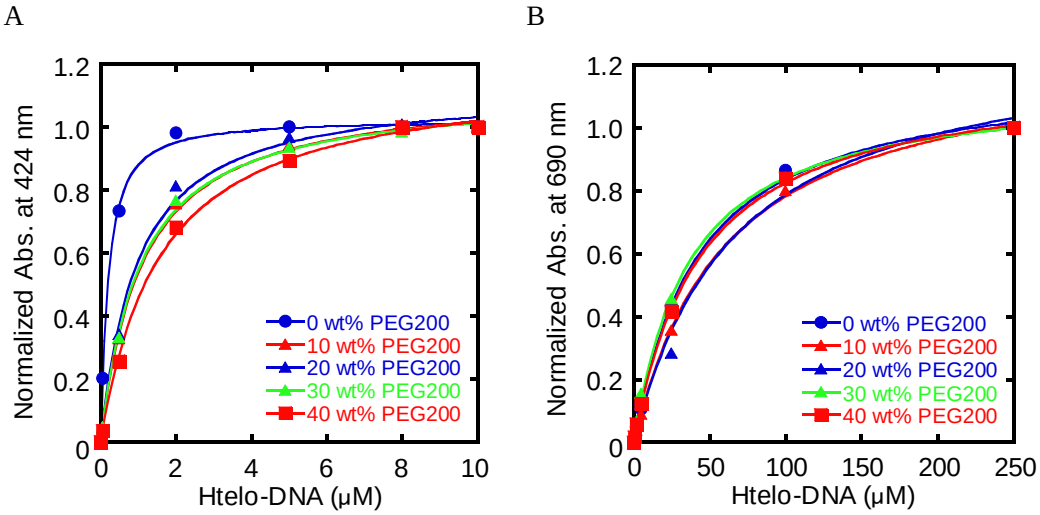

Fig. 3-16. Plots of normalized absorbance at 424 nm of 1 μM TMPyP4 (A) and at 690 nm of 2.5 μM Cu-APC (B) as a function of Htelo-DNA concentration in a buffer containing 50 mM MES-LiOH (pH 7.0) and 100 mM KCl at 0-40 wt% PEG 200 at 25°C.

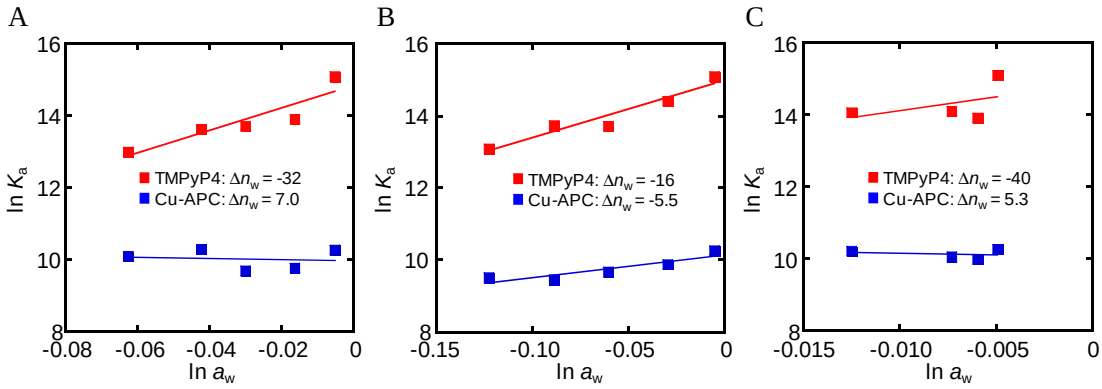

Fig. 3-17. Plots of ln K_a versus ln a_w for binding of TMPyP4 or Cu-APC with Htelo-DNA at 0 to 40 wt% PEG 200 (A), 0 to 40 wt% EG (B), and 0 to 20 wt% PEG 8000 (C).

evaluated in the present assay as well as previous reports are listed in Table 3-1. These results were in agreement with those from previous reports, which showed that more than 10 water molecules are acquired upon binding of cationic ligands to the G-quadruplex (Table 3-1) [33, 51]. More importantly, the plots of ln K_a for Cu-APC versus ln a_w showed (Fig. 3-17A) that several water molecules (7.0 ± 8.5 water molecules) were released upon Cu-APC binding to the G-quadruplex (Table 3-1). Therefore, it was possible to conclude that MC with PEG 200 reduced binding affinity of TMPyP4 to the G-quadruplex because of the hydration that occurs with G-quadruplex/TMPyP4 complex formation, although acquisition of no water molecules

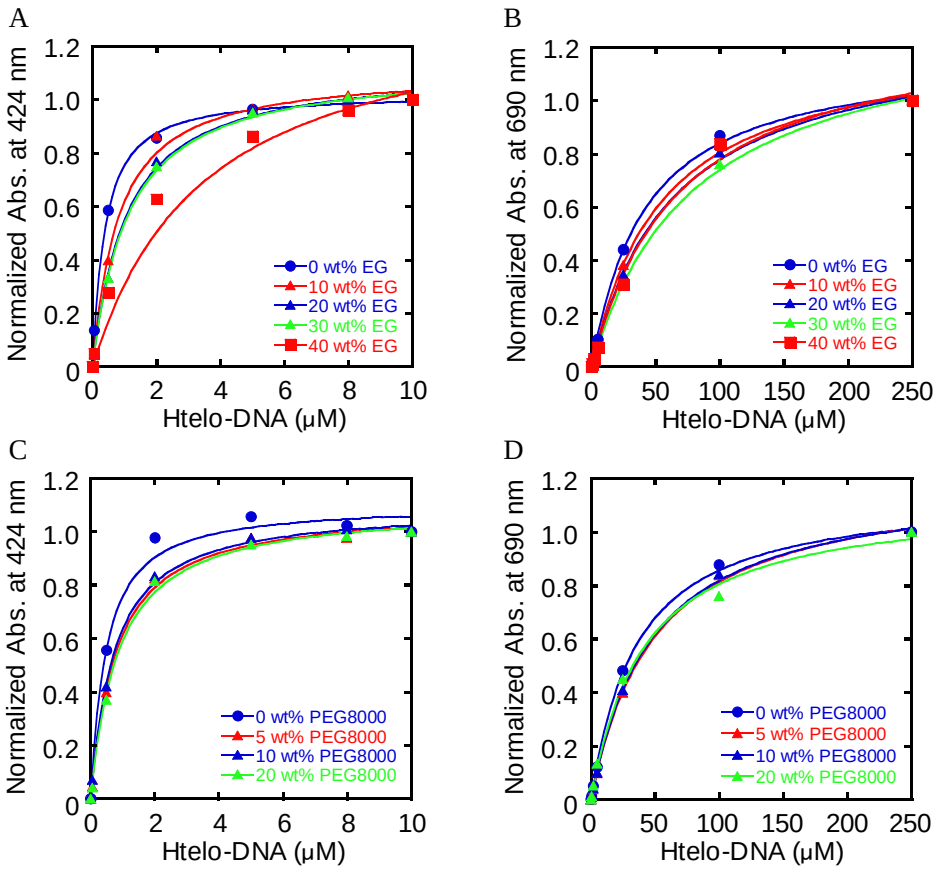

Fig. 3-18. Plots of normalized absorbance at 424 nm of 1 μM TMPyP4 (A) and 690 nm of 2.5 μM Cu-APC (B) as a function of Htelo-DNA concentration in a buffer containing 50 mM MES-LiOH (pH 7.0) and 100 mM KCl at 0-40 wt% EG at 25°C, and plots of normalized absorbance at 424 nm of 1 μM TMPyP4 (C) and 690 nm of 2.5 μM Cu-APC (D) as a function of Htelo-DNA concentration in a buffer containing 50 mM MES-LiOH (pH 7.0) and 100 mM KCl at 0-20 wt% PEG 8000 at 25°C.

during G-quadruplex/Cu-APC complex formation allowed for the maintenance of the affinity under MC conditions.

In order to further confirm the importance of water activity in the G-quadruplex/ligand complex formation, the effects of two other cosolutes such as EG and PEG 8000, which were different in size from PEG 200, were examined. Results from assays with 0~40 wt% EG (Figs. 3-18A and 3-18B for TMPyP4 and Cu-APC, respectively) showed that more water molecules were taken up upon formation of G-quadruplex/TMPyP4 complexes (16 ± 1.3 water molecules) than upon formation G-quadruplex/Cu-APC complexes (5.5 ± 1.4 water molecules) (Fig. 3-17B and Table 3-1). Results from assays with PEG 8000 (Figs. 3-18C and 3-18D for TMPyP4 and Cu-APC, respectively) showed that a significant number of water molecules (40 ± 26

water molecules) were taken up upon the G-quadruplex/TMPyP4 complex formation, despite the smaller number of water molecules (5.3 ± 7.1 water molecules) released upon the G-quadruplex/Cu-APC complex formation (Fig. 3-17C and Table 3-1). These results strongly supported the idea that anionic G-quadruplex-ligands are stronger telomerase inhibitor than cationic ligands under conditions of decreased water activity that were induced with various cosolutes.

3.4. Discussion

3.4.1 Uptake of Significant Numbers of Water Molecules upon Cationic G-Quadruplex-Ligands Binding to G-quadruplex

The results of UV-Vis titration assays with cosolutes indicated that electrostatic attraction in the G-quadruplex/ligand complex required larger numbers of water molecules than π-π stacking interaction, and this requirement for water molecules should reduce more drastically the cationic ligands binding to the G-quadruplex and the consequent telomerase inhibition under conditions of decreased water activity compared to the anionic ligands (left panel in Fig. 3-19). Previous studies on dsDNA-ligands

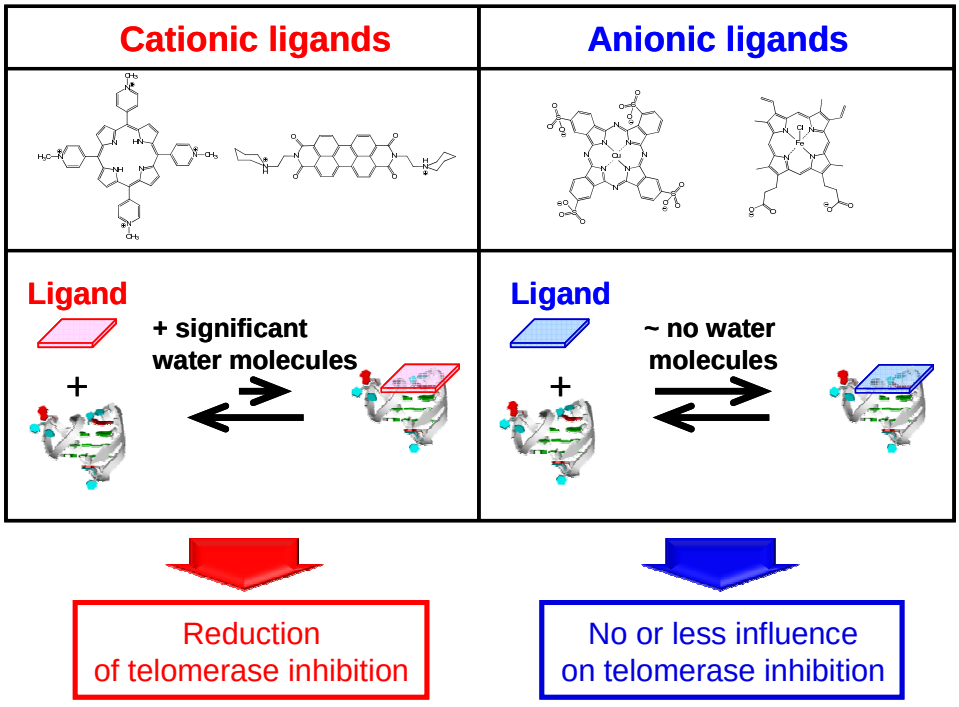

Fig. 3-19. Cationic ligands bind to G-quadruplex with uptake of many water molecules (left); in contrast, anionic ligands binding to G-quadruplex with uptake of very few water molecules (right).

showed that indirect contacts between ligands and dsDNA, including electrostatic interaction, required water molecules, and that proximal contacts displaced interfacial water molecules [47, 50, 52, 53]. For example, Hoechst 33258, which binds in the minor-groove with a cationic functional group at its terminal, is concave and closely interacts with the minor groove through hydrogen and van der Waals contacts [47, 54, 55]. Displacement of interfacial water molecules between Hoechst 33258 and the minor groove was demonstrated by X-ray crystallography as well as in thermodynamic and molecular dynamic simulation studies [47, 55-57]. However, osmotic stress studies showed that the Hoechst 33258/dsDNA complex acquired several tens of water molecules [47, 50]. These results suggest that the cationic terminal group of Hoechst 33258 binds to phosphate groups in minor groove of dsDNA through a network of water molecules [47]. Moreover, there have been other instances of water molecules bridging between other cationic ligands that bind in grooves of dsDNA [58, 59]. These findings demonstrate that water molecules are generally taken up upon formation of electrostatic interactions between the cationic ligands and dsDNA. In addition, NMR analysis showed that TMPyP4 is stacked over the top of G-quartet in a G-quadruplex from a *MYC* promoter and the cationic functional groups of TMPyP4 are in close contact with some phosphates of the G-quadruplex [60]. The results here for TMPyP4 and PIPER were consistent with those from the prior studies, and together these findings indicate that water molecules play a functional role in electrostatic interactions between DNA structures and cationic ligands by forming bridges between the DNA and the ligand.

3.4.2. Release of Several Water Molecules upon Anionic G-Quadruplex-Ligands Binding to G-quadruplex

In contrast to the cationic ligands, results of binding assays of Cu-APC to the G-quadruplex at various concentrations of PEG 200 showed that several water molecules were released when Cu-APC bound to the G-quadruplex (Fig. 3-17A). As shown in the case with Cu-APC, similar numbers of water molecules were released upon the G-quadruplex/Hemin complex formation (Fig. 3-20). These water behaviors were similar to that observed when ethidium bromide, a dsDNA-intercalator, binds to dsDNA. No water molecules were taken up upon formation of the ethidium bromide/dsDNA complex; however, binding of other dsDNA intercalators to dsDNA resulted in the acquisition of water molecules (Table 3-1) [45, 46]. These findings are attributable to the facts that ethidium bromide binds to dsDNA *via* π-π stacking interactions and that it has very few functional groups that can interact with the minor groove because of its small size. Similarly, the reason that there were almost no water

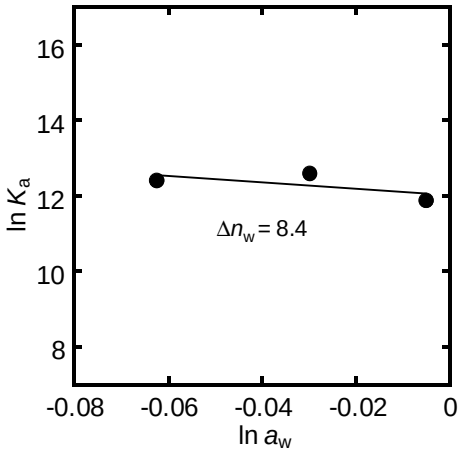

Fig. 3-20. Plots of ln K_a versus ln a_w for binding of Hemin with Htelo-DNA at 25°C.

molecules taken up upon binding of the anionic ligands, Cu-APC and Hemin, to the G-quadruplex should be that binding mode of these ligands was mainly the π-π stacking interaction due to the anionic functional groups. Furthermore, previous structural studies of G-quadruplex/ligand complexes showed that G-quadruplex-ligands are usually stacked over the top G-quartet, which may also be an important factor for the water behavior upon π-π stacking interaction. In the absence of ligands, the top G-quartet is known to form a rigid stacking interaction with a loop, of which length is more than three bases [61]. The well-ordered loop structure accumulates functional groups that can be binding sites for water molecules [61]. The end stacking interaction of G-quadruplex-ligands should alter the well-ordered loop structure bounded by water molecules, which may result in release of water molecules. Thus, to the best of our knowledge, these results indicated for the first time that decreased water activity does not reduce the binding affinity of anionic ligands for G-quadruplex and that this maintenance of binding under MC conditions resulted in the maintenance of the telomerase inhibitory effect (right panel in Fig. 3-19).

3.4.3. Other Factors Affecting Water Behavior upon G-Quadruplex/Ligands Formation

The slopes of plots of ln K_a for TMPyP4 or Cu-APC versus ln a_w depended on the cosolutes; these findings indicated that not only water activity, but also other solution factors, affected the binding affinities of these ligands (Fig. 3-18). Water molecules taken up or released upon the binding of TMPyP4 and Cu-APC, respectively, to the G-quadruplex tended to increase when cosolutes with larger weight molecule were

added (Table 3-1). A previous study on the MC effect as caused by cosolutes with different molecular weights, specifically PEG 200 and Ficoll 70, showed that these cosolutes differed in their effects on the interaction between TMPyP4 and a telomeric G-quadruplex [62]. Thus, the molecular weight of a cosolute can have an impact on some properties of a solution, and this impact may be related to the change in the number of water molecules taken up or released upon binding. The viscosity increases progressively with increases in the molecular weight of PEG [63]. The addition of EG and PEG decreases the dielectric constant of the solution, and the higher the molecular weight of PEG the larger the reduction in the dielectric constant [63]. An increase in viscosity should reduce the affinity of TMPyP4 or Cu-APC for G-quadruplex, and a decrease in the dielectric constant should enhance or reduce the affinity of TMPyP4 or Cu-APC, respectively. However, the K_a value for TMPyP4 or Cu-APC tended to decrease or increase, respectively, with the increasing concentrations of the cosolutes. Thus, these two solution properties may not be the main cause for the observed tendency in the number of taken up or released water molecules. The order of the numbers of water molecules taken up or released upon the G-quadruplex-TMPyP4 or G-quadruplex/Cu-APC complex formation, respectively, was inversely related to the numbers of hydroxyl groups in the vicinal position in the cosolutes. Previous studies on the effect of MC on formation of G-quadruplex and dsDNA demonstrated that a cosolute with fewer hydroxyl groups in the vicinal position causes more water molecules to be released during formation of an antiparallel G-quadruplex or to be taken up during formation of a DNA duplex [23, 24]. This relationship is attributable to the fact that the solvation of DNA by cosolutes with more hydroxyl groups eliminates the uptake or release of water molecules because the cosolutes with more hydroxyl groups can bind to DNA molecules directly and may be released or taken up along with the uptake or release of water molecules during formation of multi-strand DNA structure [24]. Although clarification of the influences of solution properties on G-quadruplex/ligand complex formation requires further studies, the hydration or dehydration that occurs during formation of G-quadruplex/ligand complexes may also be affected by the hydroxyl groups on the cosolutes.

3.5. Conclusions

The telomeric G-quadruplex-binding and telomerase-inhibiting capacities of G-quadruplex-ligands were systematically examined under the diluted condition and the cell nuclei-mimicking condition where λ DNA or MC cosolutes such as EG, PEG 200, and PEG 8000 exist. Although cationic ligands such as TMPyP4 and Cu-TMPyP4

bound to the telomeric G-quadruplex under the diluted condition without λ DNA and MC cosolutes, the binding affinity was drastically reduced by addition of λ DNA. The reduction should be caused by electrostatic binding to λ DNA. MC also inhibited cationic ligands from binding to the G-quadruplex. Studies on water behavior indicated that the reduced binding affinity under MC conditions is caused by uptake of water molecules upon binding of their cationic functional groups to the G-quadruplex. In accordance with these results, λ DNA and PEG 200 also decreased the telomerase inhibitory effect of cationic ligands. More importantly, both λ DNA and MC did not affect the binding capacities and the subsequent telomerase inhibitory capacities of anionic ligands such as Cu-APC, Ni-APC, Hemin, and APC, because they did not interact with dsDNA and acquire water molecules upon binding to G-quadruplex. These results indicate that anionic ligands show specific antiproliferative effect on tumor cells over normal cells *via* efficient telomerase inhibition even in cell nuclei.

3.6. References

1. Zahler, A. M.; Williamson, J. R.; Cech, T. R.; Prescott, D. M., Inhibition of Telomerase by G-Quartet DNA Structures. *Nature* **1991**, 350, 718-720.
2. Sun, D. Y.; Thompson, B.; Cathers, B. E.; Salazar, M.; Kerwin, S. M.; Trent, J. O.; Jenkins, T. C.; Neidle, S.; Hurley, L. H., Inhibition of Human Telomerase by a G-Quadruplex-Interactive Compound. *J. Med. Chem.* **1997**, 40, 2113-2116.
3. Wheelhouse, R. T.; Sun, D. K.; Han, H. Y.; Han, F. X. G.; Hurley, L. H., Cationic Porphyrins as Telomerase Inhibitors: the Interaction of Tetra-(N-methyl-4-pyridyl)porphine with Quadruplex DNA. *J. Am. Chem. Soc.* **1998**, 120, 3261-3262.
4. Mergny, J. L.; Helene, C., G-Quadruplex DNA: a Target for Drug Design. *Nat. Med.* **1998**, 4, 1366-1367.
5. Neidle, S.; Parkinson, G., Telomere Maintenance as a Target for Anticancer Drug Discovery. *Nat. Rev. Drug Discov.* **2002**, 1, 383-393.
6. Harrison, R. J.; Cuesta, J.; Chessari, G.; Read, M. A.; Basra, S. K.; Reszka, A. P.; Morrell, J.; Gowan, S. M.; Incles, C. M.; Tanious, F. A.; Wilson, W. D.; Kelland, L. R.; Neidle, S., Trisubstituted Acridine Derivatives as Potent and Selective Telomerase Inhibitors. *J. Med. Chem.* **2003**, 46, 4463-4476.
7. Davis, J. T., G-Quartets 40 Years Later: from 5 ‘-GMP to Molecular Biology and Supramolecular Chemistry. *Angew. Chem., Int. Ed.* **2004**, 43, 668-698.
8. Cheng, M. K.; Modi, C.; Cookson, J. C.; Hutchinson, I.; Heald, R. A.; McCarroll, A. J.; Missailidis, S.; Tanious, F.; Wilson, W. D.; Mergny, J. L.; Laughton, C. A.;

Stevens, M. F. G., Antitumor Polycyclic Acridines. 20. Search for DNA Quadruplex Binding Selectivity in a Series of 8,13-dimethylquino 4,3,2-kl Acridinium Salts: Telomere-Targeted Agents. *J. Med. Chem.* **2008**, 51, 963-975.

9. Drewe, W. C.; Nanjunda, R.; Gunaratnam, M.; Beltran, M.; Parkinson, G. N.; Reszka, A. P.; Wilson, W. D.; Neidle, S., Rational Design of Substituted Diarylureas: a Scaffold for Binding to G-Quadruplex Motifs. *J. Med. Chem.* **2008**, 51, 7751-7767.
10. De Cian, A.; Lacroix, L.; Douarre, C.; Temime-Smaali, N.; Trentesaux, C.; Riou, J. F.; Mergny, J. L., Targeting Telomeres and Telomerase. *Biochimie* **2008**, 90, 131-155.
11. Monchaud, D.; Teulade-Fichou, M. P., A Hitchhiker's Guide to G-Quadruplex Ligands. *Org. Biomol. Chem.* **2008**, 6, 627-636.
12. Ou, T. M.; Lu, Y. J.; Tan, J. H.; Huang, Z. S.; Wong, K. Y.; Gu, L. Q., G-Quadruplexes: Targets in Anticancer Drug Design. *ChemMedChem* **2008**, 3, 690-713.
13. Georgiades, S. N.; Abd Karim, N. H.; Suntharalingam, K.; Vilar, R., Interaction of Metal Complexes with G-Quadruplex DNA. *Angew. Chem., Int. Ed.* **2010**, 49, 4020-4034.
14. Neidle, S., Human Telomeric G-Quadruplex: the Current Status of Telomeric G-Quadruplexes as Therapeutic Targets in Human Cancer. *FEBS J.* **2010**, 277, 1118-1125.
15. Jain, A. K.; Paul, A.; Maji, B.; Muniyappa, K.; Bhattacharya, S., Dimeric 1,3-phenylene-bis(piperazinyl benzimidazole)s: Synthesis and Structure-Activity Investigations on Their Binding with Human Telomeric G-Quadruplex DNA and Telomerase Inhibition Properties. *J. Med. Chem.* **2012**, 55, 2981-2993.
16. Paul, A.; Maji, B.; Misra, S. K.; Jain, A. K.; Muniyappa, K.; Bhattacharya, S., Stabilization and Structural Alteration of the G-Quadruplex DNA Made from the Human Telomeric Repeat Mediated by Tröger's Base Based Novel Benzimidazole Derivatives. *J. Med. Chem.* **2012**, 55, 7460-7471.
17. Kim, M. Y.; Gleason-Guzman, M.; Izbicka, E.; Nishioka, D.; Hurley, L. H., The Different Biological Effects of Telomestatin and TMPyP4 Can Be Attributed to Their Selectivity for Interaction with Intramolecular or Intermolecular G-Quadruplex Structures. *Cancer Res.* **2003**, 63, 3247-3256.
18. Harrison, R. J.; Reszka, A. P.; Haider, S. M.; Romagnoli, B.; Morrell, J.; Read, M. A.; Gowan, S. M.; Incles, C. M.; Kelland, L. R.; Neidle, S., Evaluation of by Disubstituted Acridone Derivatives as Telomerase Inhibitors: the Importance of

G-Quadruplex Binding. *Bioorg. Med. Chem. Lett.* **2004**, 14, 5845-5849.

19. Sissi, C.; Lucatello, L.; Krapcho, A. P.; Maloney, D. J.; Boxer, M. B.; Camarasa, M. V.; Pezzoni, G.; Menta, E.; Palumbo, M., Tri-, Tetra- and Heptacyclic Perylene Analogues as New Potential Antineoplastic Agents Based on DNA Telomerase Inhibition. *Bioorgan. Med. Chem.* **2007**, 15, 555-562.
20. Zimmerman, S. B.; Minton, A. P., Macromolecular Crowding - Biochemical, Biophysical, and Physiological Consequences. *Annu. Rev. Bioph. Biom.* **1993**, 22, 27-65.
21. Minton, A. P., The Influence of Macromolecular Crowding and Macromolecular Confinement on Biochemical Reactions in Physiological Media. *J. Biol. Chem.* **2001**, 276, 10577-10580.
22. Ellis, R. J.; Minton, A. P., Cell Biology - Join the Crowd. *Nature* **2003**, 425, 27-28.
23. Nakano, S.; Karimata, H.; Ohmichi, T.; Kawakami, J.; Sugimoto, N., The Effect of Molecular Crowding with Nucleotide Length and Cosolute Structure on DNA Duplex Stability. *J. Am. Chem. Soc.* **2004**, 126, 14330-14331.
24. Miyoshi, D.; Karimata, H.; Sugimoto, N., Hydration Regulates Thermodynamics of G-Quadruplex Formation under Molecular Crowding Conditions. *J. Am. Chem. Soc.* **2006**, 128, 7957-7963.
25. Miyoshi, D.; Nakamura, K.; Tateishi-Karimata, H.; Ohmichi, T.; Sugimoto, N., Hydration of Watson-Crick Base Pairs and Dehydration of Hoogsteen Base Pairs Inducing Structural Polymorphism under Molecular Crowding Conditions. *J. Am. Chem. Soc.* **2009**, 131, 3522-3531.
26. Ninni, L.; Camargo, M. S.; Meirelles, A. J. A., Water Activity in Poly(ethylene glycol) Aqueous Solutions. *Thermochim. Acta* **1999**, 328, 169-176.
27. Kozer, N.; Kuttner, Y. Y.; Haran, G.; Schreiber, G., Protein-Protein Association in Polymer Solutions: from Dilute to Semidilute to Concentrated. *Biophys. J.* **2007**, 92, 2139-2149.
28. Minton, A. P., Molecular Crowding: Analysis of Effects of High Concentrations of Inert Cosolutes on Biochemical Equilibria and Rates in Terms of Volume Exclusion. In *Energetics of Biological Macromolecules, Pt B*, **1998**, 295, 127-149.
29. Lipscomb, L. A.; Zhou, F. X.; Presnell, S. R.; Woo, R. J.; Peek, M. E.; Plaskon, R. R.; Williams, L. D., Structure of a DNA-Porphyrin Complex. *Biochemistry* **1996**, 35, 2818-2823.
30. Arthanari, H.; Basu, S.; Kawano, T. L.; Bolton, P. H., Fluorescent Dyes Specific

for Quadruplex DNA. *Nucleic Acids Res.* **1998**, 26, 3724-3728.

31. Ren, J. S.; Chaires, J. B., Sequence and Structural Selectivity of Nucleic Acid Binding Ligands. *Biochemistry* **1999**, 38, 16067-16075.
32. Bennett, M.; Krah, A.; Wien, F.; Garman, E.; McKenna, R.; Sanderson, M.; Neidle, S., A DNA-Porphyrin Minor-Groove Complex at Atomic Resolution: the Structural Consequences of Porphyrin Ruffling. *Proc. Natl. Acad. Sci. USA* **2000**, 97, 9476-9481.
33. Chen, Z.; Zheng, K. W.; Hao, Y. H.; Tan, Z., Reduced or Diminished Stabilization of the Telomere G-Quadruplex and Inhibition of Telomerase by Small Chemical Ligands under Molecular Crowding Condition. *J. Am. Chem. Soc.* **2009**, 131, 10430-10438.
34. Tahara, H.; Shin-ya, K.; Seimiya, H.; Yamada, H.; Tsuruo, T.; Ide, T., G-Quadruplex Stabilization by Telomestatin Induces TRF2 Protein Dissociation from Telomeres and Anaphase Bridge Formation Accompanied by Loss of the 3 ‘ Telomeric Overhang in Cancer Cells. *Oncogene* **2006**, 25, 1955-1966.
35. Han, H. Y.; Hurley, L. H., G-Quadruplex DNA: a Potential Target for Anti-Cancer Drug Design. *Trends Pharmacol. Sci.* **2000**, 21, 136-142.
36. Tuntiwechapikul, W.; Taka, T.; Bethencourt, M.; Makonkawkeyoon, L.; Lee, T. R., The Influence of pH on the G-Quadruplex Binding Selectivity of Perylene Derivatives. *Bioorg. Med. Chem. Lett.* **2006**, 16, 4120-4126.
37. Travascio, P.; Bennet, A. J.; Wang, D. Y.; Sen, D., A Ribozyme and a Catalytic DNA with Peroxidase Activity: Active Sites Versus Cofactor-Binding Sites. *Chem. Biol.* **1999**, 6, 779-787.
38. Yamauchi, T.; Miyoshi, D.; Kubodera, T.; Nishimura, A.; Nakai, S.; Sugimoto, N., Roles of Mg^{2+} in TPP-Dependent Riboswitch. *FEBS Lett.* **2005**, 579, 2583-2588.
39. Kim, N. W.; Piatyszek, M. A.; Prowse, K. R.; Harley, C. B.; West, M. D.; Ho, P. L. C.; Coviello, G. M.; Wright, W. E.; Weinrich, S. L.; Shay, J. W., Specific Association of Human Telomerase Activity with Immortal Cells and Cancer TTAGGG Repeats. *Science* **1994**, 266, 2011-2015.
40. Yu, H. Q.; Zhang, D. H.; Gu, X. B.; Miyoshi, D.; Sugimoto, N., Regulation of Telomerase Activity by the Thermodynamic Stability of a DNA·RNA Hybrid. *Angew. Chem., Int. Ed.* **2008**, 47, 9034-9038.
41. Xu, Y.; Noguchi, Y.; Sugiyama, H., The New Models of the Human Telomere d[AGGG(TTAGGG)$_3$] in K^+ Solution. *Bioorgan. Med. Chem.* **2006**, 14, 5584-5591.

42. Ambrus, A.; Chen, D.; Dai, J. X.; Bialis, T.; Jones, R. A.; Yang, D. Z., Human Telomeric Sequence Forms a Hybrid-Type Intramolecular G-Quadruplex Structure with Mixed Parallel/Antiparallel Strands in Potassium Solution. *Nucleic Acids Res.* **2006**, 34, 2723-2735.
43. Luu, K. N.; Phan, A. T.; Kuryavyi, V.; Lacroix, L.; Patel, D. J., Structure of the Human Telomere in K^+ Solution: an Intramolecular (3+1) G-Quadruplex Scaffold. *J. Am. Chem. Soc.* **2006**, 128, 9963-9970.
44. Arora, A.; Maiti, S., Effect of Loop Orientation on Quadruplex-TMPyP4 Interaction. *J. Phys. Chem. B* **2008**, 112, 8151-8159.
45. Qu, X. G.; Chaires, J. B., Contrasting Hydration Changes for Ethidium and Daunomycin Binding to DNA. *J. Am. Chem. Soc.* **1999**, 121, 2649-2650.
46. Qu, X. G.; Chaires, J. B., Hydration Changes for DNA Intercalation Reactions. *J. Am. Chem. Soc.* **2001**, 123, 1-7.
47. Kiser, J. R.; Monk, R. W.; Smalls, R. L.; Petty, J. T., Hydration Changes in the Association of Hoechst 33258 with DNA. *Biochemistry* **2005**, 44, 16988-16997.
48. Degtyareva, N. N.; Wallace, B. D.; Bryant, A. R.; Loo, K. M.; Petty, J. T., Hydration Changes Accompanying the Binding of Minor Groove Ligands with DNA. *Biophys. J.* **2007**, 92, 959-965.
49. Yu, H. J.; Ren, J. S.; Chaires, J. B.; Qu, X. G., Hydration of Drug-DNA Complexes: Greater Water Uptake for Adriamycin Compared to Daunomycin. *J. Med. Chem.* **2008**, 51, 5909-5911.
50. Anuradha; Alam, M. S.; Chaudhury, N. K., Osmolyte Changes the Binding Affinity and Mode of Interaction of Minor Groove Binder Hoechst 33258 with Calf Thymus DNA. *Chem. Pharm. Bull.* **2010**, 58, 1447-1454.
51. Arora, A.; Balasubramanian, C.; Kumar, N.; Agrawal, S.; Ojha, R. P.; Maiti, S., Binding of Berberine to Human Telomeric Quadruplex - Spectroscopic, Calorimetric and Molecular Modeling Studies. *FEBS J.* **2008**, 275, 3971-3983.
52. Kopka, M. L.; Yoon, C.; Goodsell, D.; Pjura, P.; Dickerson, R. E., The Molecular-Origin of DNA Drug Specificity in Netropsin and Distamycin. *Proc. Natl. Acad. Sci. USA* **1985**, 82, 1376-1380.
53. Bailly, C.; Chessari, G.; Carrasco, C.; Joubert, A.; Mann, J.; Wilson, W. D.; Neidle, S., Sequence-Specific Minor Groove Binding by Bis-benzimidazoles: Water Molecules in Ligand Recognition. *Nucleic Acids Res.* **2003**, 31, 1514-1524.
54. Pjura, P. E.; Grzeskowiak, K.; Dickerson, R. E., Binding of Hoechst-33258 to the Minor Groove of B-DNA. *J. Mol. Biol.* **1987**, 197, 257-271.

55. Quintana, J. R.; Lipanov, A. A.; Dickerson, R. E., Low-Temperature Crystallographic Analyses of the Binding of Hoechst-33258 to the Double-Helical DNA Dodecamer C-G-C-G-A-A-T-T-C-G-C-G. *Biochemistry* **1991**, 30, 10294-10306.
56. Haq, I.; Ladbury, J. E.; Chowdhry, B. Z.; Jenkins, T. C.; Chaires, J. B., Specific Binding of Hoechst 33258 to the $d(CGCAAATTTGCG)_2$ Duplex: Calorimetric and Spectroscopic Studies. *J. Mol. Biol.* **1997**, 271, 244-257.
57. Tang, G. Q.; Tanaka, N.; Kunugi, S., Effects of Pressure on the DNA Minor Groove Binding of Hoechst 33258. *Bull. Chem. Soc. Jpn.* **1998**, 71, 1725-1730.
58. Brown, D. G.; Sanderson, M. R.; Skelly, J. V.; Jenkins, T. C.; Brown, T.; Garman, E.; Stuart, D. I.; Neidle, S., Crystal-Structure of a Berenil Dodecanucleotide Complex - the Role of Water in Sequence-Specific Ligand-Binding. *EMBO J.* **1990**, 9, 1329-1334.
59. Nguyen, B.; Lee, M. P. H.; Hamelberg, D.; Joubert, A.; Bailly, C.; Brun, R.; Neidle, S.; Wilson, W. D., Strong Binding in The DNA Minor Groove by an Aromatic Diamidine with a Shape That Does Not Match the Curvature of the Groove. *J. Am. Chem. Soc.* **2002**, 124, 13680-13681.
60. Phan, A. T.; Kuryavyi, V.; Gaw, H. Y.; Patel, D. J., Small-Molecule Interaction with a Five-Guanine-Tract G-Quadruplex Structure from the Human *MYC* Promoter. *Nat. Chem. Biol.* **2005**, 1, 167-173.
61. Fujimoto, T.; Nakano, S.; Sugimoto, N.; Miyoshi, D., Thermodynamics-Hydration Relationships within Loops That Affect G-Quadruplexes under Molecular Crowding Conditions. *J. Phys. Chem. B* **2013**, 117, 963-972.
62. Hansel, R.; Lohr, F.; Foldynova-Trantirkova, S.; Bamberg, E.; Trantirek, L.; Dotsch, V., The Parallel G-Quadruplex Structure of Vertebrate Telomeric Repeat Sequences Is Not The Preferred Folding Topology under Physiological Conditions. *Nucleic Acids Res.* **2011**, 39, 5768-5775.
63. Nakano, S.; Hirayama, H.; Miyoshi, D.; Sugimoto, N., Dimerization of Nucleic Acid Hairpins in the Conditions Caused by Neutral Cosolutes. *J. Phys. Chem. B* **2012**, 116, 7406-7415.

4. Development of an Assay for Telomerase Activity without False Negative Results

4.1. Introduction

In most human cancer cells, telomerase is highly-activated and plays a key role of the immortal cell proliferation, although the activity has not been detected in various normal somatic cells [1, 2]. Thus, telomerase has been suggested as a promising marker for cancer diagnosis. Several studies showed the association between the telomerase activity and a number of prognostic and clinopathological features in colorectal cancer [3-9]. For the diagnosis with telomerase activity as a marker, the assay for telomerase activity, which is precise and sensitive, is required.

A conventional assay for telomerase activity is TRAP assay (Fig. 2-13) [1]. In the assay, a telomerase reaction is carried out using an artificial oligodeoxynucleotide called TS primer, which serves as a primer for telomerase similarly to telomeric DNA. Following the telomerase reaction, the reaction products are amplified by PCR using TS primer as a forward primer. Finally, the amplification products are analyzed electrophoretically. Although TRAP assay is a powerful tool due to its high sensitivity, it is still difficult to apply to practical cancer diagnostics. This is because the assay is susceptible to polymerase inhibition by clinical extract, which leads to the false negative result [10]. Thus, many research groups have developed other telomerase assays based on various sensors or methodologies, such as optical fiber [11], magnetic resonance reader [12], magneto-mechanical detector [13], ISFET [14], electrochemical method [15], photonic microring device [16], and surface plasmon resonance method [14, 17]. In general, such assays do not utilize any signal amplification processes like PCR and were therefore less sensitive than TRAP assays. Other groups proposed telomerase assays with novel signal amplification processes involving enzymes [18-21], DNAzymes [22-24], and nanoparticles [25-28], instead of PCR. Although some of these assays with novel amplification reactions detected telomerase activity with high sensitivity, the enzymes used for catalysis-based amplification may be inhibited by components in clinical samples. Thus, a novel sensitive telomerase assay that can avoid such false negative results has been required. Here, to meet the requirement, a telomerase assay based on A-PCR [29, 30] on MBs and subsequent application of CPT [31] involving a Probe RNA and RNase H is reported.

4.2. Materials and Methods

4.2.1. Materials and Reagents

All deoxyribo-oligonucleotides were HPLC purification-grade deoxyribo-oligonucleotides, and were purchased from Tsukuba Oligo Service Co., Ltd., or were provided in a TRAPEZE telomerase detection kit from EMD Millipore Corporation (Billerica, MA, USA). λ DNA was purchased from Takara Bio Inc. All ribo-oligonucleotides were HPLC purification-grade ribo-oligonucleotides, and were purchased from Tsukuba Oligo Service Co., Ltd. HeLa and NHDF cells were provided in TRAPEZE telomerase detection kits and purchased from Toyobo Co., Ltd. (Osaka, Japan), respectively. RNase H was purchased from Takara Bio Inc. (Shiga, Japan). The polymerase used for PCR was the TaKaRa LA Taq HS that was provided the in TaKaRa LA Taq Hot Start Version from Takara Bio Inc. Streptavidin-coated MBs were Dynabeads M-280 purchased from Life Technologies Corporation (Carlsbad, CA, USA). Dynabeads M-280 were washed three times in a buffer containing 10 mM Tris-HCl (pH 7.5) and 2 M KCl before use. Cu-APC was purchased from Sigma-Aldrich corporation.

4.2.2. Preparation of Cell Lysate

A pellet of 10^6 cells was suspended in 200 μL of cold 3-**[(**3-Cholamidopropyl**)**dimethylammonio]-1-propanesulfonate (CHAPS) lysis buffer provided in the TRAPEZE telomerase detection kit. The cell lysate solution was dispensed into small volume aliquots and stored at -80°C. Each cell lysate aliquot was diluted in cold CHAPS lysis buffer as appropriate before use.

4.2.3. CPT for Model Sequence of Telomerase Products (MSTP) Detection

CPT for MSTP detection was performed to identify a probe RNA suitable for the A-PCR/CPT assay. Each type of probe RNA (100 nM) was annealed separately with each of several concentrations of MSTP in a buffer containing 50 mM Tris-HCl (pH8) and 4 mM $MgCl_2$. Each reaction solution was incubated with 0.1 U/μL RNase H at 30°C for 0.5 h, and then mixed with 50 mM Na_2EDTA to terminate the reaction; a fluorescence spectral scanning reader (Varioskan flash; Thermo Fisher Scientific Inc., Waltham, MA, USA) with excitation set to 482 nm was then used to measure the fluorescence intensity of the solution at 500-550 nm and 25°C.

4.2.4. MSTP Digestion Assay

To assess DNase activity in the HeLa cells lysates, HeLa cells lysate was incubated with MSTP, and subject to a digestion assay. MSTP (100 nM) was incubated at 37°C for 60 min with HeLa cell lysate solution containing 0 or 125 cells/μL in a buffer of 20 mM

Tris-HCl (pH 8.0) and 4 mM $MgCl_2$ or 10 mM Na_2EDTA. Each sample was then analyzed *via* gel electrophoresis on a 10% denaturing urea polyacrylamide gel in Tris-borate-EDTA buffer (pH 8.5) at 400 V. Each gel was stained with SYBR Gold nucleic acid gel stain (Life Technologies Corporation) and imaged using a fluorescence image analyzer (FLA-5100; Fuji photo film Co., Ltd., Tokyo, Japan).

4.2.5. Telomerase Reaction

Each telomerase reaction solution (10 μL) contained 1×TRAP buffer (TRAPEZE telomerase detection kit), 1×dNTPs (TRAPEZE telomerase detection kit), non-modified TS primer (TRAPEZE telomerase detection kit), HeLa cells lysate, and one of several concentrations of λ DNA; each mixture was incubated at 37°C for 60 min, heated at 95°C for 10 min, and cooled at 4°C. To generate telomerase reaction products that could be immobilized on MBs, 1 μM biotinylated TS primer was used instead of the non-modified TS primer.

4.2.6. Immobilization of Telomerase Reaction Products on MBs

A vortex was used to mix 10 μL of telomerase reaction product, which was generated with 1 μM biotinylated TS primer, with prewashed MBs (Dynabeads M-280) that were in 10 μL of a buffer containing 10 mM Tris-HCl (pH 7.5) and 2 M KCl; these 20 μL were mixed at 25°C for 30 min. The treated MBs were then subject to three sequential washes, each with 20 μL of buffer containing 10 mM Tris-HCl (pH 7.5) and 1 M NaCl, and one last wash with 20 μL of water.

4.2.7. A-PCR Amplification of Telomerase Reaction Products

A-PCR amplification of telomerase reaction products was carried out in a solution containing telomerase reaction products (telomerase reaction solutions or MBs with telomerase reaction products), 1×LA PCR Buffer II (Mg^{2+} plus), 1×dNTPs, any one of several concentrations of TS primer, 1 μM CX-ext primer, and 0.05 U/μL TaKaRa LA Taq HS, for 30 cycles with each cycle comprising denaturation at 95°C for 30 s, annealing at 59°C for 30 s, and extension at 72°C for 30 s. After A-PCR amplification, the reaction mixtures were cooled and stored at 4°C.

4.2.8. CPT for Detection of A-PCR Products

A-PCR products were detected by CPT. Each CPT reaction mixture (100 μL) contained A-PCR reaction mixture with products (10 μL), 100 nM probe RNA 2, 50

mM Tris-HCl (pH8), and 4 mM $MgCl_2$; each mixture was incubated with 0.1 U/μL RNase H at 37°C for 20 min. Na_2EDTA (50 mM) was added to terminate the reaction; a fluorescence spectral scanning reader (Varioskan flash) set with excitation at 482 nm was used to measure the fluorescence intensity of each solution at 500-550 nm and 25°C.

4.2.9. Normal PCR Amplification of Telomerase Reaction Products

PCR amplification of telomerase reaction products was carried out in a reaction mixtures that each contained telomerase reaction products, 1×LA PCR Buffer II (Mg^{2+} plus) (Takara Bio Inc.), 1×dNTPs (TRAPEZE telomerase detection kit), TS primer (TRAPEZE telomerase detection kit), Primer Mixture solution (TRAPEZE telomerase detection kit), and 0.05 U/μL TaKaRa LA Taq HS (Takara Bio Inc.); amplification occurred over 30 cycles, each comprising denaturation at 95°C for 30 s, annealing at 59°C for 30 s, and extension at 72°C for 30 s. After PCR amplification, each reaction mixture was cooled and stored at 4°C. The PCR products were analyzed by native gel electrophoresis on a 10% nondenaturing polyacrylamide gel in Tris-borate-EDTA buffer (pH 8.5) at 400 V. The gels were stained with GelStar nucleic acid gel stain and imaged using a fluorescent image analyzer (FLA-5100).

4.2.10. One-Step TRAP Assay (Conventional TRAP Assay)

Each one-step TRAP assay was carried out in a solution containing 1×TRAP buffer (TRAPEZE telomerase detection kit), 1×dNTPs (TRAPEZE telomerase detection kit), non-modified 1 μM TS primer, Primer Mixture solution (TRAPEZE telomerase detection kit), 0.05 U/μL TaKaRa LA Taq HS (Takara Bio Inc.), and HeLa cells lysate as follows: telomerase reaction for one cycle with incubation at 37°C for 30 min, and PCR for 30 cycles with denaturation at 95°C for 30 s, annealing at 59°C for 30 s, and extension at 72°C for 30 s; after each complete series of cycles, the solution was cooled at 4°C. The one-step TRAP products were analyzed by native gel electrophoresis on a 10% nondenaturing polyacrylamide gel in Tris-borate-EDTA buffer (pH 8.5) at 400 V. The gels were stained with GelStar nucleic acid gel stain and imaged using a fluorescent image analyzer (FLA-5100).

4.3. Results and Discussion

4.3.1. Detection Principle

Figure 4-1 depicts the principle of the telomerase assay described here. In principle,

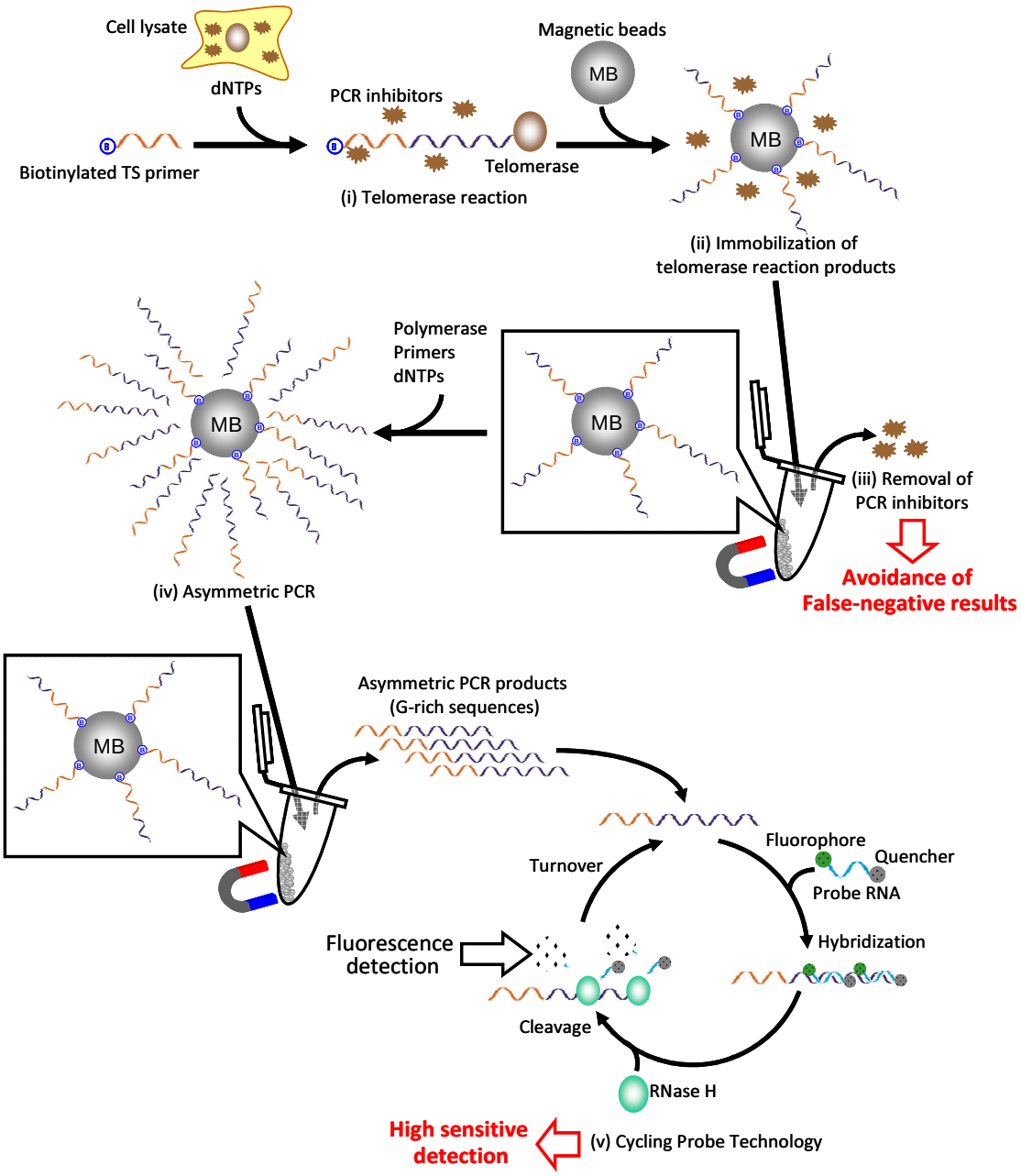

Fig. 4-1. Strategy for the telomerase assay based on A-PCR on MBs and CPT: (i) telomerase in crude clinical extract elongates the telomeric DNA sequence from biotinylated TS primer, (ii) telomerase reaction products are immobilized on MBs *via* interaction between biotin and streptavidin, (iii) MBs coated with the telomerase products are washed to remove PCR inhibitors, (iv) the G-rich sequences of the telomerase products are preferentially amplified *via* A-PCR, and (v) amplified G-rich sequences are detected by CPT.

the assay includes the following steps: (i) telomerase elongates telomeric DNA sequence *via* a biotinylated TS primer (Table 4-1), which serves as a substrate for telomerase elongation, (ii) the biotin-labelled telomerase reaction products are immobilized on streptavidin-coated MBs *via* interaction between biotin and streptavidin, (iii) MBs coated with telomerase products are washed to remove sample contaminants including PCR inhibitors, (iv) the G-rich sequences of the telomerase products are preferentially amplified by A-PCR, and (v) amplified G-rich sequences are then detected *via* CPT. In CPT, a probe RNA with a fluorophore (fluorescein isothiocyanate; FITC) and a quencher (4-(dimethylaminoazo)benzene-4-carboxylic acid; Dabcyl) at the 5' end and 3' end, respectively, hybridizes with the G-rich sequences. The hybridized probe RNA is hydrolyzed by RNase H, which recognizes RNA/DNA duplex and selectively hydrolyzes RNA in heteroduplexes. Before hydrolysis, fluorescence from FITC is quenched by fluorescence resonance energy transfer (FRET) due to proximity between FITC and Dabcyl. However, the hydrolysis of the probe RNA separates FITC from Dabcyl, which results in enhancement of the FITC fluorescence. Additionally, each reaction, including the hybridization of the probe RNA with the telomerase reaction products and the hydrolysis of the hybridized probe RNA by RNase H, occurs iteratively, which leads to a catalytic amplification of FITC signal. Importantly, in principle, the false negative results caused by PCR inhibitors should be completely avoided, and the combined application of A-PCR and CPT should lead to highly sensitive and selective detection of telomerase activity.

4.3.2 Design of the Probe RNA

The sequence and design of the probe RNA used for CPT is responsible for the sensitivity of this assay. Reducing the length of the probe should show lower background signals because FITC should be in closer proximity to Dabcyl; however, affinity between the probe and telomerase products should be lower with shorter probes. Conversely, longer probes should exhibit higher affinity for telomerase products and higher background signal. To optimize the probe RNA, four probes with FITC and Dabcyl at the 5' end and 3' end, respectively, were designed; the probes differed from one another in length and in sequence (Table 4-1).

First, the RNase H reaction was carried out separately for each probe with 100 nM of probe in the absence or the presence of 100 nM MSTP (Table 4-1) at 37 °C for 30 min. For probe 1, an obvious peak of fluorescence with a maximum intensity around 520 nm was observed in the presence of both RNase H and MSTP (Fig. 4-2A). In contrast, in the absence of MSTP, the peak at 520 nm was clearly smaller, and the fluorescence at

Table 4-1. RNA oligonucleotides used in this study

Name	Sequence	Modification
Probe 1 [a]	5'-CCCUAA-3'	5'-FITC/3'-Dabcyl
Probe 2 [a]	5'-CCCUAACCC-3'	5'-FITC/3'-Dabcyl
Probe 3 [a]	5'-CUAACCCUAAC-3'	5'-FITC/3'-Dabcyl
Probe 4 [a]	5'-CCCUAACCCUAACCC-3'	5'-FITC/3'-Dabcyl
MSTP [b]	5'-$(GGGTTA)_{16}$-3'	none
TS primer [c]	5'-AATCCGTCGAGCAGAGTT-3'	none
Biotinylated TS primer [d]	5'-AATCCGTCGAGCAGAGTT-3'	5'-biotinylation
CX-ext [e]	5'-GTGCCCTTACCCTTACCCTTACCCTAA-3'	none

[a] Probes are FRET-modified complementary RNAs to telomere sequence. [b] MSTP is a model sequence of a telomerase product. [c] TS primer is a substrate DNA for telomerase and a forward primer for PCR amplification of telomerase reaction products. [d] Biotinylated TS primer is a TS primer with a 5' biotin moiety for immobilization on streptavidin-coated magnetic beads. [e] CX-ext is a reverse primer for PCR amplification of telomerase reaction products.

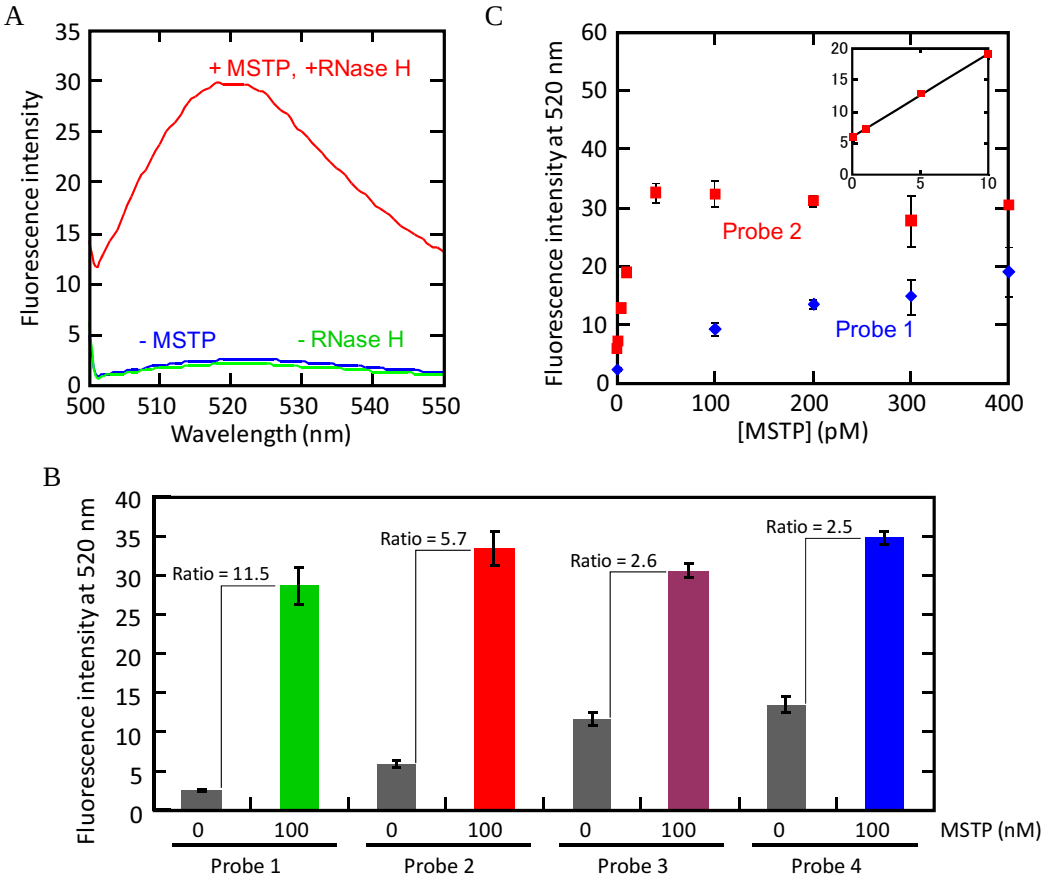

Fig. 4-2. (A) Fluorescence spectra with probe 1 in the absence of 0.1 U/μL RNase H (green) or 100 nM MSTP (blue), or presence of both (red). (B) Fluorescence at 520 nm with probes 1-4 in the absence or presence of 100 nM MSTP. Each value is the average calculated from the three replicate data sets and each error bar represents the standard deviation. (C) Plots of fluorescence at 520 nm with probe 1 or probe 2 vs. MSTP concentration. Each data point is the average calculated from the three replicate data sets and each error bar represents the standard deviation.

520 nm was about an eighteenth part of that in the presence of both RNase H and MSTP (Fig. 4-2A). Additionally, the fluorescence in the absence of RNase H was almost identical to that in the absence of MSTP. These results indicate that probe 1 hybridized with MSTP and that as expected RNase H hydrolyzed only the hybridized probe. Each other probe (probes 2, 3, and 4) also exhibited more fluorescence in the presence of MSTP than that in the absence of MSTP (Fig. 4-2B). However, the signal/background ratio values of probe 3 (2.6) and probe 4 (2.5) were less than those of probe 1 (11.5) and probe 2 (5.7). This difference occurred because, in the absence of MSTP, longer probes (probes 3 and 4) resulted in higher background fluorescence than did shorter probes (probes 1 and 2, Fig. 4-2B). The sensitivities of probes 1 and 2 were further investigated by carrying out the RNase H reaction with different concentrations (0-400 pM) of MSTP. The fluorescence at 520 nm of probe 1 decreased gradually as the concentration of MSTP decreased (Fig. 4-2C). However, the fluorescence from probe 2 with concentrations of MSTP between 80-400 pM were similar to each other and higher than those from probe 1; the fluorescence from probe 2 did decrease with decreases in MSTP concentration from 0-60 pM MSTP (Fig. 4-2C). Furthermore, a linear relationship between MSTP concentration and probe 2 fluorescence was found; the correlation equation for this relationship was probe 2 fluorescence at 520 nm = 6.01 + 1.31 × (MSTP concentration (pM)) (R^2 = 0.9986) in the range of 0-10 pM (inset in Fig. 4-2C). Since a probability of that the fluorescence of the blank sample is larger than the 3.3 times of its standard deviation (δ) is too low (0.05%) according to a standard normal distribution, the reliable detection limit with probe 2 was calculated to be 0.99 pM using the following equation (1):

$$DL = 3.3\,\delta / S \quad (1)$$

where DL is the detection limit; δ is the standard deviation of the blank sample; and S is the slope of the correlation equation obtained by the linear relationship. The reaction volume was 100 μL; therefore, CPT with probe 2 should be detected MSTP at concentrations as low as 0.1 fmol. This concentration is two orders of magnitude lower

than that detectable with conventional gel electrophoresis analysis, 10 fmol (Fig. 4-3). These results showed that probe 2 is suitable for CPT and detection of telomerase reaction products.

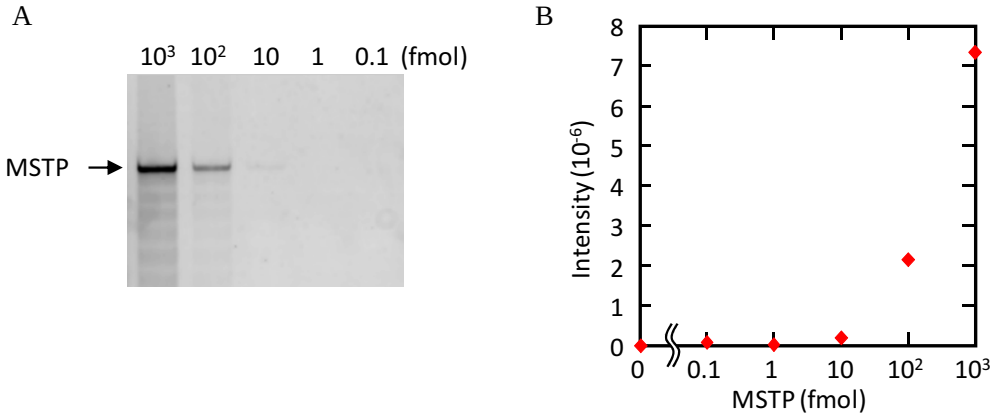

Fig. 4-3. (A) Electrophoresis results of five different amounts of MSTP. (B) Relationship between band intensity of and amount of MSTP.

4.3.3. Inhibition of Degradation of Telomerase Reaction Products by Decoy DNA

Cell lysate used without any prior purification contains various intracellular biomolecules, including DNase, that can degrade the products of telomerase reactions. Therefore, contaminants such as DNase can lead to false negative results from telomerase assays. To confirm that such problems occur, MSTP with or without HeLa cells lysate was kept in a buffer containing 50 mM MES-LiOH (pH 7.0) and 4 mM $MgCl_2$ at 37°C for 60 min, and the degradation of MSTP was analyzed *via* gel electrophoresis. In the absence of HeLa cell lysate, a band corresponding to MSTP was observed (Fig. 4-4A); however, addition of HeLa cells lysate reduced the MSTP band. Moreover, when EDTA was used instead of Mg^{2+}, addition of HeLa cells lysate did not reduce MSTP band (Fig. 4-4A). Since DNase requires divalent cations to activate the enzyme [32], these results indicated that DNase in cell lysate can degrade telomerase reaction products. To prevent such degradation, it was reasoned that addition of excess decoy DNA could prevent DNase from degrading the telomerase reaction products because the decoy DNA should serve as a competitive substrate for DNase. This assumption was confirmed by performing telomerase reaction with HeLa cells lysate in the absence or presence of various concentrations of λ DNA as the decoy DNA. The telomerase reaction mixtures were diluted 50-fold to reduce the influence of the decoy λ DNA on subsequent PCR; the telomerase reaction products were then amplified *via* PCR. PCR products were monitored *via* gel electrophoresis (Fig. 4-4B). In the absence

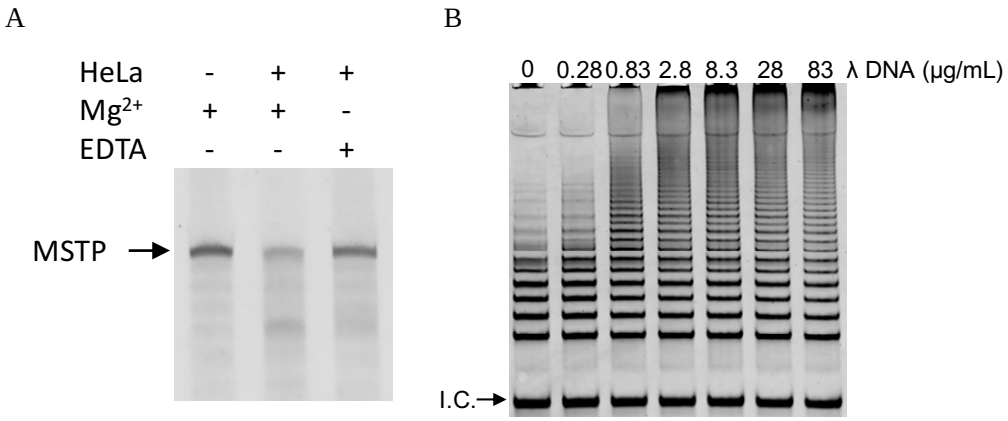

Fig. 4-4. (A) Electrophoresis of MSTP-based telomerase reaction products in the absence or presence of HeLa cells lysates, Mg^{2+}, and EDTA. (B) Electrophoresis of PCR-amplified telomerase reaction products synthesized in the presence of various concentrations of λ DNA.

of λ DNA, long telomerase products were not abundant (Fig. 4-4B), indicating that DNase in HeLa cells lysate degraded the telomerase reaction products. However, long telomerase products were observed telomerase reactions containing λDNA, and the abundance of long products increase with increasing concentrations of λ DNA (Fig. 4-4B). These results indicate that λ DNA efficiently inhibited DNase from degrading the telomerase reaction products by serving as a competitive substrate for DNase. Thus, addition of excess decoy DNA is a useful, easy, and cost-effective method for avoiding false negative results caused by DNase.

4.3.4. Optimization of Primers Concentrations for A-PCR

In the present assay, CPT with probe RNA and RNase H is used to achieve high sensitivity. A target DNA for CPT should be ssDNA, which can binds to probe RNA. Not normal PCR but A-PCR is appropriate for generating the target DNA, because the predominant product of A-PCR is ssDNA extended from a primer that is present in much higher concentrations than its partner primer [29, 30]. However, extremely different concentrations between the forward primer and the reverse primer can generate undesired artifact products. Thus, to optimize the concentration ratio of forward/reverse primers, telomerase reaction products in the absence or presence of 200 HeLa cells lysate were amplified by A-PCR with 1 μM to 50 μM TS primer and 1 μM CX-ext primer [33, 34] (Table 4-1) as the forward and reverse primers, respectively. The CX-ext primer (5'-GTGCCCTTACCCTTACCCTTACCCTAA-3') is complementary to four telomere repeats but contains a single base mismatch at the same position in each of

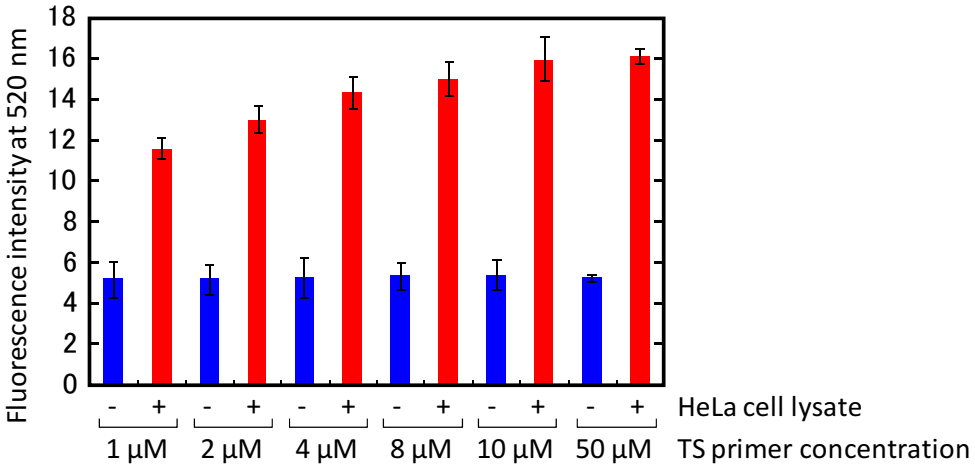

Fig. 4-5. Fluorescence at 520 nm of probe 2 resulting from CPT with telomerase reaction products amplified *via* A-PCR using five different concentrations of TS primer. Each value is the average calculated from the three replicate data sets and each error bar represents the standard deviation.

three of the telomere repeats, and has three additional non-complementary nucleotides at its 5' end [33, 34]. Therefore, the CX-ext primer functions as a reverse primer that reduces PCR-associated artifacts [33, 34]. CPT with probe 2 was used to detect the products amplified *via* A-PCR. In the absence of HeLa cell lysate, the fluorescence from probe 2 at 520 nm was identical to the fluorescence from probe 2 without MSTP (Compare the intensity from probe 2 without MSTP in Fig. 4-2 (B) and the intensity from probe 2 without HeLa cell lysate shown in Fig. 4-5). In addition, the fluorescence without HeLa cell lysate did not depend on the concentration of TS primer (Fig. 4-5). These results indicate that even highly concentrated TS primer did not generate any artifacts when paired with CX-ext primer, even though highly concentrated primers often cause PCR-associated artifacts. On the contrary, in the presence of HeLa cells lysate, the fluorescence from probe 2 with each concentration of TS primer was higher than that in the absence of HeLa cells lysate (Fig. 4-5). In addition, increases in the primer concentration up to 10 μM TS primer enhanced the fluorescence at 520 nm, and the fluorescence with 50 μM TS primer was almost the same as that with 10 μM TS primer. These results indicated that the amount of ssDNA that comprised telomere repeats increased as the concentration of TS primer increased up to 10 μM. Thus, 10 μM TS primer and 1 μM CX-ext primer were used in each subsequent assay.

4.3.5. Detection of Telomerase Activity in Cells Lysate

Based on the results described above, telomerase activity in HeLa cells lysate could

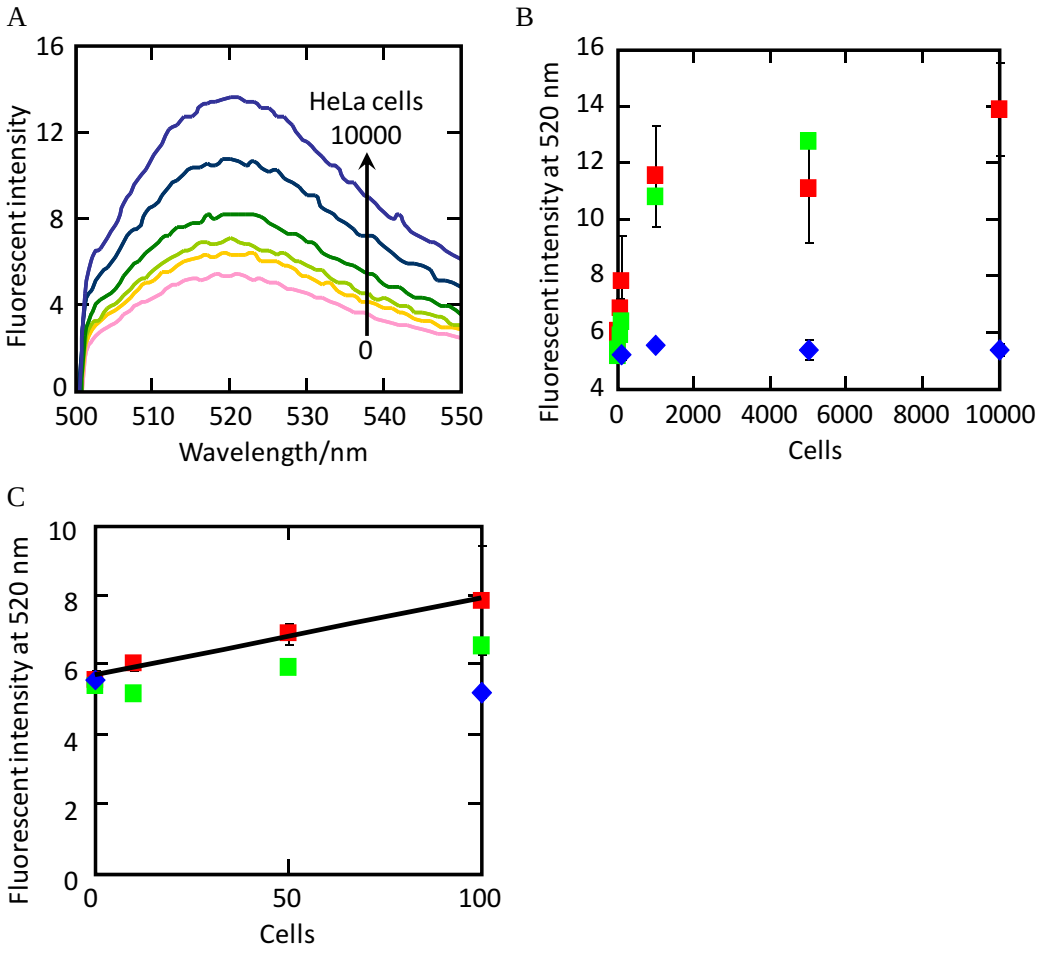

Fig. 4-6. (A) Fluorescence spectra results from the A-PCR/CPT assays run with lysate with various concentrations of HeLa cells. (B, C) Plots of fluorescence intensity at 520 nm vs. the number of cells (red square: HeLa cells, blue diamond: NHDF cells, green square: HeLa cells in the presence of 5000 NHDF cells). Each data point for HeLa cells (red square) and NHDF cells (blue diamond) is the average calculated from the three replicate data sets, and each error bar represents the standard deviation.

be detected as follows: (i) Telomerase reaction carried out in the presence of λ DNA at 37°C for 60 min. (ii) Telomerase reaction products immobilized on MBs at 25°C for 30 min, and then washed with clean buffer. (iii) Telomerase reaction products on MBs amplified over 30 cycles of A-PCR with 10 μM TS primer and 1 μM CX-ext primer. (iv) A-PCR products detected by CPT with probe 2. These procedures were carried out with various numbers of HeLa cells (Fig. 4-6A). The fluorescence at 520 nm increased as a function of the number of HeLa cells (red square in Fig. 4-6B). A linear relationship between fluorescence intensity and HeLa cell number was also found; the correlation equation was fluorescence intensity = 5.71 + 0.022 × (number of HeLa cell) (R^2 =

0.984) within the range of 0-100 cells (red square in Fig. 4-6C). Based on this linear relationship, the limit of detection was calculated to be 50 cells using the above equation (1). These results indicate that the difference between the signal from 50 HeLa cells and that from no HeLa cells was statistically significant and the sensitivity of the present assay is higher than that of the common TRAP assay [35, 36]. In contrast, 100, 1000, 5000, or 10000 NHDF cells, which have no telomerase activity, caused no fluorescence when used in our assay ((the fluorescent intensity with NHDF cells) - (the fluorescence intensity with no cells) < 0.01) (blue diamond in Figs. 4-6B and 4-6C). These results demonstrate that the fluorescence intensity depends on the telomerase activity. In addition, the fluorescence intensity when probing samples from 100–10000 NHDF cells was almost the same as that when probing samples lacking cells, although RNA is very unstable especially in clinical samples. This lack of background probably resulted because the probe RNA was added into each CPT reaction mixture after most components of the cell extracts were separated from the telomerase reaction products. Thus, the probe RNA was not degraded by irrelevant components of the cell extracts, thereby avoiding false-positive results. These results indicate that this assay should be useful for detecting cancer cells with high sensitivity and specificity. Importantly, it was also found that, due to the high sensitivity, the fluorescence corresponding to the number of HeLa cells in the presence of 5000 NHDF cells (green square in Fig. 4-6B) was identical to that in the absence of NHDF cells. These results indicate that the assay allows the accurate detection of cancer cells even in the presence of a large excess of normal cells. Therefore, the assay should be practical for the detection of cancer cells in clinical samples.

4.3.6. Eliminating False Negative Results Caused by PCR Inhibitors

PCR inhibitors that exist in cells quantitatively reduce PCR amplification. The previous study showed that bile salt, heparin, and hemoglobin inhibited PCR at ≤ 1 mg/mL, ≤ 1 IU/mL, and ≤ 1 mg/mL order or less, respectively [37]. The washing process on MBs in the present assay should eliminate the false negative results caused by such inhibitors. Therefore, effects of these PCR inhibitors—bile salt (1 mg/mL), heparin (2 IU/mL), and hemoglobin (1 mg/mL)—on the common one-step TRAP assay and our A-PCR/CPT assay were investigated; both assays were runs with HeLa cells lysate. In the one-step TRAP assay, all reagents for telomerase reaction and PCR, and the PCR inhibitors are included together in the reaction solution during the telomerase reaction and the PCR. The gel resulting from the one-step TRAP assay showed that ladder-like bands corresponding to the TRAP assay products and an internal control

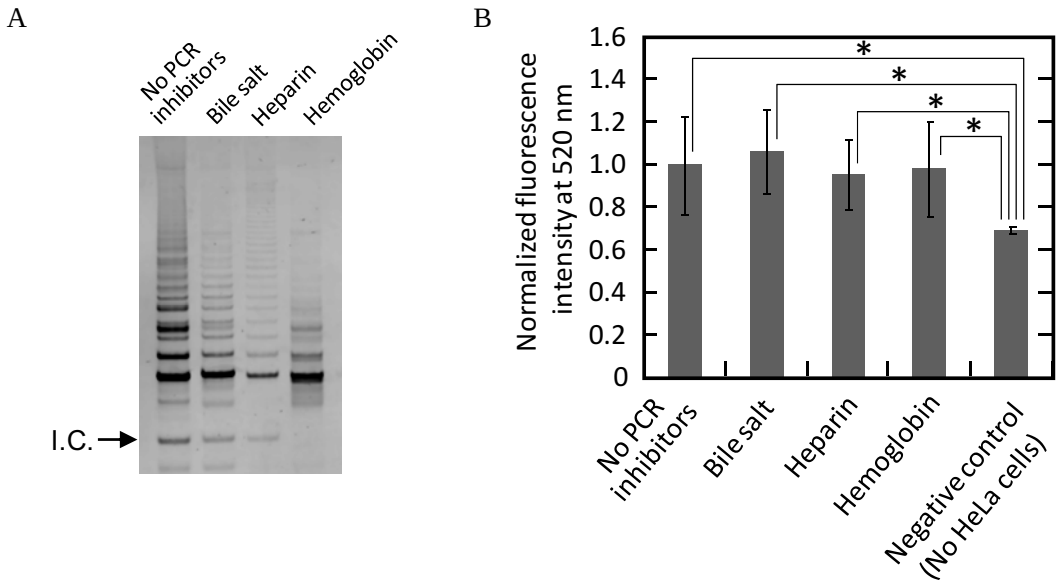

Fig. 4-7. (A) Electrophoresis results from the one-step TRAP assay in the absence or presence of individual PCR inhibitors. (B) Fluorescence intensity results from the A-PCR/CPT assay with or without individual PCR inhibitors. Each value is the average calculated from the five replicate data sets and each error bar represents the standard deviation. * p <0.05.

band corresponding to PCR products from a 36-bp template were evident in the absence of PCR inhibitors (lane 1 in Fig. 4-7A). However, each inhibitor drastically reduced the amount of TRAP assay product and the internal control PCR products (lanes 2-4 in Fig. 4-7A). These results indicate that a reduction of TRAP assay products was caused, at least in part, by PCR inhibitors. In contract, the fluorescence intensity results from the A-PCR/CPT assay showed that the fluorescence at 520 nm was similar regardless of the presence or absence of bile salt, hemoglobin, or heparin, and their fluorescence was significantly larger than that from the negative control without HeLa cells (p value <0.05) (Fig. 4-7B). These results indicate that the A-PCR/CPT assay, unlike the common one-step TRAP assay, can detect telomerase activity and simultaneously avoid the false negative results caused by PCR inhibitors including bile salt, heparin, and hemoglobin. Thus, the present assay should detect cancer cells with more accurately than the common one-step TRAP assay in the presence of PCR inhibitors.

4.3.7. Comparison with Other Telomerase Assays

Among a lot of telomerase assays developed so far, some have a washing procedure, in which telomerase reaction products immobilized on a solid phase such as a substrate and a particle are washed (Table 4-2) [13-17, 19, 20, 26-28, 38]. Their detection should

Table 4-2. Comparison of telomerase assays with a washing process.

Principle	Cell	Detection limit (cells)	Detection time [c]	Ref.
Magneto-mechanical detection of MB with telomerase products	HeLa	100	> 30 min	13
Telomerase reaction analysis by ISFET	293T	65±10 cells/μL [a]	1 h	14
SPR analysis of telomerase reaction	293T	18±3 cells/μL [a]	1 h	14
Electrochemical detection using ferrocene-based telomeric G-quadruplex-ligand	HeLa	80-280 [b]	1 h 15 min	15
Detection of resonance wavelength shift caused by telomerase reaction	J-82 HT-1376	100 cells in buffer 1000 cells in urine	1 h 30 min	16
SPR analysis of telomerase reaction	T47-D	100 cancer cells in 100000 normal cells	10 min	17
ELISA for telomerase products	293T	37500	> Over night	19
QCM analysis of BCIP precipitation catalyzed by alkaline phosphatase, which is linked to telomerase products	HeLa	1000	11 h	20
Detection of Ag stain on AuNP with telomerase products	HeLa	10	7 h	26
Detection of ECL ($Ru(bpy)_3^{2+}$) modified probe DNA on AuNP, which binds to	HeLa	500	2 h 30 min	27
Detection of ECL ligand ($[Ru(NH_3)_6]^{3+}$) bound to DNA on AuNP, which binds to	HeLa	10	4 h 30 min	28
Luminescence analysis of luminol oxidation by G-quadruplex DNAzyme of probe DNA	HeLa	1000	17 h	38
Combination of A-PCR of telomerase products on MB and CPT	HeLa	50 (5 cells/μL)	2 h 50 min (Telomerase reaction: 30 min, PCR: 1 h 30 min, CPT: 20 min)	This thesis

ISFET: ion-sensitive field-effect transmitter, SPR: surface plasmon resonance, ELISA: enzyme-linked immunosolbent assay, QCM: quartz crystal microbalance, BCIP: 5-bromo-4-chloro-3-indolyl phosphate, AuNP: Au nanoparticle, ECL: electrochemiluminescence,

[a] Detection limit of numbers of cancer cells (293T) is not shown in ref. 14. [b] Good correlation between electrochemical signal and numbers of cancer cells (HeLa cells) were observed in the range of 80-280 cancer cells. [c] Detection time does not include manual procedures.

not be affected by clinical samples due to the washing procedure. Thus, like the present assay, these assays can also be suitable for clinical application. Especially, the assays utilizing detection principles of Ag stain on Au nanoparticle (AuNP) with telomerase product on a chip [26] and $[Ru(NH_3)_6]^{3+}$ bound to DNA on AuNP, which binds to telomerase product [28], showed a higher sensitivity of cancer cells (10 HeLa cells for both assays) than the present assay (50 HeLa cells) (Table 4-2). However, they take a long time (7 h and 4.5 h, respectively) (Table 4-2). In contrast, magneto-mechanical analysis of MB with telomerase reaction products takes a relatively short time (30 min), but its detection limit is 100 HeLa cells [13], which twice as many as that of the present assay (Table 4-2). Although SPR analysis of telomerase reaction also achieved a rapid detection, it can not be compared with the present assay because of different target

cancer cells [17] (Table 4-2). Furthermore, the present assay should enable a short detection because it uses PCR. Previously, PCR was cumbersome and took long hours. However, current improvement of DNA polymerases and development of lab-on-a-chip (LoC) technology for PCR allows DNA amplification in about 10 minutes or less [39-41]. Thus, the present assay with LoC technology should enable the detection of cancer cells in 1.5 hour (1 hour for telomerase reaction, 10 minutes for PCR, and 20 minutes for CPT). In the future, patients may be informed their cancer diagnosis on the same day utilizing a LoC chip performing the present assay.

4.3.8. Evaluation of Telomerase Inhibitory Effects of Anionic Phthalocyanine

Telomeric DNA can form four-stranded DNA called G-quadruplex [42, 43]. G-quadruplex does not serve as a substrate DNA for telomerase [44]; therefore, G-quadruplex-ligands that inhibit telomerase activity are promising as anticancer drugs [45]. For development of G-quadruplex-ligands, a quantitative evaluation of the telomerase inhibitory effects of such ligands is required. Reportedly, the common one-step TRAP assay is not appropriate for such evaluation because G-quadruplex-ligands can also inhibit PCR and lead to false negative results [46]. In contrast, the A-PCR/CPT assay can accurately evaluate the inhibitory effects of these ligands because this assay should eliminate PCR inhibition as demonstrated above. To assess this supposition, the A-PCR/CPT assay was used to evaluate the effects of a G-quadruplex-ligand on telomerase activity. For this purpose, the A-PCR/CPT assay was carried out with lysate from 1000 HeLa cells and in the presence of 0-20 μM

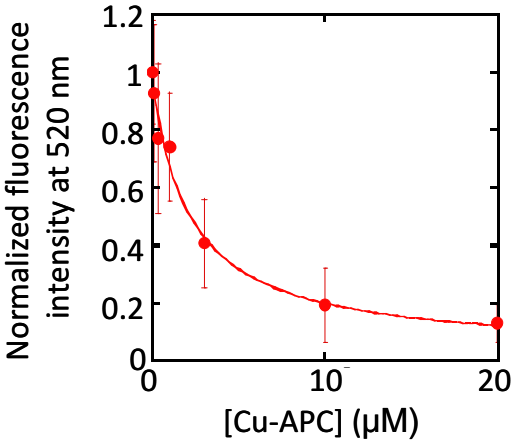

Fig. 4-8. Fluorescence intensity results from the A-PCR/CPT assay in the presence of various concentration of Cu-APC. Each data point is the average calculated from the three replicate data sets and each error bar represents the standard deviation.

Cu-APC, which binds to G-quadruplex DNA specifically over dsDNA and inhibits telomerase activity [47-50]. The normalized fluorescence intensity at 520 nm was plotted versus the concentration of Cu-APC, and the fluorescence decreased as a function of the concentration of Cu-APC (Fig. 4-8). This result indicates that Cu-APC inhibited telomerase. Based on the plot, the IC50 value of Cu-APC for telomerase activity was estimated to be 2.2 ± 0.5 μM. The value is identical to the IC50 value (1.2 or 1.4 μM) obtained by an improved TRAP assay [47, 50], which reduced the influence of Cu-APC on PCR by diluting the telomerase reaction products with Cu-APC. Therefore, the A-PCR/CPT assay can be used to screen for G-quadruplex-ligands that inhibit telomerase activity.

4.4. Conclusions

A telomerase assay based on A-PCR [29, 30] on MBs and subsequent application of CPT [31] involving a probe RNA and RNase H was developed. CPT with probe RNA 2 (5'-CCCUAACCC-3') detected MSTP comprising 5'-$(GGGTTA)_{16}$-3' with detection limit of 0.1 fmol; therefore, CPT was two orders of magnitude more sensitive than conventional gel electrophoresis analysis. Furthermore, this telomerase assay with probe RNA 2 could be used to specifically and sensitively detect HeLa cells among cell populations comprising predominantly NHDF cells. The detection limit of this assay for HeLa cells was 50 cells; therefore, this assay was more sensitive than the common TRAP assay. Moreover, it was shown that the assay eliminated false negative results caused by common components of clinical samples that inhibit PCR such as bile salt, hemoglobin, and heparin. These results demonstrated that the assay developed here is practical for detecting cancer cells in clinical samples.

4.5. References

1. Kim, N. W.; Piatyszek, M. A.; Prowse, K. R.; Harley, C. B.; West, M. D.; Ho, P. L. C.; Coviello, G. M.; Wright, W. E.; Weinrich, S. L.; Shay, J. W., Specific Association of Human Telomerase Activity with Immortal Cells and Cancer TTAGGG Repeats. *Science* **1994**, 266, 2011-2015.
2. Masutomi, K.; Yu, E. Y.; Khurts, S.; Ben-Porath, I.; Currier, J. L.; Metz, G. B.; Brooks, M. W.; Kaneko, S.; Murakami, S.; DeCaprio, J. A.; Weinberg, R. A.; Stewart, S. A.; Hahn, W. C., Telomerase Maintains Telomere Structure in Normal Human Cells. *Cell* **2003**, 114, 241-253.
3. Vidaurreta, M.; Maestro, M.; Rafael, S.; Veganzones, S.; Sanz-Casla, M.; Cerdan, J.; Arroyo, M., Telomerase Activity in Colorectal Cancer, Prognostic Factor and

Implications in the Microsatellite Instability Pathway. *World J. Gastroentero.* **2007**, 13, 3868-3872.

4. Uen, Y. H.; Lin, S. R.; Wu, D. C.; Su, Y. C.; Wu, J. Y.; Cheng, T. L.; Chi, C. W.; Wang, J. Y., Prognostic Significance of Multiple Molecular Markers for Patients with Stage II Colorectal Cancer Undergoing Curative Resection. *Ann. Surg.* **2007**, 246, 1040-1046.
5. Saleh, S.; Lam, A. K. Y.; Ho, Y. H., Real-Time PCR Quantification of Human Telomerase Reverse Transcriptase (hTERT) in Colorectal Cancer. *Pathology* **2008**, 40, 25-30.
6. Lam, A. K. Y.; Ong, K.; Ho, Y. H., Aurora Kinase Expression in Colorectal Adenocarcinoma: Correlations with Clinicopathological Features, p16 Expression, and Telomerase Activity. *Hum. Pathol.* **2008**, 39, 599-604.
7. Lam, A. K. Y.; Saleh, S.; Smith, R. A.; Ho, Y. H., Quantitative Analysis of Survivin in Colorectal Adenocarcinoma: Increased Expression and Correlation with Telomerase Activity. *Hum. Pathol.* **2008**, 39, 1229-1233.
8. Soreide, K.; Gudlaugsson, E.; Skaland, I.; Janssen, E. A. M.; Van Diermen, B.; Korner, H.; Baak, J. P. A., Metachronous Cancer Development in Patients with Sporadic Colorectal Adenomas - Multivariate Risk Model with Independent and Combined Value of hTERT and Survivin. *Int. J. Colorectal Dis.* **2008**, 23, 389-400.
9. Lam, A. K. Y.; Ong, K.; Ho, Y. H., hTERT Expression in Colorectal Adenocarcinoma: Correlations with p21, p53 Expressions and Clinicopathological Features. *Int. J. Colorectal Dis.* **2008**, 23, 587-594.
10. Kim, N. W.; Wu, F., Advances in Quantification and Characterization of Telomerase Activity by the Telomeric Repeat Amplification Protocol (TRAP). *Nucleic Acids Res.* **1997**, 25, 2595-2597.
11. Schmidt, P. M.; Lehmann, C.; Matthes, E.; Bier, F. F., Detection of Activity of Telomerase in Tumor Cells Using Fiber Optical Biosensors. *Biosens. Bioelectron.***2002**, 17, 1081-1087.
12. Grimm, J.; Perez, J. M.; Josephson, L.; Weissleder, R., Novel Nanosensors for Rapid Analysis of Telomerase Activity. *Cancer Res.* **2004**, 64, 639-643.
13. Weizmann, Y.; Patolsky, F.; Lioubashevski, O.; Willner, I., Magneto-Mechanical Detection of Nucleic Acids and Telomerase Activity in Cancer Cells. *J. Am. Chem. Soc.* **2004**, 126, 1073-1080.
14. Sharon, E.; Freeman, R.; Riskin, M.; Gil, N.; Tzfati, Y.; Willner, I., Optical, Electrical and Surface Plasmon Resonance Methods for Detecting Telomerase

Activity. *Anal. Chem.* **2010**, 82, 8390-8397.

15. Sato, S.; Kondo, H.; Nojima, T.; Takenaka, S., Electrochemical Telomerase Assay with Ferrocenyl Naphthalene Diimide as a Tetraplex DNA-Specific Binder. *Anal. Chem.* **2005**, 77, 7304-7309.
16. Kim, K. W.; Shin, Y.; Perera, A. P.; Liu, Q.; Kee, J. S.; Han, K.; Yoon, Y.-J.; Park, M. K., Label-Free, PCR-Free Chip-Based Detection of Telomerase Activity in Bladder Cancer Cells. *Biosens. Bioelectron.* **2013**, 45, 152-157.
17. Maesawa, C.; Inaba, T.; Sato, H.; Iijima, S.; Ishida, K.; Terashima, M.; Sato, R.; Suzuki, M.; Yashima, A.; Ogasawara, S.; Oikawa, H.; Sato, N.; Saito, K.; Masuda, T., A Rapid Biosensor Chip Assay for Measuring of Telomerase Activity Using Surface Plasmon Resonance. *Nucleic Acids Res.* **2003**, 31, e4.
18. Xu, S. Q.; He, M.; Yu, H. P.; Wang, X. Y.; Tan, X. L.; Lu, B.; Sun, X.; Zhou, Y. K.; Yao, Q. F.; Xu, Y. J.; Zhang, Z. R., Bioluminescent Method for Detecting Telomerase Activity. *Clin. Chem.* **2002**, 48, 1016-1020.
19. Kha, H.; Zhou, W.; Chen, K.; Karan-Tamir, B.; Miguel, T. S.; Zeni, L.; Kearns, K.; Mladenovic, A.; Rasnow, B.; Robinson, M.; Wahl, R. C., A Telomerase Enzymatic Assay That Does Not Use Polymerase Chain Reaction, Radioactivity, or Electrophoresis. *Anal. Biochem.* **2004**, 331, 230-234.
20. Pavlov, V.; Willner, I.; Dishon, A.; Kotler, M., Amplified Detection of Telomerase Activity Using Electrochemical and Quartz Crystal Microbalance Measurements. *Biosens. Bioelectron.* **2004**, 20, 1011-1021.
21. Ding, C. F.; Li, X. L.; Ge, Y.; Zhang, S. S., Fluorescence Detection of Telomerase Activity in Cancer Cells Based on Isothermal Circular Strand-Displacement Polymerization Reaction. *Anal. Chem.* **2010**, 82, 2850-2855.
22. Pavlov, V.; Xiao, Y.; Gill, R.; Dishon, A.; Kotler, M.; Willner, I., Amplified Chemiluminescence Surface Detection of DNA and Telomerase Activity Using Catalytic Nucleic Acid Labels. *Anal. Chem.* **2004**, 76, 2152-2156.
23. Yi, X.; Pavlov, V.; Gill, R.; Bourenko, T.; Willner, I., Lighting up Biochemiluminescence by the Surface Self-Assembly of DNA-Hemin Complexes. *Chembiochem* **2004**, 5, 374-379.
24. Xiao, Y.; Pavlov, V.; Niazov, T.; Dishon, A.; Kotler, M.; Willner, I., Catalytic Beacons for the Detection of DNA and Telomerase Activity. *J. Am. Chem. Soc.* **2004**, 126, 7430-7431.
25. Patolsky, F.; Gill, R.; Weizmann, Y.; Mokari, T.; Banin, U.; Willner, I., Lighting-up the Dynamics of Telomerization and DNA Replication by

CdSe-ZnS Quantum Dots. *J. Am. Chem. Soc.* **2003**, 125, 13918-13919.

26. Zheng, G. F.; Daniel, W. L.; Mirkin, C. A., A New Approach to Amplified Telomerase Detection with Polyvalent Oligonucleotide Nanoparticle Conjugates. *J. Am. Chem. Soc.* **2008**, 130, 9644-9645.
27. Zhou, X. M.; Xing, D.; Zhu, D. B.; Jia, L., Magnetic Bead and Nanoparticle Based Electrochemiluminescence Amplification Assay for Direct and Sensitive Measuring of Telomerase Activity. *Anal. Chem.* **2009**, 81, 255-261.
28. Li, Y.; Liu, B. W.; Li, X.; Wei, Q. L., Highly Sensitive Electrochemical Detection of Human Telomerase Activity Based on Bio-Barcode Method. *Biosens. Bioelectron.* **2010**, 25, 2543-2547.
29. Innis, M. A.; Myambo, K. B.; Gelfand, D. H.; Brow, M. A. D., DNA Sequencing with *Thermus aquaticus* DNA Polymerase and Direct Sequencing of Polymerase Chain Reaction-amplified DNA. *Proc. Natl. Acad. Sci. USA* **1988**, 85, 9436-9440.
30. Williams, J. F., Optimization Strategies for the Polymerase Chain Reaction. *Biotechniques* **1989**, 7, 762-769.
31. Bekkaoui, F.; Poisson, I.; Crosby, W.; Cloney, L.; Duck, P., Cycling Probe Technology with RNase H Attached to an Oligonucleotide. *Biotechniques* **1996**, 20, 240-248.
32. Campbell, V. W.; Jackson, D. A., The Effect of Divalent Cations on the Mode of Action of DNase I. *J. Biol. Chem.* **1980**, 255, 3726-3735.
33. Krupp, G.; Kuhne, K.; Tamm, S.; Klapper, W.; Heidorn, K.; Rott, A.; Parwaresch, R., Molecular Basis of Artifacts in the Detection of Telomerase Activity and a Modified Primer for a More Robust 'TRAP' Assay. *Nucleic Acids Res.* **1997**, 25, 919-921.
34. Saldanha, S. N.; Andrews, L. G.; Tollefsbol, T. O., Analysis of Telomerase Activity and Detection of Its Catalytic Subunit, hTERT. *Anal. Biochem.* **2003**, 315, 1-21.
35. Gang, Z. R.; Wang, X. W.; Yuan, J. H.; Guo, L. X.; Xie, H., Using a Non-radioisotopic, Quantitative TRAP-based Method Detecting Telomerase Activities in Human Hepatoma Cells. *Cell Res.* **2000**, 10, 71-77.
36. Tian, T.; Peng, S.; Xiao, H.; Zhang, X. E.; Guo, S.; Wang, S. R.; Zhou, X.; Liu, S. M., Highly Sensitive Detection of Telomerase Based on a DNAzyme Strategy. *Chem. Commun.* **2013**, 49, 2652-2654.
37. Abu al-Soud, W.; Radstrom, P., Purification and Characterization of PCR-inhibitory Components in Blood Cells. *J. Clin. Microbiol.* **2001**, 39,

485-493.

38. Niazov, T.; Pavlov, V.; Xiao, Y.; Gill, R.; Willner, I., DNAzyme-functionalized Au Nanoparticles for the Amplified Detection of DNA or Telomerase Activity. *Nano Lett.* **2004**, 4, 1683-1687.
39. Zhang, C. S.; Xing, D., Miniaturized PCR Chips for Nucleic Acid Amplification and Analysis: Latest Advances and Future Trends. *Nucleic Acids Res.* **2007**, 35, 4223-4237.
40. Majeed, B.; Jones, B.; Tezcan, D. S.; Tutunjyan, N.; Haspeslagh, L.; Peeters, S.; Fiorini, P.; Op de Beeck, M.; Van Hoof, C.; Hiraoka, M.; Tanaka, H.; Yamashita, I., Silicon Based System for Single-Nucleotide-Polymorphism Detection: Chip Fabrication and Thermal Characterization of Polymerase Chain Reaction Microchamber. *Jpn. J. Appl. Phys.* **2012**, 51, 04DL01-04DL01-9.
41. Tanaka, H.; Fiorini, P.; Peeters, S.; Majeed, B.; Sterken, T.; Op de Beeck, M.; Hayashi, M.; Yaku, H.; Yamashita, I., Sub-Micro-Liter Electrochemical Single-Nucleotide-Polymorphism Detector for Lab-on-a-Chip System. *Jpn. J. Appl. Phys.* **2012**, 51, 04DL02-1-04DL02-6.
42. Sundquist, W. I.; Klug, A., Telomeric DNA Dimerizes by Formation of Guanine Tetrads between Hairpin Loops. *Nature* **1989**, 342, 825-829.
43. Williamson, J. R.; Raghuraman, M. K.; Cech, T. R., Mono-valent Cation Induced Structure of Telomeric DNA - the G-quartet Model. *Cell* **1989**, 59, 871-880.
44. Zahler, A. M.; Williamson, J. R.; Cech, T. R.; Prescott, D. M., Inhibition of Telomerase by G-Quartet DNA Structures. *Nature* **1991**, 350, 718-720.
45. Sun, D. Y.; Thompson, B.; Cathers, B. E.; Salazar, M.; Kerwin, S. M.; Trent, J. O.; Jenkins, T. C.; Neidle, S.; Hurley, L. H., Inhibition of Human Telomerase by a G-Quadruplex-Interactive Compound. *J. Med. Chem.* **1997**, 40, 2113-2116.
46. De Cian, A.; Cristofari, G.; Reichenbach, P.; De Lemos, E.; Monchaud, D.; Teulade-Fichou, M. P.; Shin-Ya, K.; Lacroix, L.; Lingner, J.; Mergny, J. L., Reevaluation of Telomerase Inhibition by Quadruplex Ligands and Their Mechanisms of Action. *Proc. Natl. Acad. Sci. USA* **2007**, 104, 17347-17352.
47. Yaku, H.; Murashima, T.; Miyoshi, D.; Sugimoto, N., Anionic Phthalocyanines Targeting G-quadruplexes and Inhibiting Telomerase Activity in the Presence of Excessive DNA Duplexes. *Chem. Commun.* **2010**, 46, 5740-5742.
48. Yaku, H.; Murashima, T.; Miyoshi, D.; Sugimoto, N., Specific Binding of Anionic Porphyrin and Phthalocyanine to the G-quadruplex with a Variety of *in Vitro* and *in Vivo* Applications. *Molecules* **2012**, 17, 10586-10613.

49. Yaku, H.; Fujimoto, T.; Murashima, T.; Miyoshi, D.; Sugimoto, N., Phthalocyanines: a New Class of G-quadruplex-ligands with Many Potential Applications. *Chem. Commun.* **2012**, 48, 6203-6216.
50. Yaku, H.; Murashima, T.; Miyoshi, D.; Sugimoto, N., Study on Effects of Molecular Crowding on G-quadruplex-ligand Binding and Ligand-mediated Telomerase Inhibition. *Methods* **2013**, 64, 19-27.

5. Perspective

5.1. Elucidation of Rules to Design Anticancer Drugs with Efficient Telomerase Inhibitory Effect

Most G-quadruplex-ligands developed to date are cationic for telomerase inhibition by strong binding to G-quadruplex *via* electrostatic attractive interaction [1-3]. However, this thesis elucidated that anionic functional groups of G-quadruplex-ligands contribute to G-quadruplex-binding and telomerase-inhibiting capacites of the ligands under abundant dsDNA condition and MC conditions. In addition, large π-planar compounds such as phthalocyanine and porphyrin preferentially accumulated in cancer cells [4], and anionic compounds are expected to exhibit long blood retention properties and high transfection efficiency because they do not participate in electrostatic interactions with lipoproteins or seric proteins [5, 6]. Consequently, it was demonstrated that large π-planar compounds with anionic functional groups can be new scaffolds to develop G-quadruplex-ligands as anticancer drugs. This strategy may also be useful to improve the capacity of numerous G-quadruplex-ligands reported previously.

Furthermore, recent bioinformatic studies have shown that many putative G-quadruplex-forming sequences in the genome are enriched in the promoter regions of oncogenes including *c-MYC, c-kit, HRAS* and *KRAS* [1, 2, 7-10]. These bioinformatic studies strongly indicate that G-quadruplexes can influence carcinogenesis by modulating transcription of oncogenes. Importantly, some G-quadruplex-ligands regulate the expression of these oncogenes by binding to G-quadruplexes in the promoter regions [1, 2, 7, 8]. Thus, anionic G-quadruplex-ligands are also expected to bind to G-quadruplexes in the promoter regions of oncogenes and regulate their expression.

5.2. Development of an Assay for Telomerase Activity without False Negative Results

The conventional telomerase activity assay, TRAP assay, is not applicable for practical cancer diagnostics, because it is susceptible to polymerase inhibition by clinical extract, which leads to the false negative results [11]. To solve the problem, the novel telomerase assay utilizing A-PCR on MBs and CPT technology was developed in this thesis. Because of high-sensitive detection of cancer cells and avoidance of false negative results that preclude a clinical application of the conventional TRAP assay, the present assay should make a contribution to an accurate cancer diagnosis. For a clinical application of the present assay, it is preferable that all the procedures are automated using LoC technology. Various LoC devices utilizing MBs have already been developed,

because attachment of MBs to the target molecules including DNA, RNA, and proteins allows for the manipulation [12]. Also, the author's group succeeded to develop a silicon based PCR chip, which allows a rapid PCR amplification (30 cycles for 15 minutes) using only 2 μL of PCR solution [13, 14]. Therefore, the LoC device performing the present assay can be realized in the future.

Among various cancer diagnoses, a cervical cancer diagnosis may most need the LoC device with the present assay. Although cervical cancer is usually diagnosed by cervical cytology, the diagnosis is not accurate and depends on a proficiency of a cytotechnologist. Recently, DNA testing of human papillomavirus (HPV), of which infection is the first step for the cervical cancer development, was approved for the accurate diagnosis by Food and Drug Administration (FDA). However, HPV DNA testing should also be unuseful, because most HPV infections are temporary and 90% of infections are gone in 2 years without causing cervical cancer. Thus, it is critically important to detect only HPV with a high risk for cervical cancer. Previous studies on a cervical cancer development showed that E6 and E7 proteins of HPV with such a high risk activate hTERT expression by interacting with transcriptional repressors including USF1 and USF2 [15], and activators including c-Myc/Mac heterodimer [16, 17]. Therefore, the LoC device with the present assay should be of great help in the accurate diagnosis of cervical cancer.

5.3. References

1. Monchaud, D.; Teulade-Fichou, M. P., A Hitchhiker's Guide to G-Quadruplex Ligands. *Org. Biomol. Chem.* **2008**, 6, 627-636.
2. Ou, T. M.; Lu, Y. J.; Tan, J. H.; Huang, Z. S.; Wong, K. Y.; Gu, L. Q., G-Quadruplexes: Targets in Anticancer Drug Design. *ChemMedChem* **2008**, 3, 690-713.
3. Georgiades, S. N.; Abd Karim, N. H.; Suntharalingam, K.; Vilar, R., Interaction of Metal Complexes with G-Quadruplex DNA. *Angew. Chem., Int. Ed.* **2010**, 49, 4020-4034.
4. Spikes, J. D., Phthalocyanines as Photosensitizers in Biological-Systems and for the Photodynamic Therapy of Tumors. *Photochem. Photobiol.* **1986**, 43, 691-699.
5. Nicolazzi, C.; Mignet, N.; de la Figuera, N.; Cadet, M.; Ibad, R. T.; Seguin, J.; Scherman, D.; Bessodes, M., Anionic Polyethyleneglycol Lipids Added to Cationic Lipoplexes Increase Their Plasmatic Circulation Time. *J. Control. Release* **2003**, 88, 429-443.

6. Mignet, N.; Richard, C.; Seguin, J.; Largeau, C.; Bessodes, M.; Scherman, D., Anionic pH-Sensitive Pegylated Lipoplexes to Deliver DNA to Tumors. *Int. J. Pharm.* **2008**, 361, 194-201.
7. Luedtke, N. W., Targeting G-Quadruplex DNA with Small Molecules. *Chimia* **2009**, 63, 134-139.
8. Neidle, S., Human Telomeric G-Quadruplex: the Current Status of Telomeric G-Quadruplexes as Therapeutic Targets in Human Cancer. *FEBS J.* **2010**, 277, 1118-1125.
9. Huppert, J. L.; Balasubramanian, S., Prevalence of Quadruplexes in the Human Genome. *Nucleic Acids Res.* **2005**, 33, 2908-2916.
10. Todd, A. K.; Johnston, M.; Neidle, S., Highly Prevalent Putative Quadruplex Sequence Motifs in Human DNA. *Nucleic Acids Res.* **2005**, 33, 2901-2907.
11. Kim, N. W.; Wu, F., Advances in Quantification and Characterization of Telomerase Activity by the Telomeric Repeat Amplification Protocol (TRAP). *Nucleic Acids Res.* **1997**, 25, 2595-2597.
12. Gijs, M. A. M., Magnetic Bead Handling on-Chip: New Opportunities for Analytical Applications. *Microfluid. Nanofluid.* **2004**, 1, 22-40.
13. Tanaka, H.; Fiorini, P.; Peeters, S.; Majeed, B.; Sterken, T.; Op de Beeck, M.; Hayashi, M.; Yaku, H.; Yamashita, I., Sub-Micro-Liter Electrochemical Single-Nucleotide-Polymorphism Detector for Lab-on-a-Chip System. *Jpn. J. Appl. Phys.* **2012**, 51, 04DL02-1-04DL02-6.
14. Majeed, B.; Jones, B.; Tezcan, D. S.; Tutunjyan, N.; Haspeslagh, L.; Peeters, S.; Fiorini, P.; Op de Beeck, M.; Van Hoof, C.; Hiraoka, M.; Tanaka, H.; Yamashita, I., Silicon Based System for Single-Nucleotide-Polymorphism Detection: Chip Fabrication and Thermal Characterization of Polymerase Chain Reaction Microchamber. *Jpn. J. Appl. Phys.* **2012**, 51, 04DL01-04DL01-9.
15. McMurray, H. R.; McCance, D. J., Human Papillomavirus Type 16 E6 Activates TERT Gene Transcription through Induction of c-*Myc* and Release of USF-Mediated Repression. *J. Virol.* **2003**, 77, 9852-9861.
16. Wang, J.; Xie, L. Y.; Allan, S.; Beach, D.; Hannon, G. J., Myc Activates Telomerase. *Gene. Dev.* **1998**, 12, 1769-1774.
17. Wu, K. J.; Grandori, C.; Amacker, M.; Simon-Vermot, N.; Polack, A.; Lingner, J.; Dalla-Favera, R., Direct Activation of *TERT* Transcription by c-MYC. *Nat. Genet.* **1999**, 21, 220-224.

6. Publications

6.1. Main Papers

1. **Anionic Phthalocyanines Targeting G-Quadruplexes and Inhibiting Telomerase Activity in the Presence of Excessive DNA Duplexes**

   Hidenobu Yaku, Takashi Murashima, Daisuke Miyoshi, Naoki Sugimoto

   Chem. Commun. **2010**, 46, 5740-5742.

2. **Study on Effects of Molecular Crowding on G-Quadruplex-Ligand Binding and Ligand-Mediated Telomerase Inhibition**

   Hidenobu Yaku, Takashi Murashima, Hisae Tateishi-Karimata Shu-ichi Nakano, Daisuke Miyoshi, Naoki Sugimoto

   Methods **2013**, 64, 19-27.

3. **A Highly Sensitive Telomerase Activity Assay that Eliminates False-Negative Results Caused by PCR Inhibitors**

   Hidenobu Yaku, Takashi Murashima, Daisuke Miyoshi, Naoki Sugimoto

   Molecules **2013**, 18, 11751-11767.

6.2. Related Papers

1. Design of Allele-Specific Primers and Detection of the Human ABO Genotyping to Avoid the Pseudopositive Problem

   Hidenobu Yaku, Tetsuo Yukimasa, Shu-ichi Nakano, Naoki Sugimoto, Hiroaki Oka

   Electrophoresis **2008**, 29, 4130-4140.

2. Development of Technology for Electrochemical SNP Genotyping - Electrochemical Discrimination for Individual Differences in DNA Sequences -

   Hidenobu Yaku, Tetsuo Yukimasa, Shu-ichi Nakano, Naoki Sugimoto, Hiroaki Oka

   Matsushita Technical Journal **2008**, 54, 40-45.

3. Sub-Micro-Liter Electrochemical Single-Nucleotide-Polymorphism Detector for Lab-on-a-Chip System

   Hiroyuki Tanaka, Paolo Fiorini, Sara Peeters, Bivragh Majeed, Tom Sterken, Maaike Op de Beek, Miho Hayashi, Hidenobu Yaku, Ichiro Yamashita

   Jpn. J. Appl. Phys. **2012**, 51, 04DL02-1-04DL02-6.

4. Multiple and Cooperative Binding of Fluorescence Light-up Probe Thioflavin T with Human Telomere DNA G-Quadruplex

   Valerie Gabelica, Ryuichi Maeda, Takeshi Fujimoto, Hidenobu Yaku, Takashi Murashima, Naoki Sugimoto, Daisuke Miyoshi

   Biochemistry **2013**, 52, 5620-5628.

5. *In Vitro* Assays Predicting of Telomerase Inhibitory Effect of G-Quadruplex Ligands in Cell Nuclei

   Hidenobu Yaku, Takashi Murashima, Daisuke Miyoshi, Naoki Sugimoto

   J. Phys. Chem. B, in press.

6. A Simple “Add and Measure” FRET-Based Telomeric Tandem Repeat Sequence Detection and Telomerase Assay Method

   Koji Kawamura, Hidenobu Yaku, Daisuke Miyoshi, Takashi Murashima

   Org. Biomol. Chem., in press.

6.3. Reviews

1. 電気化学的 SNP タイピング技術

   夜久英信

   核酸化学のニュートレンド DNA・RNA の新たな可能性を拓く（化学同人） **2011**, 17, 188-195.

2. Phthalocyanines: a New Class of G-Quadruplex-Ligands with Many Potential Applications

   Hidenobu Yaku, Takeshi Fujimoto, Takashi Murashima, Daisuke Miyoshi and Naoki Sugimoto

   Chem. Commun. (Feature Article & Front Cover) **2012**, 48, 6203-6216.

3. Specific Binding of Anionic Porphyrin and Phthalocyanine to the G-Quadruplex with a Variety of *in Vitro* and *in Vivo* Applications

   Hidenobu Yaku, Takashi Murashima, Daisuke Miyoshi, Naoki Sugimoto

   Molecules **2012**, 17, 10586-10613.

7. Presentations

7.1. International Conferences

1. Roles of Anionic Functional Groups in G-Quadruplex-Ligands for Efficient Telomerase Inhibition

   Hidenobu Yaku, Takashi Murashima, Daisuke Miyoshi, Naoki Sugimoto

   The 37th International Symposium on Nucleic Acids Chemistry 2010, Hamagin Hall "VIA MARE" (Yokohama, Japan), 2010/11

2. G-Quadruplex-Ligands with Negative Charges under Cell-Mimicking Conditions

   Daisuke Miyoshi, Hidenobu Yaku, Takashi Murashima, Naoki Sugimoto

   SECOND TRAINING SCHOOL on G-QUADRUPLEXES "Self-Assembled Guanosine Structures for Molecular Electronic Devices", Spa, Belgium, 2011/9

3. A New Fluorescent Light-up Probe for DNA

   Daisuke Miyoshi, Hidenobu Yaku, Takeshi Fujimoto, Takashi Murashima, Naoki Sugimoto

   The 38th International Sympoisum on Nucleic Acid Chemistry, Hokkaido University (Hokkaido, Japan), 2011/11

4. PCR-Free Detection of Telomerase Activity in HeLa Cells Based on Catalytic Signal Amplification with RNase H

   Hidenobu Yaku, Takashi Murashima, Daisuke Miyoshi, Naoki Sugimoto

   The 38th International Symposium on Nucleic Acid Chemistry, Hokkaido University (Hokkaido, Japan), 2011/11

5. Thioflavine-T as Human Telomeric G-Quadruplex Probe

   Daisuke Miyoshi, Valerie Gabelica, Ryuichi Maeda, Takeshi Fujimoto, Hidenobu Yaku, Takashi Murashima, Naoki Sugimoto

   XX International Roundtable on Nucleosides, Nucleotides and Nucleic Acids, McGill University (Montreal, Canada), 2012/8

6. PCR-Free Telomerase Assay with Cycling Probe Technology

Hidenobu Yaku, Takashi Murashima, Daisuke Miyoshi, Naoki Sugimoto

XX International Roundtable on Nucleosides, Nucleotides and Nucleic Acids, McGill University (Montreal, Canada), 2012/8

7. Quantitative Analysis for the DNA Stability toward the Development of New Functional Materials

   Naoki Sugimoto, Hidenobu Yaku, Takashi Murashima Daisuke Miyoshi, S. Nakano T. Endoh and H. Tateishi-Karimata

   4th EuCheMS Chemistry Congress, Prague, Czech Republic, 2012/8

8. Diminished Electrostatic Attraction in G-Quadruplex-Ligand Complex Leading to to Reduction of Telomerase Inhibitory Effect under Cell-Nuclei Mimicking Condition

   Hidenobu Yaku, Takashi Murashima, Daisuke Miyoshi and Naoki Sugimoto

   The 39th International Symposium onNucleic Acids Chemistry, Nagoya University (Nagoya, Japan), 2012/11

9. Biomolecule-Ligand Noncovalent Complexes: Mass Spectrometry as a Key to Interpret Solution Fluorescence Data

   Daisuke Miyoshi, Ryuichi Maeda, Takeshi Fujimot, Hidenobu Yaku, Takashi Murashima, Naoki Sugimoto, Adrien Marchand, Frederic Rosu, Valerie Gabelica

   61st ASMS (American Society for Mass Spectrometry) Conference, Minneapolis Convention Center (Minneapolis, Minnesota, USA) 2013/6

10. Molecular Crowding Effects on Functions of G-Quadruplex Ligands

    Hidenobu Yaku, Takashi Murashima, Hisae Tateishi-Karimata, Shu-ichi Nakano, Naoki Sugimoto, Daisuke Miyoshi

    4th International Meeting on G-Quadruplex Nucleic Acids, Nanyang Technological University (Nanyang Avenue, Singapore), 2013/7

11. G-Quadruplex-Based Drug Delivery Carrier in Response to Target mRNA

    Hidenobu Yaku, Takashi Murashima, Daisuke Miyoshi, Naoki Sugimoto

    The 40th International Symposium on Nucleic Acid Chemistry, Kanagawa Univessity (Yokohama, Japan), 2013/11

12. FRET-based detection of G-quadruplexes in the 5'-UTR of cancer related mRNAs

Ryuichi Maeda, Valerie Gabelica, Hidenobu Yaku, Takashi Murashima, Naoki Sugimoto, Daisuke Miyoshi

The 40th International Symposium on Nucleic Acid Chemistry, Kanagawa Univessity (Yokohama, Japan), 2013/11

7.2. Domestic Conferences

1. 擬陽性を抑制するアレル特異的 DNA プライマーの開発

夜久英信・行政哲男・岡弘章・杉本直己

日本化学会第 87 春季年会, 関西大学, 2007/3

2. 擬似細胞核内環境下におけるアニオン性 G-quadruplex リガンドのテロメラーゼ阻害効果

夜久 英信・村嶋 貴之・三好 大輔・杉本 直己

第 5 回バイオ関連化学シンポジウム, つくば国際会議場, 2011/9

3. 生命分子の挙動に及ぼす分子環境の効果(31) RNase H とプローブ RNA を用いたサイクリングプローブ技術による PCR フリーのテロメラーゼ活性検出技術の開発

夜久英信・村嶋貴之・三好大輔・杉本直己

日本化学会第９２春季年会, 慶應義塾大学, 2012/3

4. チオフラビン T による DNA 四重らせん構造の蛍光検出

前田龍一・藤本健史・夜久英信・村嶋貴之・杉本直己・三好大輔

日本化学会第９２春季年会, 慶應義塾大学, 2012/3

5. FRET を利用した新規なテロメラーゼ活性測定法の開発

河村浩司・夜久英信・三好大輔・村嶋貴之

第 6 回バイオ関連化学シンポジウム, 北海道大学, 2012/9

6. 生命分子の挙動に及ぼす分子環境の効果 (43) チオフラビン T による核酸四重らせん構造の高感度検出

前田龍一、Gabelica, Valerie、藤本健史、夜久英信、村嶋貴之、杉本直己、三好　大輔

日本化学会第 93 春季年会, 立命館大学, 2013/3

7. G-quadruplex を利用した標的 mRNA 応答型ドラッグデリバリーシステムの開発

   夜久 英信・村嶋 貴之・三好 大輔・杉本 直己

   第 7 回バイオ関連化学シンポジウム, 名古屋大学, 2013/9

8. FRET を利用した mRNA 四重らせん構造の特異的検出

   前田 龍一・Gabelica Valerie・夜久 英信・村嶋貴之・杉本 直己・三好 大輔

   第 7 回バイオ関連化学シンポジウム, 名古屋大学, 2013/9

Acknowledgements

I greatly appreciate Prof. Naoki Sugimoto for giving me the opportunity to engage in this study, and for his guidance and encouragement.

I express my gratitude to Profs. Daisuke Miyoshi and Takashi Murashima for their valuable guidance and suggestions for conducting this study and polishing this thesis.

I express my thanks to Drs. Tamaki Endoh, Syuntaro Takahashi, Hisae Tateishi, and postdoctoral fellows for their continuous encouragement.

I express my appreciation to Prof. Shu-ichi Nakano for his helpful guidance in developing SNP genotyping technology.

I am deeply grateful to Mr. Sugihara Hirokazu (Panasonic Corporation), Dr. Hiroaki Oka (Panasonic Corporation), and Mr. Tetsuo Yukimasa (Panasonic Corporation) for developing SNP genotyping technology together and for their suggestions.

I appreciate Drs. Daisuke Ueda (Panasonic Corporation) and Ayumu Tsujimura (Panasonic Corporation), and Mr. Atsushi Omote (Panasonic Corporation) for supporting me.

I would like to thank Miss. Chieko Hijiriyama, Mr. Atsushi Niwafumi, and the past and present members of Biomolecular Chemistry Laboratory and Biomolecular Design Laboratory in Konan University for their kind support.

Finally, I thank my family for their support.